CRYSTAL STRUCTURE AND ELASTIC CONSTANTS OF AMMONIUM FLUOBERYLLATE BY X-RAY DIFFRACTION

By

ANITA GARG

DEPARTMENT OF PHYSICS

INDIAN INSTITUTE OF TECHNOLOGY KANPUR

MAY 1980

CRYSTAL STRUCTURE AND ELASTIC CONSTANTS OF AMMONIUM FLUOBERYLLATE BY X-RAY DIFFRACTION

A Thesis Submitted
in Partial Fulfilment of the Requirements
for the Degree of

DOCTOR OF PHILOSOPHY

By

ANITA GARG

to the

DEPARTMENT OF PHYSICS

INDIAN INSTITUTE OF TECHNOLOGY KANPUR

MAY 1980

TO

MY DAUGHTER

ANKUR

CERTIFICATE

Certified that the work presented in this thesis entitled "CRYSTAL STRUCTURE AND ELASTIC CONSTANTS OF AMMONIUM FLUOBERYLLATE BY X-RAY DIFFRACTION" has been carried out by Anita Garg under my supervision and has not been submitted elsewhere for a degree.

R. Srivastava

(R. C. Srivastava)
Professor
Department of Physics
Indian Institute of Technology
Kanpur, India

Dated. 20.12.1980

ACKNOWLEDGEMENTS

With great pleasure, I express my appreciation and gratitude to Professor R. C. Srivastava for his keen interest, guidance and encouragement throughout the course of this work.

I am grateful to Professor A. S. Parasnis for his valuable advice and generous help. Special thanks are due to Professor C. J. L. Lock and Mr. R. Faggiani of McMaster University, Canada for helping me use their facilities. I must also acknowledge with thanks the many helpful suggestions of Professor W. A. Wooster of Crystal Structure Ltd., Cambridge, U.K.

My warm and sincere thanks are due to Professors A. K. Majumdar, R. K. Ray, G. K. Mehta, H. D. Bist and T. M. Srinivasan for their help and cooperation in several ways.

I am thankful to A. K. Nigam and A. Agarwal for their help, care and sympathy which I mostly took for granted and always received in abundance. Thanks are also due to Y. Chandra and Shri M. L. Pandey for their help at various stages of the work.

I cannot express in words the help, cooperation and understanding received from my husband, Vijay.

Finally I must thank Mr. Nihal Ahmad for careful typing and Shri Lallu Singh and H. L. Panda for neat cyclostyling.

Financial assistance received from C.S.I.R. is gratefully acknowledged.

Anita Garg

CONTENTS

APPENDIX

LIST OF TABLES

LIST OF FIGURES

SYNOPSIS

In the present work the crystal structure and elastic properties of single crystals of Ammonium Fluoberyllate, $(NH_4)_2BeF_4$, have been investigated at room temperature using X-ray diffraction techniques. The work is presented in four chapters and two appendices.

Chapter I gives the general introduction and theoretical background of the work done. Section A of this chapter gives a brief survey of different methods of crystal structure determination and refinement. It also describes the analysis of anisotropic temperature factors in terms of rigid body motion of molecules in crystals. Section B gives a brief account of the theory of thermal diffuse scattering (TDS) of X-rays as applied to the determination of elastic constants. The relations between the intensity of diffuse reflections and elastic constants based on Voigt's theory as well as Laval's theory of elasticity have been described in this section.

The experimental procedure for measuring intensities and corrections etc. has been described in Chapter II. Section A gives the measurement of 3-dimensional intensity data for crystal structure determination and Section B describes the determination of the intensity of diffuse

reflection for evaluation of elastic constants. For the study of diffuse reflection, the incident beam has been monochromatized using a curved quartz crystal monochromator. The monochromator assembly was designed so as to be accommodated on GE-XRD-6 diffractometer. Various corrections viz. divergence, polarization, skew, absorption and general scattering applied to measured intensity of diffuse reflection are also discussed in this section. In order to determine the absolute values of elastic constants, the direct beam intensity I_o has been determined using the Compton scattering of diamond as an intermediate standard. This is described in Appendix I.

Chapter III deals with the determination and discussion of the crystal structure of $(NH_4)_2BeF_4$. The structure has been refined to an R value of 0.049. The structure consists of two kinds of ammonium tetrahedra, $(NH_4)_I$ and $(NH_4)_{II}$ which are hydrogen bonded to BeF_4 tetrahedra. The large thermal anisotropy of fluorine atoms has been analysed in terms of rigid body libration of BeF_4 group. As a consequence of this the foreshortening of individual Be-F bond length by about 0.02 Å has been accounted for. Other structural features have been correlated with the known results of Raman spectrum of $(NH_4)_2BeF_4$.

The results of the study of TDS of X-rays have been discussed in Chapter IV. The reciprocal lattice points

(relps.) used to calculate all the elastic constants of $(NH_4)_2BeF_4$ are 004, 020, 040, 400, 301 and 031. For different directions of propagation of the thermal wave, the graphs between the ratio of diffuse intensity to incident intensity and square of wavelength of the corresponding thermal wave for all the above relps. have been drawn and shown in Appendix II. According to Voigt's theory of elasticity there will be 9 elastic constants for orthorhombic $(NH_4)_2BeF_4$ whose values in units of 10^{11} dynes cm^{-2} are $C_{11} = 3.82$, $C_{22} = 3.56$, $C_{33} = 2.45$, $C_{44} = 0.96$, $C_{55} = 1.01$, $C_{66} = 0.79$, $C_{12} = 1.78$, $C_{13} = 1.52$, $C_{23} = 1.41$. The accuracy of C_{44}, C_{55}, C_{66}; C_{11}, C_{22}, C_{33}; C_{12}, C_{13}, C_{23} is estimated to be 5%, 8%, 10% respectively. Laval's theory requires 15 elastic constants for the orthorhombic system. This is so as certain constants which are required to be equal in Voigt's theory may not be equal in Laval's theory. The differences in such elastic constants have not been found to be significant for $(NH_4)_2BeF_4$ as they are within the experimental errors involved in the method. Isodiffusion contours have been drawn around the node (400) and thus information about thermal vibration amplitudes has been obtained. The mean sound velocity in the crystal has been calculated from elastic constants and Debye temperature for $(NH_4)_2BeF_4$ has been evaluated as 381 K. The constant velocity surfaces have been plotted in different sections.

The other bulk properties viz. bulk modulus, shear modulus etc. of polycrystalline aggregate of $(NH_4)_2BeF_4$ have been evaluated from single crystal elastic stiffness constant (C_{ij}) and elastic compliance constant (S_{ij}) values. A qualitative correlation between structure and elastic constant values is also indicated in this chapter.

1. INTRODUCTION AND THEORY

Since the establishment of fundamental principles of X-ray diffraction by Von Laue, W. H. Bragg and W. L. Bragg, X-ray diffraction has become one of the major tools of studying the arrangement of atoms in crystals. It also yields information about the motion of atoms about their mean position which in turn may be employed to give useful information about the related physical properties of the crystals.

The compound undertaken in the present study is Ammonium fluoberyllate, $(NH_4)_2BeF_4$, which has been the subject of considerable interest since the discovery of its ferroelectric transition at 175 K (Pepinsky and Jona, 1957)[1] and more recently of its non-ferroelectric transition at 182 K (Makita and Yamauchi, 1974)[2]. Unlike proper ferroelectrics such as triglycine sulphate and $BaTiO_3$, $(NH_4)_2BeF_4$ (called AFB hereafter) has very different and peculiar properties. Recently Levanyuk and Sannikov[3] have proposed an improper ferroelectric model for AFB, in which free energy is represented by two characteristic parameters. Although many investigations have been made, the mechanism of phase transition in AFB is still unknown. Hence it is of interest to study more about its physical properties. Keeping this in

view, crystal structure and elastic properties of AFB have been investigated at room temperature (305 K) in the paraelectric phase, using X-ray diffraction method. Brief theoretical background of crystal structure analysis as well as determination of elastic constants by X-ray methods is given in the following sections.

1.A.1 Crystal Structure Analysis

The scattering of X-rays by matter is essentially the scattering due to electrons. A measurement of positions and intensities of the diffraction maxima forms the basic set of data for structure analysis. The positions are used for identifying the crystal planes and determining the geometry of the unit cell. The space group symmetry information is derived from the systematically absent reflections in different classes of reflections in the intensity data. The intensity of reflections is related to electron density distribution which in turn depends on the atomic positions. The intensity data therefore can in principle be used to determine the crystal structure.

Structure Factor (F_{hkl})

At a diffraction maximum, i.e. the reflection hkl, the sum of amplitudes of the wavelets scattered by all the atoms in the unit cell is given by

$$F_{hkl} = \sum_{j=1}^{J} f_j \exp[\, 2\pi i \, (hx_j + ky_j + lz_j) \,] \qquad (1.1)$$

where f_j is the atomic scattering factor of the j^{th} atom located at the position (x_j, y_j, z_j) in the unit cell and J is the total number of atoms in the unit cell.

Equation (1.1) can also be written as

$$F_{hkl} = \sum_{j=1}^{J} f_j \cos \phi_j + i \sum_{j=1}^{J} f_j \sin \phi_j \qquad (1.2)$$

$$\text{i.e. } |F_{hkl}| = \sqrt{\left(\sum_{j=1}^{J} f_j \cos \phi_j\right)^2 + \left(\sum_{j=1}^{J} f_j \sin \phi_j\right)^2} \qquad (1.3)$$

where $\phi_j = 2\pi (hx_j + ky_j + lz_j)$ is called the phase of the the structure amplitude $|F_{hkl}|$.

Fourier (F_o) Synthesis

Since a crystal is a period structure in three dimensions, it can be represented by a 3-dimensional electron density function $\rho(x_j, y_j, z_j)$, which varies continuously over the volume of the unit cell. The structure factor then can be written as

$$F_{hkl} = \int_{o}^{V} \rho(xyz) \exp[2\pi i \, (hx+ky+lz)] dv \qquad (1.4)$$

where V is the volume of unit cell. Since the electron density $\rho(xyz)$ is periodic in three dimensions, it can be

represented by a 3-dimensional fourier series

$$\rho(xyz) = \sum_{h} \sum_{k=-\infty}^{+\infty} \sum_{l} C_{hkl} \exp[-2\pi i(hx+ky+lz)] \qquad (1.5)$$

The fourier coefficients C_{hkl} turn out to be F_{hkl}/V and hence

$$\rho(xyz) = \frac{1}{V} \sum_{h} \sum_{k=-\infty}^{+\infty} \sum_{l} F_{hkl} \exp[-2\pi i (hx+ky+lz)] \qquad (1.6)$$

Thus if F_{hkl} are known, a three dimensional plot of $\rho(xyz)$ could be obtained and the peaks would show the positions of atoms.

Phase Problem

The complex form of the expression (1.1) for the structure factor merely means that the phase of the scattered wave is not simply related to that of the incident wave. The phase, however, is not an observable quantity, the only observable quantity being the intensity which is proportional to $|F_{hkl}|^2$. Hence the experimental data I_{hkl} (intensity of the reflection hkl) which only gives the information about $|F_{hkl}|$ (as $I_{hkl} \propto |F_{hkl}|^2$) and no direct information about phase of the diffracted beam is not sufficient for performing fourier synthesis.

In the absence of any direct information about phases of the diffraction maxima (reflections), the crystal structures

are solved by extracting the information about phases indirectly by one of the many methods or their combinations which may suit a given problem. Some of these are mentioned below.

Patterson Synthesis

Instead of F_{hkl}/V, measurable quantity $|F_{hkl}|^2/V$, i.e. I_{hkl}/V are used as fourier co-efficients. The resulting synthesis gives information about interatomic vectors from which the atomic positions of many atoms may be derived using image seeking or vector convergence procedures in suitable crystal structures.

Heavy Atom Method

If the unit cell of the crystal contains a few heavy atoms whose positions are known (by Patterson synthesis or symmetry) then a fourier synthesis, phased with these atoms only, is done and it may reveal a few more atoms. The remaining atoms could be located by successive use of F_o synthesis phased with more atoms.

Direct Methods[4]

It is a class of methods in which attempt is made to derive the phases of the structure factors without previously having postulated any atomic positions. For fairly large structures having nearly equal atoms, these methods have been used with great success.

1.A.2 Refinement of the Structure

Once the model of the structure has been proposed, it is necessary to improve the preliminary co-ordinates so as to obtain best correspondence between the calculated ($|F^c_{hkl}|$) and the observed ($|F^o_{hkl}|$) structure factors. The following procedures, their variants or combinations are generally used.

Difference Fourier Synthesis

The difference synthesis uses ($F^o_{hkl} - F^c_{hkl}$) as the fourier co-efficients, i.e.

$$\rho_o - \rho_c = \frac{1}{V} \sum_h \sum_{k=-\infty}^{+\infty} \sum_l (F^o_{hkl} - F^c_{hkl}) \exp[-2\pi i(hx+ky+lz)] \qquad (1.7)$$

When the proposed model exactly matches the actual crystal structure, the difference map is characterized by essentially a flat topography. If the proposed structure deviates in any way from the actual structure, a topography characteristic of the deviation is observed which helps in locating the unresolved atoms in F_o synthesis as well as in determining the anisotropy of thermal vibration of different atoms.

Least Squares Refinement

To obtain a better agreement between F^o_{hkl} and F^c_{hkl}, different parameters p_j (j=1,...n; where n is the total

number of variable parameters) on which F^c_{hkl} are dependent, e.g. atomic positions, temperature factors, scale factors, etc. are systematically varied such that

$$M = \sum_{hkl} \omega_{hkl} \left(|F^o_{hkl}| - |k F^c_{hkl}| \right)^2$$

is a minimum; ω_{hkl} is the weight alloted to each reflection and k is the scale factor. Taking first derivative of M w.r.t. different parameters p_j and equating them to zero, leads to n normal equations which can be written in the matrix form as follows

$$[C]_{nxn} \cdot [X]_{nx1} = [V]_{nx1} \qquad (1.8)$$

where $$C_{ij} = \sum_{hkl} \omega_{hkl} \frac{\partial |kF^c_{hkl}|}{\partial p_i} \frac{\partial |kF^c_{hkl}|}{\partial p_j}$$

$$X_j = \Delta p_j$$

and $$V_j = \sum_{hkl} \omega_{hkl} (\Delta F_{hkl}) \frac{\partial |kF^c_{hkl}|}{\partial p_j}$$

or $$[X]_{nx1} = [C]^{-1}_{nxn} \cdot [V]_{nx1}$$

Thus one can get the value of X_j i.e. Δp_j, the required shift in the parameter for a better fit. This refinement process is repeated until the shift in each parameter becomes small as compared to its standard deviation.

It is advisable to compute the difference map after each refinement cycle to inspect for any significant features.

1.A.3 Figure of Merit

The reliability index R is taken as the figure of merit of the structure. It is defined as follows .

$$R = \frac{\sum_n \left| |F^o_{hkl}| - |F^c_{hkl}| \right|}{\sum_n |F^o_{hkl}|} \qquad (1.9)$$

where n is the total number of observations. Smaller the value of R, the better is the agreement of proposed model with the observed one. If weights are given to different reflections, a weighted R factor, ωR, may be defined as follows

$$\omega R = \left[\frac{\sum_n \omega (F^o_{hkl} - F^c_{hkl})^2}{\sum_n \omega (F^o_{hkl})^2} \right]^{1/2} \qquad (1.10)$$

1.A.4 Thermal Motion Analysis

Atoms undergo thermal motion at all temperatures and thus electrons of each atom sweep out a large average volume which may be regarded as triaxial ellipsoid in the most general case of anisotropic thermal vibrations. The shape will be sphere if the thermal vibrations are isotropic. The thermal motion causes the effective atomic scattering curve f of the atom to fall off more rapidly with the scattering angle θ. For the isotropic case

$$f = f_o \exp \left[- B_o (\sin^2 \theta / \lambda^2) \right] \qquad (1.11)$$

where f_o is the scattering factor of the static atom and B_o is the isotropic temperature factor and λ is the wave-length of the X-rays scattered. In the early stages of the crystal structure refinement, it is sufficiently good approximation to take the temperature factor as isotropic but as the refinement approaches the final stages, each atomic motion may be approximated by a triaxial ellipsoid which is different for each non-equivalent atom. This leads to the anisotropic temperature factor which for j^{th} atom of the unit cell is defined as follows

$$f_j = f_{oj} \exp[-(B_{11}h^2+B_{22}k^2+B_{33}l^2+2B_{12}hk+2B_{13}hl+2B_{23}kl)] \quad (1.12)$$

The normal modes of vibration of a simple molecule are constituted by molecular (internal) modes and lattice (external) modes. The former involve the stretching or bending of bonds within a molecule and have relatively high frequencies while the latter describe the translation and rotation (i.e. libration) of each molecule essentially as a rigid unit and hence have low frequencies. At ordinary temperatures, the mean square displacement of an atom resulting from the molecular modes is only a few per-cent of that produced by the lattice modes and hence it is a reasonable approximation to neglect the former contribution at room temperature.

The mean square displacement of any atom of the unit cell in the direction $\vec{l}$ specified by unit vectors $(\vec{i}_1, \vec{i}_2, \vec{i}_3)$

can be written as

$$\overline{u^2} = \sum_{i=1}^{3} \sum_{k=1}^{3} U_{ik} l_i l_k$$

where U_{ik} are the components of the symmetric tensor U obtained from the anisotropic temperature factors B_{ik}. For a rigid body motion of a molecule (or a part of it), this displacement can be expressed in terms of two symmetric tensors T and L, each with six independent components (Cruickshank, 1956)[5]. T gives the translational vibration of the centre of masses and L the angular oscillation (libration) about axes through the centre. The value of $\overline{u^2}$ in a direction $\vec{l}$ at a point r in the rigid body is then given by

$$\overline{u^2} = \sum_{i=1}^{3} \sum_{k=1}^{3} U_{ik} l_i l_k = \sum_{i=1}^{3} \sum_{k=1}^{3} (T_{ik} l_i l_k + L_{ik} (\vec{l} \times \vec{r})_i (\vec{l} \times \vec{r})_k) \qquad (1.14)$$

There is an equation of this type for each atom of the molecule, hence T and L tensors for the molecule can be calculated. An important consequence of the rigid body libration is that it can account for the apparent shortening of the bond lengths due to angular oscillations.

If the libration axes are not constrained to intersect in a known point (e.g. centre of symmetry of the molecule) an additional non-symmetric tensor S[6] called the screw tensor has also to be used to correlate the L and T tensors.

When this tensor is included in the analysis, the fit of observed and calculated U's is independent of origin but the components of S and T vary with it. To avoid this arbitrariness, S is symmetrized and values of S and T are calculated w.r.t. the principal axes of L.

The amplitudes of angular oscillation can be used to calculate the average frequencies of the rotational branches of the normal lattice vibrations. Each of the rotational branches may be approximated[7] by a constant frequency and the mean square amplitude of angular oscillation in radian^2 is then given by the following equation

$$(L)_I = \frac{h}{8\pi^2 I} \left(\frac{1}{\nu} \coth \frac{h\nu}{kT}\right) \qquad (1.15)$$

where I is the moment of inertia of the molecule about the axis of libration.

1.B.1 Thermal Diffuse Scattering (TDS)

Due to thermal motion of atoms at all temperatures, there is a diffusely reflected part of the radiation which can provide very useful information about many physical properties of the crystal, e.g. elastic properties, Debye temperature etc. Excellent summaries of the theory of X-ray diffuse scattering are presented by Born (1942-1943)[8], James (1950)[9], Slater (1958)[10], Wooster (1962)[11] and

Cochran (1969)[12]. The theory has been placed on firm footing by the experimental work of Laval (1938-1957)[13], Lonsdale and Smith (1941,1942)[14] and Ramachandran and Wooster (1951)[15].

The idea of determination of elastic constants from the study of diffuse X-ray reflections originates from the theory of Waller (1923-1928)[16] and Faxen (1923)[17]. According to this theory, atoms constituting the crystalline medium vibrate continuously at all temperatures, the amplitude of vibration increases with an increase of temperature. These vibrations resolve into thermal waves which are superimposed on the static periodicity of the crystal. Consequently regular periodicity of the crystal gets modulated by each thermal wave and gives rise to a series of dynamic stratifications corresponding to each set of lattice planes (hkl). Coherent reflections from these dynamic stratifications will be possible at angles slightly different from Bragg angle of the static plane. The intensity of such a reflection will depend on the amplitude of modulation which is given by the amplitude of corresponding thermal wave. The latter is again dependent on the frequency of the wave, being smaller the higher the frequency owing to the equipartition of energy among the different modes of vibration. Thus the intensity of a dynamic reflection corresponding to a particular thermal wave can be indirectly employed

to give its frequency. The wavelength (λ), which is reciprocal of the wave vector ($\vec{q}$) and the direction of propagation of the wave depend on the geometry of dynamic reflection, i.e. the angles of incidence and reflection with respect to the static planes. By proper choice of geometry, it is possible to pick out for observation the dynamic reflection due to a particular thermal wave having a definite wave-length and a definite direction of propagation. The wavelength and frequency of a particular thermal wave being known, its velocity can be determined. Since the thermal waves corresponding to small wave vectors can be identified with the acoustic waves, their velocity in a particular direction can be related to the elastic constants of the crystal. This elegant theory of Waller has been mathematically formulated by Laval (1943)[13] so as to explicitly express the intensity of diffuse reflections in terms of elastic constants. Essential features of his treatment are described below.

Thermal vibrations of a crystal consisting of N unit cells and g atoms per unit cell can be resolved into 3Ng independent waves. Assuming the thermal waves to be plane and neglecting absorption and dispersion and excluding the Compton scattering, the total amplitude scattered by a crystal vibrating under the influence of 3Ng thermal waves can be shown to consist of two components:

1. Laue Bragg reflection having the same frequency as that of the incident beam but having atomic scattering factor, f_j, reduced by thermal motion.

2. The second component consists of diffracted radiation due to thermal vibrations. For polyatomic lattice one wave vector corresponds to a number of thermal waves having different frequencies. So no exact information about frequencies can be obtained from the intensity of diffuse reflections. But for very long waves, i.e. short wave vectors ($\vec{q} \to 0$), the frequency of the three (one longitudinal and two transverse) acoustical waves approaches zero while that of optical branch remains still high, the amplitude scattered by optical branch becomes inappreciably low, whereas that due to acoustical branch remains high (except in a rare case where there is a low frequency optical mode present). Hence for small wave vectors, only acoustical modes are primarily effective in producing diffuse reflections and therefore amplitudes of vibrations of thermal waves with polarization α can be taken to be same for all atoms. Considering only first order diffuse reflection where only elastic waves having their wave vectors $\vec{q}$ equal to $\pm XQ$ (Fig. 1.1, where X is the reciprocal lattice point (relp.) nearest to Q) contribute, the fraction of the incident intensity I'_d / I_o reflected in the first order for region of reciprocal space close to a relp. from the equation of Laval (1943)[13] is given as follows

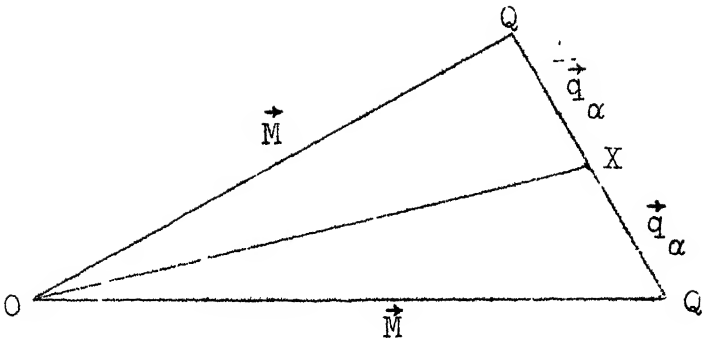

Fig. 1.1 Vector diagram for first order diffuse reflection. (Ω is the pole of diffusion; X is the reciprocal point nearest to it.)

$$\sigma_1 = \frac{I_d'}{I_o} = \frac{\epsilon^2 N F_T^2 kT}{V} \frac{|\vec{X}|^2}{|\vec{q}|^2} \sum_{\alpha=1}^{3} \frac{\cos^2(\vec{X}, A_\alpha)}{\rho V_\alpha^2} \qquad (1.16)$$

where

N is the total number of unit cells in the crystal.

F_T is the structure factor of the plane hkl under consideration at temperature T.

V is the volume of the unit cell.

$\vec{X}$ is the reciprocal lattice vector $\vec{OX}$.

$\vec{q}$ is the wave vector of the thermal wave.

ρ is the density of the crystal.

A_α, V_α are the amplitudes and velocities respectively of the three acoustical waves having wave vector $\vec{q}$.

In the above equation all the terms except the summation are known or can be readily evaluated. This summation has been evaluated by Jahn (1942)[13] and is given by

$$\sum_{\alpha=1}^{3} \frac{\cos^2(\vec{X}, A_\alpha)}{\rho V_\alpha^2} = K\,[uvw]_{hkl} \tag{1.17}$$

$$= L^2A_{11}^{-1} + M^2A_{22}^{-1} + N^2A_{33}^{-1} + 2LMA_{12}^{-1} + 2MNA_{23}^{-1} + 2NLA_{31}^{-1} \tag{1.18}$$

where L, M, N and u,v,w are the direction cosines of $\vec{X}$ and $\vec{q}$ respectively with respect to orthogonal crystal axes and $(A^{-1})_{ij}$ are the elements of the matrix A^{-1} which is inverse of the matrix A whose elements are given by

$$\begin{bmatrix} A_{11} \\ A_{22} \\ A_{33} \\ A_{23} \\ A_{13} \\ A_{12} \end{bmatrix} = \begin{bmatrix} C_{11} & C_{66} & C_{55} & 2C_{56} & 2C_{15} & 2C_{16} \\ C_{66} & C_{22} & C_{44} & 2C_{24} & 2C_{46} & 2C_{26} \\ C_{55} & C_{44} & C_{33} & 2C_{35} & 2C_{35} & 2C_{45} \\ C_{56} & C_{24} & C_{34} & (C_{23}+C_{44}) & (C_{36}+C_{45}) & (C_{25}+C_{46}) \\ C_{15} & C_{46} & C_{35} & (C_{36}+C_{45}) & (C_{13}+C_{55}) & (C_{14}+C_{56}) \\ C_{16} & C_{26} & C_{45} & (C_{25}+C_{46}) & (C_{14}+C_{56}) & (C_{12}+C_{66}) \end{bmatrix} \begin{bmatrix} u^2 \\ v^2 \\ w^2 \\ vw \\ wu \\ uv \end{bmatrix} \tag{1.19}$$

where C_{rs} are the elastic constants of the crystal.

$\therefore$ (1.16) becomes

$$\sigma_1 = \frac{I_d'}{I_o} = \frac{\epsilon^2 N F_T^2 kT}{V} \frac{|\vec{X}|^2}{|\vec{q}|^2} K[uvw]_{hkl} \tag{1.20}$$

The form of the elastic constant matrix given above corresponds to the theory of elasticity which was given by Voigt (1910)[19] by treating crystalline medium as homogeneous to all scales and also by Cauchy and Born (1915)[20] by treating interatomic forces as central forces. Both these approaches led to the same conclusion that the stress and

strain tensors are symmetric, thus leading to 36 elastic constants which reduce down to 21 in the most general case by the symmetry requirement that $C_{rs} = C_{sr}$. A detailed account of the theory of elasticity has been given by Wooster (1938)[21], Love (1944)[22], Nye (1957)[23], Krishnan (1958)[24], Huntington (1958)[25] and Bhagavantam (1966)[26].

1.B.2 Second Order Diffuse Reflection

Laval has shown that 2nd order diffuse reflection (σ_2) from a pole of diffusion will be produced only by the combined action of the pairs of waves, the wave vectors $\vec{q}_\alpha$ and $\vec{q}_\beta$ of which add vectorially to $\pm\vec{Q}\vec{X}$ as shown in fig. 1.2 below.

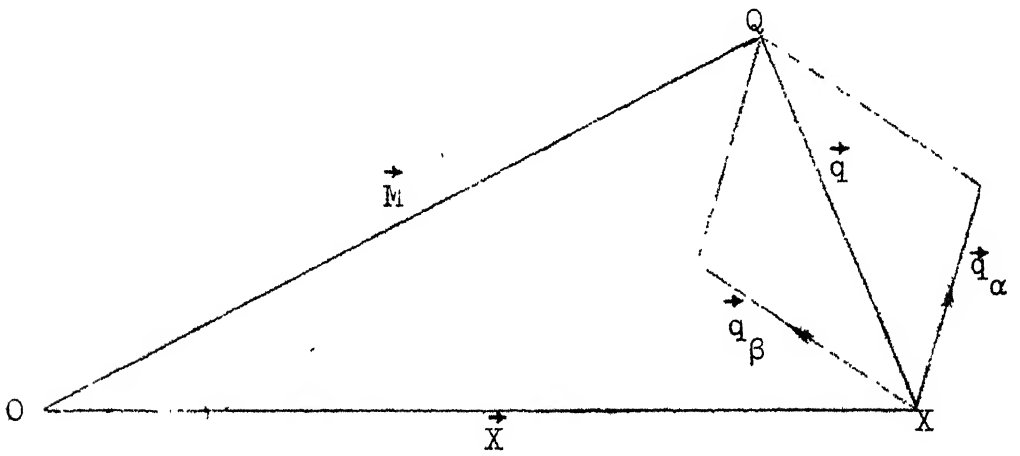

Fig. 1.2. Vector diagram for second order diffuse reflection.

Ramachandran and Wooster (1951)[15], making certain approximations in view of the fact that $\sigma_2 << \sigma_1$, have derived the following expression for σ_2.

$$\sigma_2 = \frac{\pi^3}{2} \frac{N(kT)^2}{V} F_T^2 \frac{|\vec{X}|^4}{|\vec{q}|} K'[uvw]_{hkl} \qquad (1.21)$$

where $K'[uvw]_{hkl} = \sum_{\alpha=1}^{3} \frac{\cos^4(\vec{X}\cdot\vec{A}_\alpha)}{\rho^2 V_\alpha^4}$

Thus the second order correction is more important at high temperatures and for higher order reflections.

1.B.3 Simplified Formula of Diffuse Reflection for Orthorhombic Case

In general a given measurement of diffuse intensity depends on several elastic constants, but by a proper choice of reflecting planes and wave normals, each measurement can be made to depend on only one or two elastic constants. Also expression for $K[uvw]_{hkl}$ becomes simpler for crystals of higher symmetry. For an orthorhombic crystal, according to Voigt's theory, there are 9 unique elastic constants and the matrix equation (1.19) takes the following form[11]

$$\begin{bmatrix} A_{11} \\ A_{22} \\ A_{33} \\ A_{23} \\ A_{13} \\ A_{12} \end{bmatrix} = \begin{bmatrix} C_{11} & C_{66} & C_{55} & 0 & 0 & 0 \\ C_{66} & C_{22} & C_{44} & 0 & 0 & 0 \\ C_{55} & C_{44} & C_{33} & 0 & 0 & 0 \\ 0 & 0 & 0 & (C_{23}+C_{44}) & 0 & 0 \\ 0 & 0 & 0 & 0 & (C_{13}+C_{55}) & 0 \\ 0 & 0 & 0 & 0 & 0 & (C_{12}+C_{66}) \end{bmatrix} \begin{bmatrix} u^2 \\ v^2 \\ w^2 \\ vw \\ wu \\ uv \end{bmatrix} \qquad (1.22)$$

With the help of these A_{ij}'s, the expressions for different $K[uvw]_{hkl}$ for simple directions of propagation of thermal waves have been derived and are given in Table 1.1. These relations have been used for evaluation of the elastic constants of AFB.

1.B.4 New Theory of Elasticity

Laval (1951a)[13] pointed out that the central force assumption of Born leads to atoms inside a crystalline medium being rigid impenetrable spheres. But a crystalline solid consists of rigid positive ions distributed in a periodic array in a continuous fluid of electrons. The forces acting on the whole mass of the crystal chiefly determine the elastic properties of the crystal. These forces are produced by the relative displacement of the ions as well as by the interaction of the ions with the surrounding deformed electronic medium. The former type of forces can be taken to be sensibly central but not the latter one. On account of these considerations Laval showed that the stress and strain tensors are not symmetric and would have 9 components each. This would give rise to 81 elastic constants which due to their symmetry property $C_{rs} = C_{sr}$ become 45 and the matrix equation (1.19) would take the following form

Table 1.1

Relation Between $K[uvw]_{hkl}$, C_{ij} (old theory) and C'_{ij} (new theory) for Orthorhombic System

Direction cosines u,v,w of thermal wave through node(hkl)	Expression for $K[uvw]_{hkl}$ According to Old theory	New theory
	a b Plane**	
$[100]_{h00}$	$1/C_{11}$	$1/C'_{11}$
$[100]_{0k0}$	$1/C_{66}$	$1/C'_{99}$
$[100]_{hk0}$	$L^2/C_{11}+M^2/C_{66}$	$L^2/C'_{11}+M^2/C'_{99}$
$[010]_{h00}$	$1/C_{66}$	$1/C'_{66}$
$[010]_{0k0}$	$1/C_{22}$	$1/C'_{22}$
$[010]_{hk0}$	$L^2/C_{66}+M^2/C_{22}$	$L^2/C'_{66}+M^2/C'_{22}$
$[1/\sqrt{2},1/\sqrt{2},0]_{h00}$	$2(C_{22}+C_{66})/P1$	$2(C'_{22}+C'_{99})/P1$
$[1/\sqrt{2},1/\sqrt{2},0]_{0k0}$	$2(C_{11}+C_{66})/P1$	$2(C'_{11}+C'_{66})/P1$

$$P1=[C_{11}(C_{22}+C_{66})+C_{22}C_{66}-2C_{12}C_{66}-C_{12}^2]$$

$$P1=[(C'_{11}+C'_{66})(C'_{22}+C'_{99})-(C'_{12}+C'_{69})^2]$$

...Contd.

Table 1.1 contd.

Direction cosines u,v,w of thermal wave through node(hkl)	Expression for $K[uvw]_{hkl}$ According to Old theory	New theory
	* * b c Plane	
$[010]_{0k0}$	$1/C_{22}$	$1/C'_{22}$
$[010]_{001}$	$1/C_{44}$	$1/C'_{77}$
$[010]_{0kl}$	$M^2/C_{22}+N^2/C_{44}$	$M^2/C'_{22}+N^2/C'_{77}$
$[001]_{0k0}$	$1/C_{44}$	$1/C'_{44}$
$[001]_{001}$	$1/C_{33}$	$1/C'_{33}$
$[001]_{0kl}$	$M^2/C_{44}+N^2/C_{33}$	$M^2/C'_{44}+N^2/C'_{33}$
$[0,1/\sqrt{2},1/\sqrt{2}]_{0k0}$	$2(C_{44}+C_{33})/P2$	$2(C'_{77}+C'_{33})/P'2$
$[0,1/\sqrt{2},1/\sqrt{2}]_{001}$	$2(C_{22}+C_{44})/P2$	$2(C'_{22}+C'_{44})/P'2$

$$P2=[C_{22}(C_{44}+C_{33})+C_{44}C_{33}-2C_{23}C_{44}-C_{23}^2]$$

$$P'2=[(C'_{22}+C'_{44})(C'_{77}+C'_{33})-(C'_{23}+C'_{47})^2]$$

...Contd.

Table 1.1 contd.

Direction cosines u,v,w of thermal wave through node(hkl)	Expression for $K[uvw]_{hkl}$ According to Old theory	New theory
	* * a c Plane	
$[100]_{h00}$	$1/C_{11}$	$1/C'_{11}$
$[100]_{001}$	$1/C_{55}$	$1/C'_{55}$
$[100]_{h01}$	$L^2/C_{11}+N^2/C_{55}$	$L^2/C'_{11}+N^2/C'_{55}$
$[001]_{h00}$	$1/C_{55}$	$1/C'_{88}$
$[001]_{001}$	$1/C_{33}$	$1/C'_{33}$
$[001]_{h01}$	$L^2/C_{55}+N^2/C_{33}$	$L^2/C'_{88}+N^2/C'_{33}$
$[1/\sqrt{2},0,1/\sqrt{2}]_{h00}$	$2(C_{33}+C_{55})/P3$	$2(C'_{33}+C'_{55})/P3$
$[1/\sqrt{2},0,1/\sqrt{2}]_{001}$	$2(C_{11}+C_{55})/P3$	$2(C'_{11}+C'_{88})/P3$

$$P3=[C_{11}(C_{33}+C_{55})+C_{33}C_{55}-2C_{13}C_{55}-C_{13}^2]$$

$$P3=[(C'_{11}+C'_{88})(C'_{55}+C'_{33})-(C'_{58}+C'_{13})^2]$$

$$\begin{bmatrix} A_{11} \\ A_{22} \\ A_{33} \\ A_{23} \\ A_{13} \\ A_{12} \end{bmatrix} = \begin{bmatrix} C'_{11} & C'_{66} & C'_{88} & 2C'_{86} & 2C'_{18} & 2C'_{16} \\ C'_{99} & C'_{22} & C'_{44} & 2C'_{24} & 2C'_{49} & 2C'_{29} \\ C'_{55} & C'_{77} & C'_{33} & 2C'_{37} & 2C'_{35} & 2C'_{75} \\ C'_{59} & C'_{27} & C'_{34} & (C'_{23}+C'_{47}) & (C'_{39}+C'_{45}) & (C'_{79}+C'_{25}) \\ C'_{15} & C'_{76} & C'_{38} & (C'_{78}+C'_{36}) & (C'_{58}+C'_{13}) & (C'_{17}+C'_{56}) \\ C'_{19} & C'_{26} & C'_{48} & (C'_{28}+C'_{46}) & (C'_{14}+C'_{89}) & (C'_{12}+C'_{69}) \end{bmatrix} \begin{bmatrix} u^2 \\ v^2 \\ w^2 \\ vw \\ wu \\ uv \end{bmatrix} \tag{1.23}$$

For orthorhombic system, there are only 15 non-zero unique elastic constants and the matrix equation (1.23) takes the form

$$\begin{bmatrix} A_{11} \\ A_{22} \\ A_{33} \\ A_{23} \\ A_{13} \\ A_{12} \end{bmatrix} = \begin{bmatrix} C'_{11} & C'_{66} & C'_{88} & 0 & 0 & 0 \\ C'_{99} & C'_{22} & C'_{44} & 0 & 0 & 0 \\ C'_{55} & C'_{77} & C'_{33} & 0 & 0 & 0 \\ 0 & 0 & 0 & (C'_{23}+C'_{47}) & 0 & 0 \\ 0 & 0 & 0 & 0 & (C'_{58}+C'_{13}) & 0 \\ 0 & 0 & 0 & 0 & 0 & (C'_{12}+C'_{69}) \end{bmatrix} \begin{bmatrix} u^2 \\ v^2 \\ w^2 \\ vw \\ wu \\ uv \end{bmatrix} \tag{1.24}$$

These relations have been used in interpreting the results of the present study in terms of the new theory of elasticity. A great amount of theoretical and experimental work on the new theory of elasticity has been done by Laval (1951,1957)[13], Viswanathan (1955)[27], Le-Corre (1953-1958)[28], Raman and Viswanathan (1955)[29], Joel and Wooster (1957-1960)[30] and Krishnan et al. (1958)[31], but unequivocal results to verify the new theory are not yet available.

2. EXPERIMENTAL PROCEDURE

2.A.B. Specimen Preparation

Crystals of AFB were grown from aqueous solution of the salt obtained from ICN K and K Labs, New York. The crystals generally form long needles of faces (100), (001) and (101) with end faces being a pair of (010) or two pairs of (011) faces. In some of the crystals (100) face is so broad as compared to (001) or (101) that they take thin plate like shapes. Suitable single crystals are not easy to obtain. After the solution becomes supersaturated, the growth of the crystals is very fast and one gets a bundle of small transparent crystals, most of which are twinned as has also been reported by the early study of Mukherjee[32]. Only twinfree, single domain crystals were selected for crystal structure as well as diffuse scattering study by careful examination of these crystals under polarizing microscope and by taking Laue photographs.

The dimensions of the crystals were determined by a travelling microscope. The density was measured by floatation method using a solution of tetrabromomethane (ρ = 2.964 g/cm^3) and carbontetrachloride (ρ = 1.595 g/cm^3). The measured and calculated densities are listed in table 2.1.

Table 2.1

Crystal Data on Ammonium Fluoberyllate

Chemical Formula	$(NH_4)_2BeF_4$
Crystal Class	Urthorhombic
Space Group	Pnma
Axial Parameters	a= 7.6367(3)A^o b= 5.9072(2)A^o c=10.4316(3)A^o
Number of Molecules per Unit Cell	4
Volume of the Unit Cell	470.585A^{o3}
Measured Density	1.686g/cm^3
Calculated Density	1.707g/cm^3
Linear Absorption Co-efficient(μ)for MoK_α	2.4cm^{-1}

2.A Crystal Structure Determination

Suitable single crystals of size 0.1 x 0.4 x 0.2 mm were chosen for structure determination. Preliminary studies of the crystals were done photographically. Rotation, oscillation and zero layer Weissenberg photographs were taken to identify the cell axes and angles. The crystals were found to belong to orthorhombic system. Precession photographs were also taken which showed clearly the orthorhombic symmetry with the following systematic absences,

Reflections hko absent when $h = 2n+1$

and okl absent when $k+\ell = 2n+1$

indicating the space group Pnma or $Pn2_1a$.

One of the crystals, aligned about b-axis, was transferred to General Electric XRD-6 diffractometer equipped with a quarter circle goniostat. Using a proportional counter and filtered CuK_α radiation ($\lambda_{\alpha_1} = 1.5410$ Å), the lattice constants a, b, c were accurately determined from high order axial reflections. A slow scan in 2θ of the above reflections was made and a mean 2θ corresponding to half the peak intensity on either side of the peak was taken as the 2θ for calculations of lattice parameters.

Once the lattice parameters were known, the χ, ϕ and 2θ settings of the goniostat were calculated using a computer program written for IBM 7044 computer. Reflections which

were found systematically absent in the precession photographs were again checked on the diffractometer, thus confirming the space group to be either Pnma or $Pn2_1a$. The first set of three dimensional intensity data were collected on this diffractometer using the stationary crystal stationary counter technique. From a random check in different regions of the reciprocal space, the maximum width of a reflection was found to be less than 1.5°. For each reflection the intensity of the peak and the background recorded at one degree off on either side of the peak were counted for 10 seconds. Six reflections 600, 004, 223, 341, 020 and 060 of good intensity and coverying the whole range of χ, ϕ, 2θ were chosen as standard reflections whose intensities were monitored every eight hours to check for any misalignment or irradiation effects in the crystal. Irradiation effects in the crystal were found to be negligible. These have also not been reported earlier by any other worker.

In order to keep the intensity of strong reflections (>2000 c.p.s.) in the linear range of the counter, additional nickel absorbers were used in front of the counter window. The filter factor for these absorbers was determined by measuring the intensity of some reflections which lie in the linear range of the counter, with and without the absorber. The ratio of the two gives the filter factor for that absorber. There were eleven reflections for which additional

absorbers were required. Beyond 2θ angle of 110°, two thirds of the reflections had intensity almost equal to the background, hence beyond this 2θ the intensity measurements were not done. The intensity data for 670 unique reflections were recorded out of which only 410 were such that they had intensity I greater than three times the standard deviation $\sigma(I)$, i.e. $I > 3\sigma(I)$. Only these were coded as 'observed' and rest as 'unobserved' reflections.

The integrated intensity of each reflection was calculated by subtracting the mean of background counts from the counts recorded with counter set at the 2θ. Lorentz and polarization corrections were applied to each reflection through a computer program written for IBM 7044. At $\chi = 90^{\circ}$ the intensity of 020, 040 and 060 reflections was noted as a function of ϕ with ϕ varying from 0° to 360°. The maximum variation was less than 5% hence absorption correction was not applied.

Three dimensional intensity data were again collected on Syntex $P2_1$ automatic diffractometer at Material Research Centre, McMaster University, Canada. Using a graphite crystal monochromatic MoK_{α} radiation ($\lambda_{\alpha} = 0.71069$ Å), integrated intensities for 1267 reflections upto $2\theta = 55^{\circ}$ in two octants hkl and $hk\bar{l}$ were measured from a crystal ground into the shape of a cylinder of radius 0.075 mm and length (along b) 0.30 mm. For different reflections, the scan rate

depended upon the peak intensity. Two reference reflections $2\bar{2}1$ and 301 were monitored throughout the data collection (at intervals of 14 reflections). The random fluctuation in the intensity of these reflections was less than 10%. Background intensity was measured on either side of and one degree removed from each peak. The measured intensities were corrected for Lorentz and polarization corrections. Since linear absorption co-efficient μ (calculated theoretically) for AFB is very low (=2.4 cm^{-1}) and crystal used is of small size, it is not considered necessary to apply absorption correction. Averaging equivalent reflections in two octants gave 673 unique reflections out of which 411 were coded as 'observed' reflections ($I > 3\sigma(I)$) based on counting statistics. The lattice parameters calculated from high order axial reflections are given in Table 2.1.

2.B Thermal Diffuse Scattering

Two types of experimental arrangements, one based on the photographic method and the other on the diffractometer with ionization counter are used for recording the diffuse X-ray reflections. For a detailed study of these reflections from a single crystal, the diffractometer is more suitable as the intensity measurement is more accurate and the crystal specimen can be conveniently manipulated to allow a continuous survey of whole hemisphere of the reciprocal space with smooth

and fine controllable motions. A GE-XRD-6 diffractometer equipped with a goniostat as mentioned in the earlier section has been used here also. The X-ray beam used is monochromatic MoK_α obtained from a curved quartz crystal monochromator. The absolute value of the incident beam intensity (I_o) is obtained from Compton scattering of diamond as an intermediate standard, details of which are given in Appendix I.

2.B.1 Method of Monochromatization

Balanced Filters

In the present case, the monochromatization was first tried with balanced filter of Zr (Z = 40) and Y (Z = 39). Zr was available in the form of a thin foil but not Y, hence high purity Y_2O_3 powder pressed into a thin pellet was used. Several trials were made to match the two intensities at all points except the peak reflection, but none of them was very satisfactory. Sometimes the match was perfect on lower angle side but not on the higher angle side and vice-versa. In few trials the match was perfect but only in small regions of 2θ. This was due to the fact that very thin (∿0.1 mm) pellets are needed and it is very difficult to ensure uniformity of thickness. Also considering the fact that there is a small portion of the white radiation which is transmitted more by one filter than by the other, this method was abandoned in favour of a crystal monochromator.

Crystal Monochromator

For the study of diffuse reflections, curved crystal monochromator has been used by many earlier workers [33]. The curved quartz crystal monochromator used here has been accommodated between the goniostat and the X-ray tube by shifting the tube mount and turning it about its axis from its normal geometry. The reflection $(10\bar{1}1)$ from quartz single crystal of dimensions 4 x 1.3 x 0.03 cm has been used as the monochromatic beam. The quartz crystal was pressed in the brass die for MoK_α radiation. The die was placed on a turn table with fine controllable angular motion so as to properly orient it with respect to the incident beam to obtain $(10\bar{1}1)$ reflection of quartz which occurs at $2\theta = 12.18^\circ$. The turn table was put on a mount with two X-Y controllable motions and with the help of these motions, the distance and position of the crystal were adjusted so as to focus the monochromatic beam at the crystal and at the same time make it coincident with the zero of the 2θ arm. The die was supplied by Ch. Beaudouin, Paris; the other parts of the monochromator assembly were designed and fabricated for this work.

The reflected beam from the quartz crystal was cut off by a knife edge slit S_1 of width 0.6 mm and height 2 mm, set at a distance of 35 mm from the monochromator. In order

to collimate the beam another slit S_2 of width 0.5 mm and height 2 mm was used at a distance of 75 mm from the first slit. In this way monochromatic MoK_α is allowed to impinge on the experimental crystal. The vertical and horizontal divergence of the beam were 32' and 3.52' respectively. The beam diffracted by the crystal is allowed to pass through a receiving slit S_3 of width 3 mm and height 3 mm placed in front of the detector window and at a distance of 144.5 mm from the experimental crystal. The detector unit was well shielded with lead sheets to avoid pick up of any stray counts. A sketch of the experimental arrangement is shown in fig. 2.1.

2.B.2 Intensity of Diffuse Reflection through a Crystal Plate

If crystals are taken in plate form and reflections at a glancing angle θ are considered through the crystal plate of thickness t from a set of planes nearly normal to its surface, the distance travelled in the crystal by the beam is the same and is equal to $t \sec\theta$ and hence the total volume of the crystal plate irradiated by the incident beam of cross-section S_o is $S_o t \sec\theta$ (fig. 2.2)

$$\therefore \quad NV = S_o t \sec\theta$$

X : X-ray target
L : Lead shields
T : 2θ arm
M : Monochromator assembly
C' : Quartz crystal
S, S_1 : Knife edge slits
ω : ω Circle where single crystal orienter is put
S_2 : Collimating slit
C : Specimen crystal on the goniometer head
S_3 : Receiving slit
P : Proportional counter

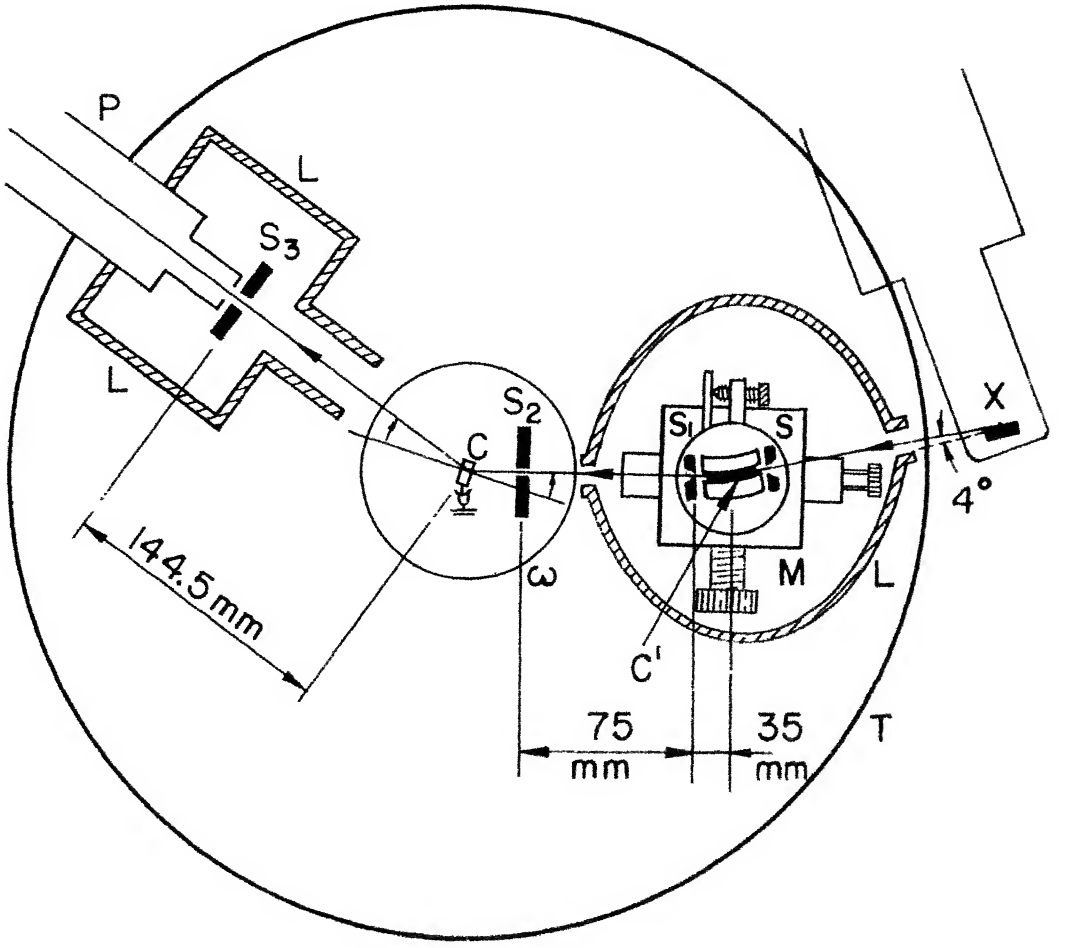

Fig.2.1 Schematic arrangement of the experimental set up for studying diffuse X-ray scattering.

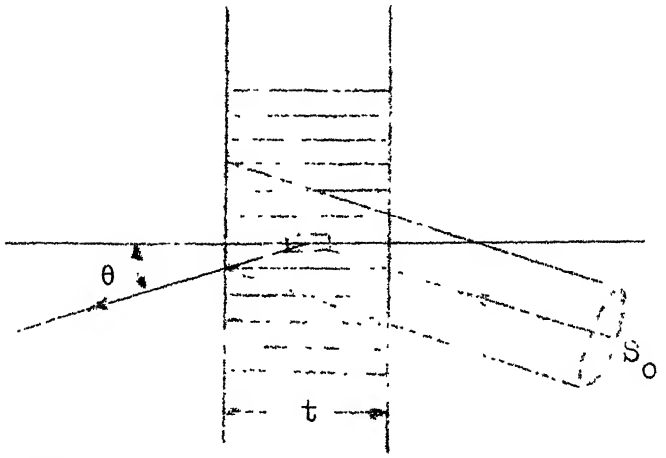

Fig. 2.2. Reflection through a crystal plate.

where N is the number of unit cells contributing to diffuse reflection and V is the volume of the unit cell. If the mosaicity of the crystal plate is also taken into account and a counter collimator slit subtending a solid angle Ω at the crystal is used for measuring the reflection, equation (1.20) becomes (James, 1967)[9]

$$\sigma_1 = \frac{I_d'}{I_o} = \frac{\varepsilon^2 kT\Omega F_T^2}{V^2} \frac{|\vec{X}|^2}{|\vec{q}|^2} K[uvw]_{hkl} e^{-\mu t \sec\theta} s_o t \sec\theta \qquad (2.1)$$

where μ is the linear absorption co-efficient of the crystal. Putting

$$\frac{I_d' \; e^{\mu t \sec\theta}}{s_o t \sec\theta} = I_d , \qquad (2.2)$$

equation (2.1) becomes

$$\sigma_1' = \frac{I_d}{I_o} = \frac{\varepsilon^2 kT\Omega}{V^2} F_T^2 \frac{|\vec{X}|^2}{|\vec{q}|^2} K[uvw]_{hkl} \qquad (2.3)$$

where I_d/I_o is the ratio of the intensity of I order diffuse

reflection (after applying absorption correction) per unit volume of the crystal to the intensity of the incident beam.

To determine the volume of the crystal immersed in the X-ray beam, the area of cross-section S_o of the beam has been measured photographically. Several photographs perpendicular to the direction of the beam were taken by placing the film at the axis of the diffractometer where the experimental crystal is placed. These photographs were magnified through an accurately known magnification factor and the cross-section measured with the help of a travelling microscope. The mean value of the width of the beam thus determined is 0.049 cm. Since the height of the crystal plates used was less than the height of the beam, the former was used to calculate the effective cross-section of the beam for calculating the immersed volume of the crystal. The height and the thickness of the plates were measured by travelling microscope. Hence knowing angle θ for each reflection, the immersed volume of the crystal can be calculated. This volume at Bragg angle for all relps. which have been used to calculate the elastic constants is given in table A of Appendix II.

For each relp., the observations of diffuse reflections have been made on either side of the corresponding Bragg reflection by mis-setting the crystal from the Bragg position. The angles of mis-set have been kept small to

ensure that the condition $\vec{q} \rightarrow 0$ is satisfied. For each observation time has been measured for 10,000 counts to obtain a counting accuracy of 1% in the intensity measurement. These measurements are given in Appendix II.

2.B.3 Correction Factors

Apart from absorption, several other correction factors to the measured intensity of diffuse reflection arise because of the experimental conditions employed. These corrections must be applied before using the observed intensities for the calculation of elastic constants. These corrections are discussed in the following.

Divergence Corrections

The finite size of the slits between the crystal and the X-ray tube and also between the crystal and the detector permits X-rays having a certain divergence to enter the detector and be counted together. The experimental observation does not, therefore, correspond to the intensity of diffuse reflection from a point in reciprocal space, but it corresponds to the effect integrated over a certain volume of reciprocal space. The divergence may be divided into three components denoted respectively by i, θ and χ divergence. The i divergence is the maximum angle between the rays falling on the crystal when they are projected on a

horizontal plane. The θ and χ divergences are the maximum angles between the reflected rays projected on a horizontal and vertical plane respectively passing through the crystal and the detector. The magnitude of i, θ, χ divergences are approximately 4', 0.8°, 4° respectively in our set up.

In order to apply i divergence correction, the detector and χ positions are kept fixed. The intensity of the Bragg reflection B(i) is measured as a function of i in the vicinity of the Bragg position θ_B (Fig. 2.3(a)). Then the intensity of diffuse reflection D(i) is measured around the point say A, having departure δ from the Bragg setting and at which diffuse reflection is being measured, as a function of i at an interval of $\delta i \sim 0.02^{\circ}$ to obtain the curve AB in fig. 2.3(b). D(i) varies slowly with i but variation of B(i) is very fast in the neighbourhood of the Bragg setting θ_B. The contribution of Bragg reflection corresponding to the point A is represented by CD. The correction term $Z(i_o)$ for the i divergence is then given by[11]

$$Z(i_o) = \int_{-\Delta/2}^{\Delta/2} G(\delta)\, B(\delta)\, d\delta \Big/ \int_{-\Delta/2}^{\Delta/2} B(\delta)\, d\delta$$

where

$$G(\delta) = \left(\tfrac{1}{2}\left(D(i_o+\delta) + D(i_o-\delta)\right) - D(i_o)\right)/D(i_o)$$

and it takes care of the asymmetry of the Bragg reflection about its centre.

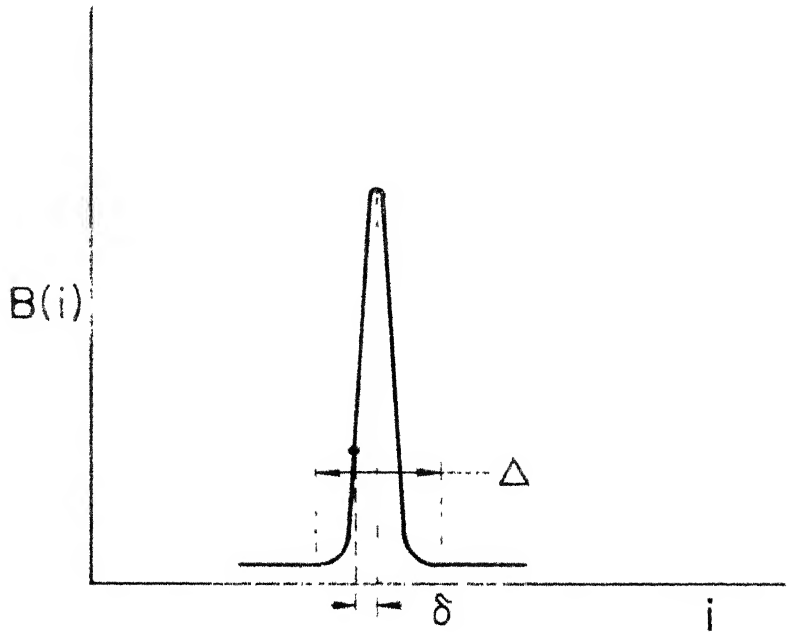

Fig.2.3(a) The curve corresponding to the variation of intensity across a Bragg reflection

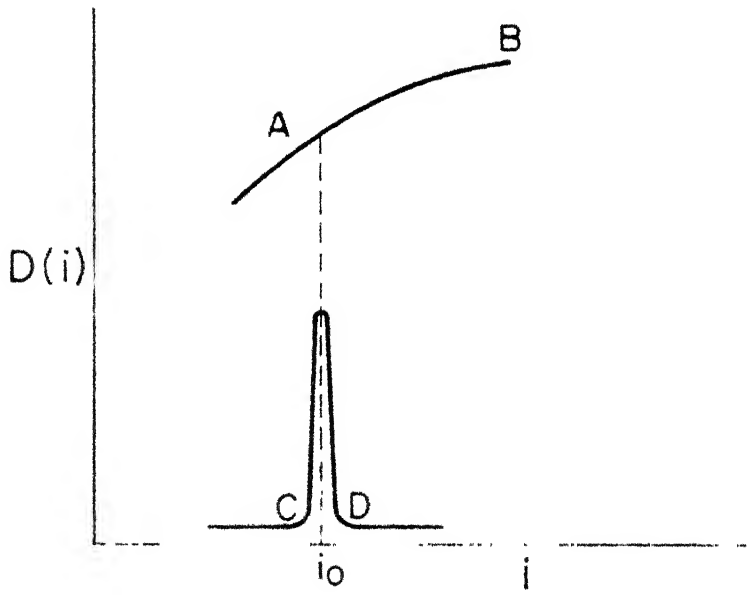

Fig.2.3(b) The curve AB corresponding to the variation of intensity, D across the diffuse reflection. The curve CD is a copy, reduced to an appropriate scale, of the Bragg reflection curve.

The evaluation of this correction factor has been done graphically. The observed diffuse intensity at any given i_o is multiplied by $(1 + Z(i_o))$ to get the corrected value.

The analysis of θ and χ divergences is carried out in a similar manner. Finally all the three correction terms are added together to give a final correction factor.

Skew Correction

During a survey of diffuse reflections, the angles of incidence (i) and reflection $(\phi/2)$ are not equal. This gives rise to an important change in the intensity of diffuse reflection I_d which is given by

$$I_d = I_d' \tfrac{1}{2} \left(1 + \frac{\sin i}{\sin(\phi - i)}\right);$$

I_d' is the observed diffuse intensity and $\tfrac{1}{2}\left(1 + \frac{\sin i}{\sin(\phi - i)}\right)$ is called the skew correction factor.

Polarization Correction

X-rays reflected from a monochromatizing crystal are partially polarized. If p_1 and p_2 are the amplitude components normal and parallel respectively to the plane of incidence, then the polarization factor is given by

$$P = (p_1^2 + p_2^2 \cos^2 \phi)$$

If α represents the angle of reflection from the monochromator crystal, then for equatorial reflections[34]

$$P = \frac{1 + \cos^2 2\alpha \cos^2 \phi}{1 + \cos^2 2\alpha}$$

Absorption Correction

For the geometry of reflection described in sec. 2.B.2, the absorption correction is $e^{-\mu t \sec\theta}$. This was so for relps. 004, 400, 020 and 040. For relps. 031 and 301, the reflecting planes were not normal to the plate surface and so the above geometry of reflection is not applicable. In these two cases the absorption correction was applied by graphical method due to Albrecht.[35]

The corrected intensity per unit volume of the crystal after applying the above mentioned corrections to the observed intensity I_d' is denoted by I_d''.

General Scattering Correction

The general scattering always accompanies Bragg and diffuse reflections and includes Compton scattering, fluorescent radiation and scattering due to optical waves. The intensity of the general scattering I_B varies very little over the region of the reciprocal space covering the reciprocal lattice point around which the observation is made. Its value is equal to the intercept on the I_d'' axis of the graph between

I_d'' against λ^2 $(= 1/q^2)$. This value when subtracted from I_d'' gives the value of I_d (I+II order) for each observation.

2.B.4 Evaluation of the Elastic Constants

Apart from I_d and I_o, the evaluation of the thermal wave vector $\vec{q}$ is also required for the evaluation of elastic constants.

Evaluation of the Wave Vector $\vec{q}$

For a particular direction of propagation of the thermal wave, the value of the wave vector $\vec{q}$ (QP_1, QP_2, QQ_1, etc. in fig. 2.4) and the corresponding angle for the diffuse reflection has been calculated trigonometrically by considering the geometrical position of the circle of reflection (intersection of sphere of reflection with the plane of diffraction) in the reciprocal lattice net for a particular setting of the crystal. The position of the circle is completely determined by the knowledge of the correct orientation of the crystal with respect to the incident beam.

From equation (2.3) it is evident that the graph between I_d''/I_o vs $\lambda^2(=1/q^2)$ for a particular lattice point and a direction of propagation of thermal wave would be a straight line having an intercept on the I_d''/I_o axis due to contribution of general scattering. This intercept I_B/I_o is subtracted from I_d''/I_o to obtain I_d/I_o which is the ratio

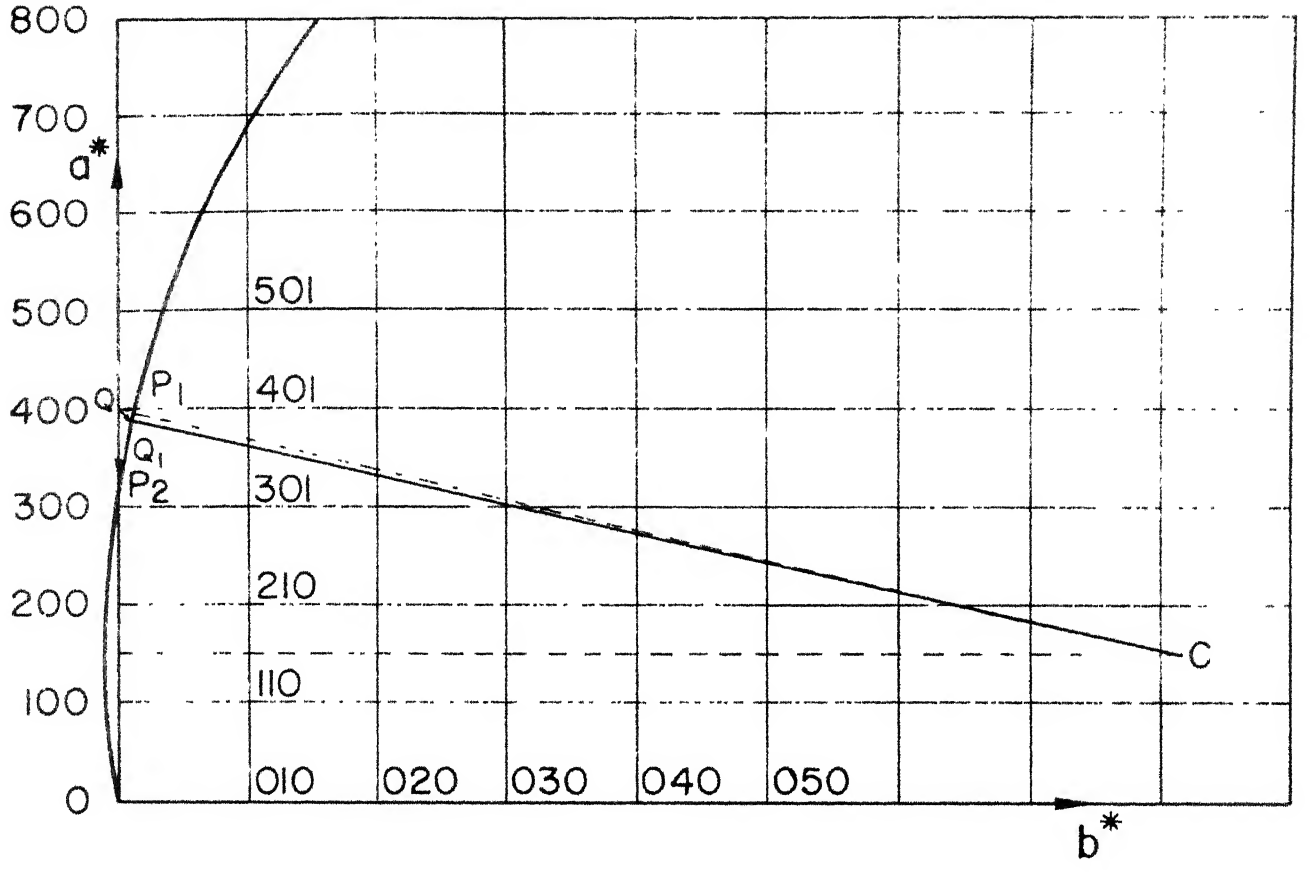

Fig.2.4 A section of the reciprocal lattice plane a^* b^* of Ammonium Fluoberyllate. The figure shows the formatiom of (400) diffuse reflection. QP_1, QP_2 and QQ_1 are the wave vectors of thermal wave propagating along $[010]_{400}$, $[\bar{1}00]_{400}$ and $[-1/\sqrt{2}, 1/\sqrt{2}, 0]_{400}$ directions respectively.

of diffuse intensity (I+II order) per unit volume to the incident intensity to which all the corrections have been applied. This when plotted against λ^2 passes through the origin. From the slope of this line the corresponding $K[uvw]_{hkl}$ can be evaluated. These graphs of I_d/I_o vs λ^2 have been drawn for all the cases and are shown in Appendix II.

Second Order Diffuse Reflection Correction

The main contribution to diffuse intensity is due to first order reflection σ_1' only. The ratio of second to first order diffuse reflection intensity as given by Ramachandran and Wooster (1951)[15], Prasad and Wooster (1955)[16] and Amoros and Amoros (1968)[37] is

$$\frac{\sigma_2'}{\sigma_1'} = \frac{\pi^3}{2} kT |\vec{x}|^2 |\vec{q}| K[uvw]_{hkl}$$

To apply second order diffuse reflection correction, $K[uvw]_{hkl}$ is first obtained from the intensity of diffuse reflection I_d (I+II order). This value of K is then used to calculate σ_2' from above equation, where σ_1' is taken equal to I_d. σ_2' thus obtained is subtracted from I_d to obtain σ_1' alone, which is then used to calculate the corrected value of elastic constants. Since these corrections are small in the crystal under study, further iterations for this correction were not found necessary.

2.B.5 Choice of Planes for Determination of the Elastic Constants

The choice of planes for studying diffuse reflection is made such that the observed diffuse flux is as large as possible. The intensity of diffuse reflection in the first order depends directly on $X^2F_T^2$ (eqn. 2.3), i.e. F_T^2/d^2 where d is the spacing corresponding to a plane hkl. Therefore only those planes for which this quantity is large, are suitable for the determination of elastic constants. Smaller 'd' will make the above quantity larger. But the theory on which the above method is based assumes that the amplitude of atomic vibrations is small as compared to the lattice spacing. The mean amplitude of atomic vibrations is of the order of 0.2 Å (Lonsdale, 1948)[38] for most crystals. Therefore planes having spacing larger than 1 Å may be assumed to fulfil the above requirement i.e. in terms of angles, planes for which diffraction angles are larger than 42° (for MoK_α) will not be suitable. Another point to be considered is the polarization factor. For crystal reflected monochromatic beam, the polarization factor for reflections in equatorial plane is given by[34]

$$P = \frac{1 + \cos^2 2\alpha \cos^2 \phi}{1 + \cos^2 2\alpha}$$

where the symbols have the same meaning as explained in sec. 2.B.3. When quartz $(10\bar{1}1)$ plane is used for monochromatization,

then for diffraction angle of 30°, the value of P is 0.8. For higher angles the intensity of diffuse reflection will be very much reduced due to this factor. Hence suitable planes which have diffraction angles larger than 30° (and less than 42°) can be used only if the value of their structure factor is quite high. Also for planes with large value of X (i.e. higher Bragg angle) intensity of second order diffuse reflection will be larger and an exact correction on this account would also be necessary. For planes having low diffraction angles (say smaller than 10°) the skew correction would be much different from unity and changes rapidly with angles, therefore a slight mis-setting of the crystal may produce large errors.

Keeping the above factors in mind, the choice of planes has been made for determining all the nine elastic constants of AFB. Indices of these planes along with their structure factors are given in table 2.2.

Table 2.2

Data corresponding to the Planes used for studying Diffuse X-ray Reflections

Indices	d in A^{o}	Diffraction Angle in deg.	Structure Facture(F_T)
Planes Studied With 100 Axis Vertical			
040	1.477	27.78	55.43
004	2.608	15.63	72.94
013	2.997	13.62	42.13
Planes Studied With 010 Axis Vertical			
004	2.608	15.63	72.94
301	2.473	16.52	70.11
400	1.909	21.41	14.53
Planes Studied With 001 Axis Vertical			
020	2.954	13.79	53.68
040	1.477	27.78	55.43

3. DETERMINATION AND DISCUSSION OF THE CRYSTAL STRUCTURE

3.1 Crystal Structure Determination

As mentioned in sec. 2.A the systematic absences in the intensity data collected photographically as well as on diffractometer indicate the space group to be Pnma or $Pn2_1a$. From the consideration of ionic sizes of SO_4^{--} and BeF_4^{--}, one can expect the BeF_4 group to have about the same size and shape as the SO_4 group[39]. The crystals of $(NH_4)_2BeF_4$ are also expected to be isomorphous[40] with $(NH_4)_2SO_4$ which belong to space group Pnma at room temperature. Hence the same space group (Pnma) was assumed for $(NH_4)_2BeF_4$. This was later confirmed by statistical tests on normalized structure factors using the programme NORMSF[41] and by satisfactory refinement of the crystal structure.

An overall isotropic temperature factor of 2.374 $Å^2$ and scale factor of 0.26 were obtained from a least squares fitted Wilson[42] plot. The trial parameters for N, Be and F were taken to be same as for N, S, O in $(NH_4)_2SO_4$ from Singh (1962)[40]. A fourier synthesis using these parameters showed clearly the well defined peaks of the above atoms.

The refinement of the structure was performed on the CDC 6400 computer at McMaster University Computer Centre using locally written full matrix least squares programme CUDLS[42]. None of the reflections seems to be affected by extinction and hence extinction correction was not applied. The atomic scattering factors for N, Be, F corrected for anomalous dispersion were taken from international tables[43] for refinement in the initial stages. These were also computed from more accurate numerical Hartree-Fock wave functions[44] and used in the later course of refinement.

The least squares refinement with isotropic temperature factor converged at R = 0.141. At this stage the anisotropic temperature factors subject to restrictions imposed by symmetry[45] were introduced. After each refinement cycle the geometry of the structure was checked for its stereochemistry. The refinement was stopped when the shift in each parameter was less than a quarter of the corresponding standard deviation. R at this stage was 0.064. Y projection of the unit cell without H positions is shown in fig. 3.1(a). A three dimensional difference fourier synthesis calculated with the final parameters of N, Be, F showed small peaks at the expected H positions. If the correct space group were $Pn2_1a$, instead of Pnma, one would expect an unusual elongation of the hydrogens along b axis in the above difference map, but no such elongation was

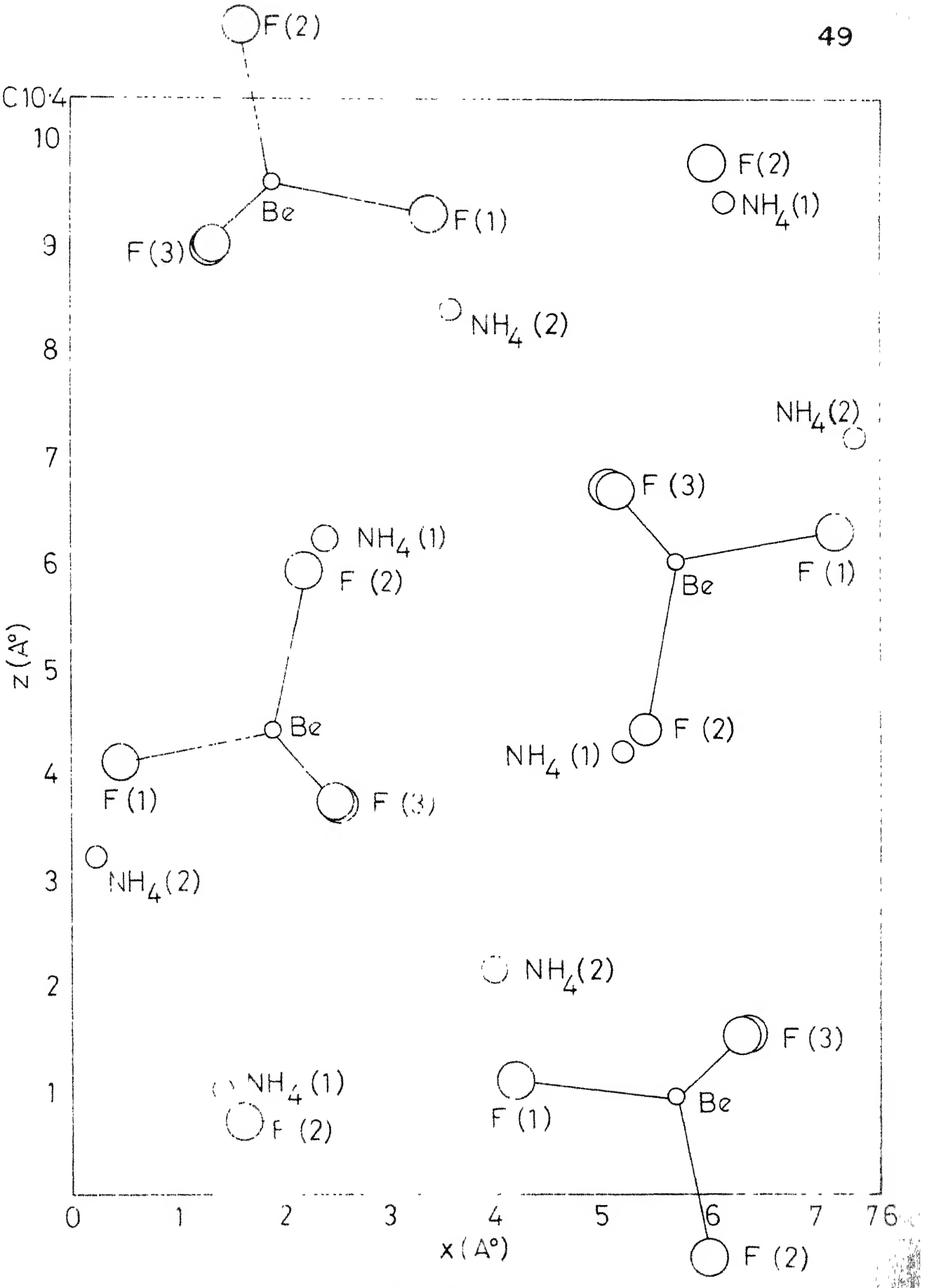

Fig.3.1(a) An XZ projection of a unit cell of $(NH_4)_2BeF_4$

observed thus further asserting the correctness of the space group Pnma. The H positions were assigned the anisotropic temperature factors of the atoms to which they are bound. The refinement of the structure with H-positions also included was done at IIT Kanpur on IBM 7044 computer using the least squares refinement programme ORFLS[46]. After three cycles of refinement a final R = 0.049 and weighted R = 0.044 were obtained. The weight ω given to a reflection was equal to $1/\sigma^2$ where σ is its standard deviation. At this stage the shift in each parameter was less than the corresponding standard deviation, the maximum and the average shift being 0.17σ and 0.02σ respectively. Y-projection of the unit cell with H positions included is shown in fig. 3.1(b).

The final atomic parameters and their standard deviations are listed in tables 3.1(a) and 3.1(b) respectively. The observed and calculated structure factors are listed in table 3.2.

3.2 Discussion of the Crystal Structure

3.2.1 General Structural Features

Symmetry operations of the space group Pnma are shown in fig. 3.2. The multiplicity of the general position in this space group is eight and there are four formula units per unit cell, both the nitrogen atoms, the beryllium atom,

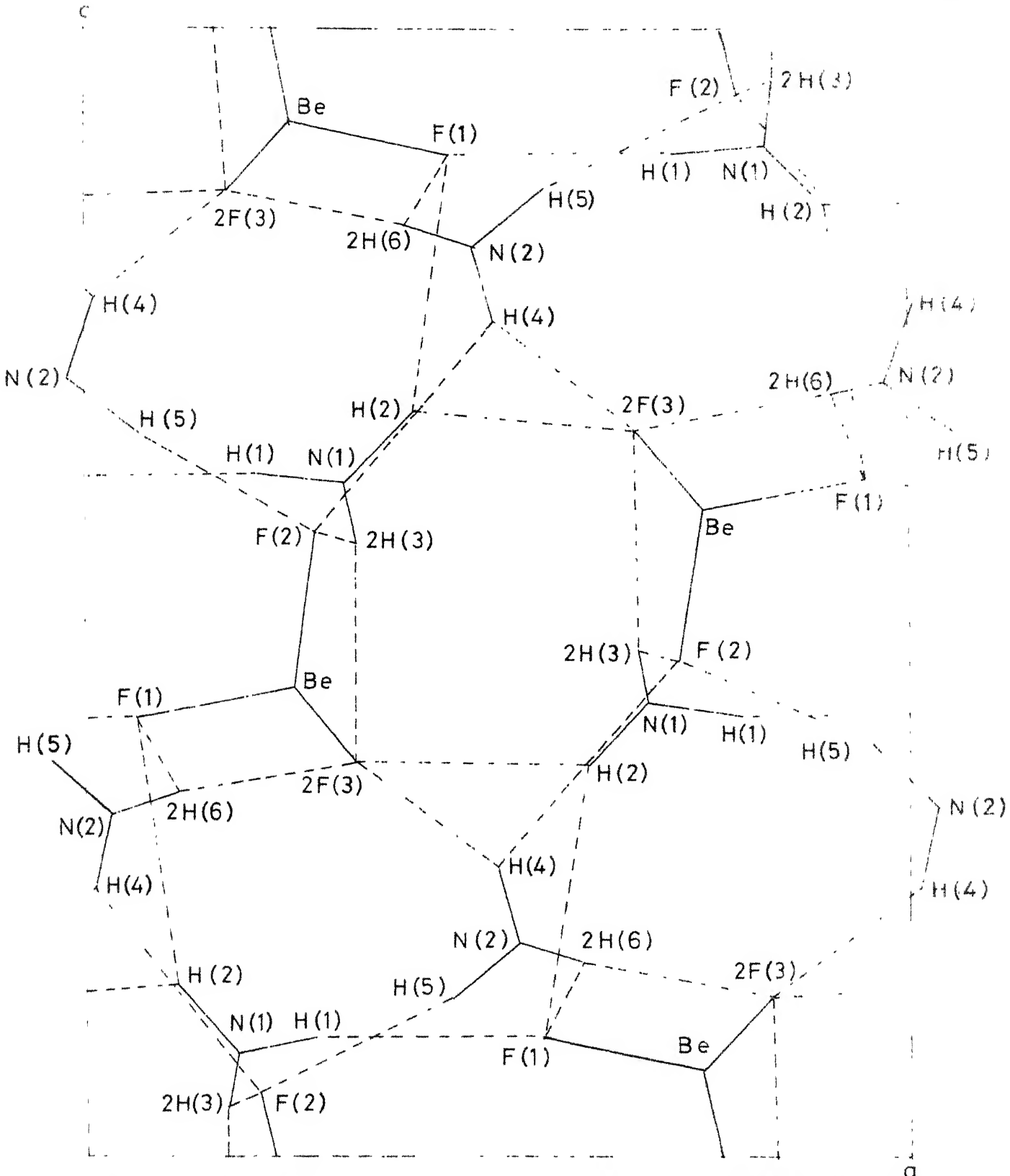

Fig.3.1(b) An XZ projection of a unit cell of $(NH_4)_2BeF_4$. Broken lines indicate hydrogen bonds

Table 3.1(a)

Positional parameters for $(NH_4)_2BeF_4$ with standard deviations in parentheses

Atom	X/a	Y/b	Z/c
N(1)	0.1804(6)	0.25	0.0968(4)
N(2)	0.4687(6)	0.25	0.8059(4)
Be	0.2466(7)	0.25	0.4180(5)
F(1)	0.0502(4)	0.25	0.3933(3)
F(2)	0.2856(4)	0.25	0.5620(3)
F(3)	0.3278(3)	0.0365(3)	0.3588(2)
H(1)	0.288(7)	0.25	0.108(4)
H(2)	0.109(7)	0.25	0.156(5)
H(3)	0.167(4)	0.115(5)	0.048(3)
H(4)	0.491(7)	0.25	0.739(5)
H(5)	0.547(7)	0.25	0.856(5)
H(6)	0.392(4)	0.115(5)	0.823(3)

Table 3.1(b)

Anisotropic temperature factors $x10^2$ with standard deviations in parentheses

Atom	B_{11}	B_{22}	B_{33}	B_{12}	B_{13}	B_{23}
N(1)	0.82(7)	1.74(12)	0.78(4)	0.0	0.05(5)	0.0
N(2)	1.14(7)	1.97(13)	0.44(3)	0.0	0.02(5)	0.0
Be	0.60(8)	1.55(16)	0.50(5)	0.0	0.03(4)	0.0
F(1)	0.83(5)	3.81(13)	1.52(5)	0.0	-0.24(4)	0.0
F(2)	2.10(7)	3.79(12)	0.49(2)	0.0	-0.13(3)	0.0
F(3)	1.69(4)	2.11(6)	1.21(2)	0.21(5)	0.24(3)	-0.62(3)

Table 3.2

Observed and Calculated Structure Factors for $(NH_4)_2BeF_4$

(* indicates the unobserved reflection)

h	k	l	F^o	F^c	h	k	l	F^o	F^c
0	0	2	10.05	10.00	1	0	7	9.55	9.57
0	0	4	73.63	72.94	1	0	8	8.38	8.39
0	0	6	11.93	11.32	1	0	9	3.29	4.25
0	0	8	6.14	6.81	1	0	10	5.02	6.08
0	0	10	1.11	0.80*	1	0	11	5.20	5.91
0	1	1	13.46	12.37	1	0	12	2.28	0.90
0	1	3	42.49	42.13	1	0	13	3.27	3.96
0	1	5	22.10	20.38	1	1	1	26.82	24.90
0	1	7	27.33	26.91	1	1	2	1.72	3.69*
0	1	9	2.21	3.22	1	1	3	5.96	5.93
0	1	11	2.65	2.63	1	1	4	27.10	27.42
0	1	13	6.74	6.30	1	1	5	8.01	7.89
0	2	0	54.06	53.68	1	1	6	10.03	9.84
0	2	2	24.05	22.40	1	1	7	7.42	7.53
0	2	4	4.66	3.68	1	1	8	1.32	1.88*
0	2	6	31.70	31.62	1	1	9	10.90	10.67
0	2	8	20.63	20.92	1	1	10	2.45	2.12*
0	2	10	10.25	10.53	1	1	11	3.59	3.53
0	2	12	2.68	2.64	1	1	12	4.07	3.29
0	3	1	16.32	15.35	1	1	13	4.33	3.91
0	3	3	12.94	12.79	1	2	1	25.42	25.45
0	3	5	5.64	4.83	1	2	2	50.02	50.69
0	3	7	21.03	20.75	1	2	3	33.93	32.91
0	3	9	4.03	5.01	1	2	4	9.08	8.71
0	3	11	3.55	3.47	1	2	5	1.82	0.74*
0	4	0	55.48	55.43	1	2	6	8.84	8.93
0	4	2	5.98	5.68	1	2	7	5.43	5.21
0	4	4	24.06	23.20	1	2	8	6.54	6.84
0	4	6	9.93	10.46	1	2	9	3.18	3.64
0	4	8	1.89	2.09	1	2	10	1.47	1.07*
0	4	10	3.52	3.34	1	2	11	1.58	0.75*
0	5	1	13.47	13.27	1	2	12	4.46	4.76
0	5	3	16.13	15.84	1	2	13	1.01	2.93*
0	5	5	11.98	13.08	1	3	1	2.25	2.12
0	5	7	9.73	9.26	1	3	2	13.99	13.42
0	5	9	3.79	3.51	1	3	3	23.58	23.01
0	6	0	15.48	15.38	1	3	4	9.46	9.41
0	6	2	0.25	1.64*	1	3	5	4.38	3.67
0	6	4	3.28	2.75	1	3	6	10.81	10.04
0	6	6	4.65	4.01	1	3	7	14.61	15.05
0	6	8	6.02	6.17	1	3	8	3.74	3.53
0	7	1	4.23	4.40	1	3	9	4.95	4.73
0	7	3	3.17	3.05*	1	3	10	2.43	1.96*
0	7	5	5.39	5.03	1	3	12	3.48	3.87
1	0	1	1.88	1.79	1	4	1	0.61	0.58*
1	0	2	28.10	26.95	1	4	2	6.93	6.29
1	0	3	9.55	11.19	1	4	3	4.64	3.80
1	0	4	44.86	45.29	1	4	4	8.11	8.14
1	0	5	9.89	9.99	1	4	5	5.56	5.47
1	0	6	26.43	25.98	1	4	6	8.66	8.87

....Contd.

Table 3.2 contd.

h	k	l	F^o	F^c	h	k	l	F^o	F^c
1	4	7	2.99	3.79	2	2	6	20.45	20.60
1	4	8	2.28	1.60*	2	2	7	5.89	5.67
1	4	9	1.01	0.64*	2	2	8	9.31	9.79
1	4	10	3.26	2.92	2	2	9	1.72	1.28*
1	4	11	2.46	2.57	2	2	10	1.88	2.61*
1	5	1	12.91	12.65	2	2	11	0.59	0.35*
1	5	2	6.10	6.52	2	2	12	4.32	4.38
1	5	3	6.86	7.23	2	3	0	24.69	24.96
1	5	4	7.85	8.58	2	3	1	4.12	2.93
1	5	5	3.44	3.33	2	3	2	1.80	3.05*
1	5	6	1.38	0.27*	2	3	3	13.69	13.91
1	5	7	2.57	2.61	2	3	4	21.74	21.71
1	5	9	4.39	4.76	2	3	5	1.54	1.24
1	5	10	0.16	0.39*	2	3	6	1.92	2.20
1	6	1	2.50	2.33*	2	3	7	1.96	1.60
1	6	2	3.55	3.83	2	3	8	8.12	8.59
1	6	3	3.65	3.96	2	3	9	7.56	7.75
1	6	4	3.89	3.88	2	3	11	4.05	4.57
1	6	5	1.73	1.23	2	3	12	1.68	1.55
1	6	6	2.00	2.30	2	4	0	10.68	10.34
1	6	8	0.95	0.68*	2	4	1	2.49	1.84
1	7	1	3.40	2.45	2	4	2	11.42	11.38
1	7	2	1.66	1.44*	2	4	3	3.96	3.83
1	7	3	5.78	5.84	2	4	4	7.29	7.67
1	7	4	1.76	1.48*	2	4	5	7.12	7.61
1	7	5	2.22	0.50*	2	4	6	7.73	7.94
2	0	0	36.31	36.07	2	4	7	1.52	0.14*
2	0	1	0.31	2.53*	2	4	8	0.84	0.12*
2	0	2	30.91	32.19	2	4	9	6.77	6.28
2	0	3	13.81	13.22	2	4	10	4.64	3.58
2	0	4	18.77	17.87	2	4	11	0.80	0.20*
2	0	5	29.03	28.34	2	5	0	8.07	8.07
2	0	6	10.32	10.63	2	5	1	10.13	10.19
2	0	7	1.81	0.85*	2	5	2	3.60	4.17
2	0	8	3.28	3.28	2	5	3	1.74	0.47*
2	0	9	13.24	14.01	2	5	4	2.59	3.01
2	0	10	9.13	10.61	2	5	5	5.92	7.07
2	0	11	2.01	1.62	2	5	6	6.49	7.24
2	0	12	4.33	3.95	2	5	8	1.67	0.43*
2	0	13	1.39	1.51	2	5	9	2.20	2.47*
2	1	0	4.36	4.54	2	6	0	1.36	0.65*
2	1	1	15.74	16.36	2	6	1	5.49	5.16
2	1	2	10.05	10.35	2	6	2	5.07	5.48
2	1	3	21.75	21.03	2	6	3	5.87	6.22
2	1	4	12.55	12.31	2	6	4	0.80	0.20*
2	1	5	13.05	12.74	2	6	5	0.74	0.40*
2	1	6	10.36	10.40	2	6	6	5.15	4.83
2	1	7	2.79	1.84	2	6	7	3.69	3.00
2	1	8	8.45	7.92	2	6	8	2.85	1.78*
2	1	9	5.49	5.48	2	7	0	6.97	6.39
2	1	10	4.92	5.67	2	7	1	1.64	0.54*
2	1	11	4.23	4.49	2	7	2	1.28	0.45*
2	1	12	0.52	1.48*	2	7	3	1.44	0.54
2	1	13	4.47	3.69	2	7	4	6.43	5.89
2	2	0	19.19	19.49	3	0	1	70.37	70.11
2	2	1	46.74	45.97	3	0	2	27.93	28.07
2	2	2	30.15	29.90	3	0	3	42.22	41.30
2	2	3	34.57	34.14	3	0	4	11.22	10.39
2	2	4	13.61	12.72	3	0	5	17.89	17.38
2	2	5	12.47	12.56	3	0	6	4.01	4.25

....Contd.

Table 3.2 contd.

h	k	l	F^o	F^c	h	k	l	F^o	F^c
3	0	7	2.75	2.36	3	6	1	4.26	4.56
3	0	8	4.44	4.20	3	6	2	2.62	3.55*
3	0	9	0.83	1.48*	3	6	3	3.23	2.30
3	0	10	1.82	0.52	3	6	4	1.43	1.21*
3	0	11	0.32	0.99*	3	6	5	1.06	0.76*
3	0	12	1.67	0.70*	3	6	7	3.67	3.44
3	1	1	6.78	6.27	3	7	1	2.00	1.37
3	1	2	16.69	17.14	3	7	2	4.42	3.72
3	1	3	5.69	4.88	4	0	0	13.62	14.53
3	1	4	6.23	6.51	4	0	1	31.84	31.34
3	1	5	8.88	9.41	4	0	2	5.17	5.41
3	1	6	19.44	18.88	4	0	3	0.81	0.56*
3	1	7	12.41	12.50	4	0	4	5.47	5.38
3	1	8	3.56	3.04	4	0	5	30.17	29.68
3	1	9	8.18	9.48	4	0	6	10.35	10.43
3	1	10	3.68	3.35	4	0	7	2.12	0.92
3	1	11	0.78	1.32*	4	0	8	11.90	12.08
3	1	12	1.66	1.23*	4	0	9	6.84	6.76
3	2	1	10.24	10.04	4	0	10	3.21	3.17
3	2	2	25.18	24.44	4	0	11	3.39	3.36
3	2	3	13.11	11.75	4	0	12	3.28	1.84*
3	2	4	3.26	3.96	4	1	0	15.92	14.85
3	2	5	1.30	1.82	4	1	1	9.40	9.06
3	2	6	2.32	1.80	4	1	2	10.73	10.16
3	2	7	20.62	20.56	4	1	3	3.76	3.07
3	2	8	0.86	0.60*	4	1	4	9.52	9.05
3	2	9	0.81	0.06*	4	1	5	1.70	0.79
3	2	10	1.14	0.49*	4	1	6	3.98	2.48
3	2	11	6.98	6.15	4	1	7	6.49	7.17
3	2	12	1.56	0.10*	4	1	8	0.59	1.15*
3	3	1	3.56	3.41	4	1	9	0.55	0.20*
3	3	2	11.20	11.05	4	1	10	7.49	7.46
3	3	3	5.81	5.17	4	1	11	0.15	0.40*
3	3	4	12.25	13.07	4	1	12	1.04	0.45*
3	3	5	4.14	3.26	4	2	0	30.72	31.33
3	3	6	6.23	6.37	4	2	1	11.33	11.18
3	3	7	9.49	9.50	4	2	2	3.24	2.51
3	3	8	8.55	9.71	4	2	3	16.97	17.07
3	3	9	4.74	5.00	4	2	4	9.36	8.80
3	3	10	2.05	1.74	4	2	5	3.75	3.51
3	3	11	1.86	0.95*	4	2	6	5.70	5.54
4	1	20	0.81	20.84	4	2	8	5.21	5.08
4	2	7	1.18	6.62	4	2	9	4.84	5.02
4	3	13	3.24	13.56	4	2	10	2.30	1.23*
4	4	1	1.34	2.61*	4	2	11	4.31	4.54
4	4	5	8.36	8.49	4	3	0	7.12	6.86
4	4	6	1.18	2.31*	4	3	1	1.36	0.35*
4	4	7	0.78	0.68*	4	3	2	11.05	11.02
4	4	8	1.87	1.71*	4	3	3	6.19	6.64
4	4	9	2.01	1.80	4	3	4	4.47	4.78
4	4	10	0.34	0.28*	4	3	5	4.19	3.83
4	5	1	3.14	3.19	4	3	6	7.78	8.37
4	5	2	12.64	13.35	4	3	7	5.23	5.87
4	5	3	0.24	0.21*	4	3	8	1.78	1.08*
4	5	4	1.86	0.74*	4	3	9	2.04	2.43
4	5	5	2.60	2.41	4	3	10	3.39	2.69
4	5	6	11.45	11.21	4	3	11	0.93	1.02*
4	5	7	5.04	4.48	4	4	0	9.98	10.46
4	5	8	0.34	1.45*	4	4	1	8.90	8.99
4	5	9	2.75	3.24	4	4	2	0.48	1.35*

....Contd.

Table 3.2 contd.

h	k	l	F_o	F_c	h	k	l	F_o	F_c
4	4	3	0.36	0.55*	5	3	3	6.23	5.98
4	4	4	0.83	0.66*	5	3	4	1.90	2.77*
4	4	5	10.11	10.44	5	3	5	15.26	16.26
4	4	6	3.54	3.43	5	3	6	1.40	1.34*
4	4	7	1.73	0.60*	5	3	7	0.57	0.74*
4	4	8	6.84	6.50	5	3	8	4.68	4.81
4	4	9	4.14	2.74	5	3	9	1.15	0.65*
4	4	10	0.50	1.44*	5	3	10	1.31	0.99
4	5	0	8.08	9.63	5	4	1	8.34	8.48
4	5	1	5.25	4.97	5	4	2	6.22	6.41
4	5	2	0.73	0.79*	5	4	3	1.47	1.57*
4	5	3	0.10	0.98*	5	4	4	1.02	1.43*
4	5	4	6.62	6.54	5	4	5	7.10	7.16
4	5	5	3.12	3.09	5	4	6	2.05	1.93*
4	5	6	3.46	3.33	5	4	8	5.46	5.33
4	5	7	1.24	2.45*	5	5	1	2.91	3.14*
4	5	8	2.58	2.25	5	5	2	5.90	6.32
4	6	0	5.82	5.58	5	5	3	5.46	5.70*
4	6	1	1.56	0.12*	5	5	4	3.99	4.75
4	6	2	1.04	0.96*	5	5	5	7.31	7.25*
4	6	3	5.80	5.23	5	5	6	2.99	2.61
4	6	4	0.61	0.88*	5	5	7	4.75	4.84
4	6	5	1.00	1.31*	5	6	1	0.54	1.34
4	6	6	2.12	2.52*	5	6	2	7.16	6.27
4	7	0	5.86	6.29	5	6	3	1.39	1.68
5	0	1	22.55	22.02	5	6	4	1.53	1.96
5	0	2	6.32	6.52	5	6	5	1.79	1.92
5	0	3	6.55	6.87	6	0	0	14.65	14.87
5	0	4	7.30	7.07	6	0	1	12.94	12.47
5	0	5	11.11	10.46	6	0	2	5.36	5.38
5	0	6	4.90	4.56	6	0	3	13.81	13.87
5	0	7	3.24	2.28	6	0	4	9.09	9.02
5	0	8	11.80	12.20	6	0	5	6.14	6.87
5	0	9	2.55	3.43*	6	0	6	7.02	7.07
5	0	10	3.70	3.57	6	0	7	3.32	2.96
5	0	11	2.96	2.74	6	0	8	3.65	4.34
5	1	1	18.64	19.26	6	0	9	6.89	6.39
5	1	2	4.60	4.22	6	1	0	2.47	1.38
5	1	3	4.41	3.80	6	1	1	0.91	0.04*
5	1	4	9.17	9.00	6	1	2	3.66	3.37
5	1	5	20.42	20.40	6	1	3	2.80	2.43
5	1	6	4.51	5.01	6	1	4	8.78	9.78
5	1	7	6.09	6.32	6	1	5	0.98	1.29*
5	1	8	1.37	2.07	6	1	6	4.52	4.60
5	1	9	0.39	2.07*	6	1	7	0.14	0.53*
5	1	10	1.21	1.31*	6	1	8	7.87	8.32
5	1	11	3.33	1.96	6	1	9	0.60	1.81*
5	2	1	2.06	2.29*	6	1	10	3.12	2.05*
5	2	2	30.09	30.27	6	2	0	13.16	13.31
5	2	3	13.21	12.83	6	2	1	15.10	15.76
5	2	4	1.64	0.71*	6	2	2	0.83	1.14*
5	2	5	6.75	6.98	6	2	3	11.31	12.06
5	2	6	8.98	9.74	6	2	4	10.21	10.72
5	2	7	7.93	8.46	6	2	5	1.14	0.93*
5	2	8	4.49	5.17	6	2	7	0.26	0.08*
5	2	9	1.10	0.35*	6	2	8	2.91	2.86
5	2	10	1.23	0.17*	6	2	9	4.73	4.29
5	2	11	0.47	0.28*	6	2	10	3.38	3.39
5	3	1	18.18	18.25	6	3	1	8.05	8.50
5	3	2	2.62	2.78	6	3	2	1.10	2.01*

....Contd.

Table 3.2 contd.

h	K	l	F^o	F^c	h	k	l	F^o	F^c
6	3	3	2.13	1.94	7	3	8	0.63	1.20*
6	3	4	6.19	6.96	7	4	1	0.59	0.25*
6	3	5	4.91	5.49	7	4	2	2.81	2.79*
6	3	6	1.88	2.52*	7	4	3	1.08	1.30*
6	3	7	2.94	2.06	7	4	4	5.96	6.01
6	3	8	5.55	5.19	7	4	5	2.73	2.01
6	3	9	0.64	1.00*	7	4	6	1.49	0.29*
6	4	0	5.30	4.96	7	5	2	4.46	3.76
6	4	1	6.60	6.71	7	5	3	2.09	1.39*
6	4	2	2.26	2.49*	8	0	0	11.60	12.57
6	4	3	5.68	5.77	8	0	1	0.54	0.75*
6	4	4	3.36	3.66	8	0	2	0.24	0.10*
6	4	5	2.28	2.89*	8	0	3	2.93	2.55*
6	4	6	1.12	2.00*	8	0	4	8.35	5.45
6	4	7	1.44	0.56	8	0	5	0.58	1.10*
6	4	8	3.10	2.54	8	0	7	0.88	0.05*
6	5	1	3.39	3.19	8	0	8	3.30	3.39
6	5	2	2.85	2.59*	8	1	0	3.49	3.05
6	5	3	1.40	2.32*	8	1	1	5.06	4.76
6	5	4	3.57	3.01	8	1	2	6.26	6.31
6	5	5	3.86	4.07	8	1	3	3.66	3.81
6	5	6	2.97	3.22*	8	1	4	1.58	2.39
6	6	1	4.73	4.36	8	1	5	3.03	3.39
6	6	2	2.24	1.47*	8	1	6	5.70	5.17
7	0	1	2.40	2.19	8	1	7	3.67	3.12
7	0	2	10.53	11.00	8	2	1	7.19	7.20
7	0	3	5.12	5.42	8	2	2	0.95	1.87*
7	0	4	10.73	10.93	8	2	3	1.71	1.92
7	0	5	4.13	4.42	8	2	5	4.76	4.09
7	0	6	3.28	3.23	8	2	6	1.22	2.71*
7	0	7	4.78	4.43	8	2	7	2.19	1.36*
7	0	8	4.09	4.41	8	3	0	5.38	4.58
7	0	9	3.91	3.69	8	3	2	4.04	3.59
7	1	1	3.21	2.41	8	3	3	2.51	1.86*
7	1	2	9.16	9.65	8	3	4	4.44	4.24
7	1	3	2.41	0.02	8	3	5	1.15	0.41*
7	1	4	3.49	4.60	8	3	6	1.29	2.54*
7	1	5	0.27	0.52*	8	4	0	4.83	4.98
7	1	7	6.73	6.58	8	4	1	0.72	1.94*
7	1	8	0.82	0.78*	8	4	2	0.87	0.06*
7	1	9	0.92	0.70*	8	4	3	1.09	1.37*
7	2	1	2.36	1.98*	9	0	2	6.85	6.52
7	2	2	7.13	7.69	9	0	3	2.01	2.15*
7	2	4	4.11	4.05	9	0	4	3.91	3.84
7	2	5	0.41	0.70*	9	0	5	1.48	0.49*
7	2	6	5.69	5.95	9	1	1	4.20	3.92
7	2	7	2.43	1.66*	9	1	2	0.57	0.99*
7	2	8	0.47	0.33*	9	1	3	1.73	1.26*
7	3	1	6.45	6.51	9	1	4	0.75	1.06*
7	3	2	3.25	3.65	9	1	5	7.42	6.97
7	3	3	6.60	6.66	9	2	1	4.66	4.12
7	3	4	2.86	3.12	9	2	2	8.40	8.06
7	3	7	2.77	2.29	9	2	3	4.26	3.59

Space group No.62 Pnma (D_{2h}^{16})

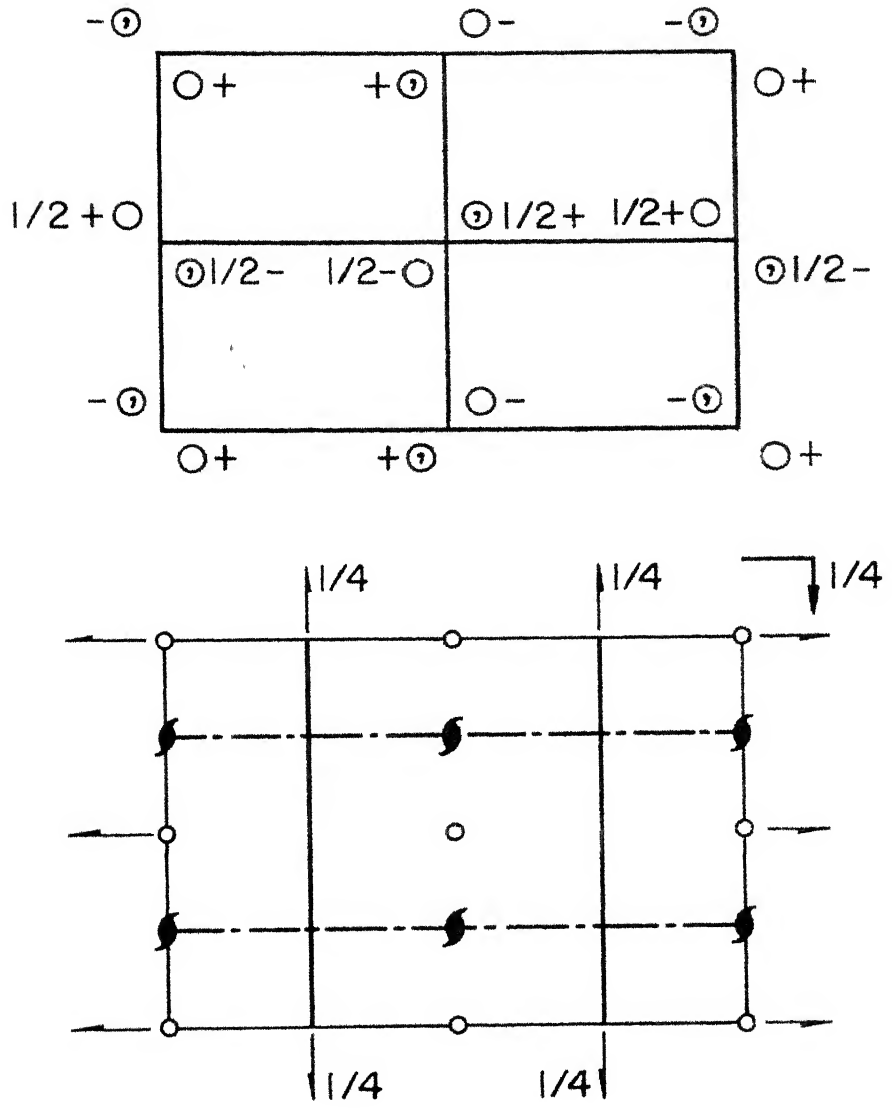

Origin at $\bar{1}$

Fig.3.2 Symmetry elements for space group Pnma.

two of the three symmetrically independent fluorine atoms and four of the six symmetrically independent hydrogen atoms lie on the mirror plane at y = 1/4 (position 4c : x, $\frac{1}{4}$, z; $\bar{x}$, $\frac{3}{4}$, $\bar{z}$; $\frac{1}{2}$ - x, $\frac{3}{4}$, $\frac{1}{2}$ + z; $\frac{1}{2}$ + x, $\frac{1}{4}$, $\frac{1}{2}$ - z). The remaining atoms occupy general position (position 8d: x, y, z; $\frac{1}{2}$ + x, $\frac{1}{2}$ - y, $\frac{1}{2}$ - z; $\bar{x}$, $\frac{1}{2}$ + y, $\bar{z}$; $\frac{1}{2}$ - x, $\bar{y}$, $\frac{1}{2}$ + z; $\bar{x}$, $\bar{y}$, $\bar{z}$; $\frac{1}{2}$ - x, $\frac{1}{2}$ + y, $\frac{1}{2}$ + z; x, $\frac{1}{2}$ - y, z; $\frac{1}{2}$ + x, y, $\frac{1}{2}$ - z).

Table 3.3(a) gives the bond length and bond angles in BeF_4^{--} ion showing fairly regular tetrahedral co-ordination. The mean Be-F bond length and the mean F-Be-F bond angle is 1.531(5) Å and 109.5°(3) respectively. When this Be-F distance was compared with other crystals[47] containing BeF_4 ions (table 3.3(a)), it was found that this distance was shorter by at least 0.02 Å. A rough estimate[48] of the shortening of Be-F bond due to the libration of BeF_4^{--} about y-axis accounted for the above discrepancy. The libration of BeF_4^{--} ion was calculated from the radial and tangential components of the mean square vibration amplitude at each fluorine atom in a manner similar to that done by Cruickshank for anthracene[49] and benzene[50]. A more rigorous treatment accounting for the foreshortening of each Be-F bond length in BeF_4^{--} ion is given in the following section 3.2.2.

Tables 3.3(b) and 3.3(c) show that NH_4 tetrahedra are somewhat distorted and have large variation in the value of

Table 3.3(a)

Interatomic Distances(A^{o}) and Angles(deg.) in BeF_4

Numerals 1 and 7 in front of atom symbols indicate symmetry positions x,y,z and x,1/2-y,z respectively

Environment of Be within a radius of 3.0 A^{o}

	Uncorrected for Libration	Corrected for Libration
1Be-1F(1)	1.522(6)	1.546
-1F(2)	1.531(6)	1.560
-1F(3)	1.535(4)	1.559
-7F(3)	1.535(4)	1.559
Mean Be-F	1.531(5)	1.556
1F(1)-1Be-1F(2)	111.0(4)	
-1Be-1F(3)	109.3(2)	
-1Be-7F(3)	109.3(2)	
1F(2)-1Be-1F(3)	108.4(2)	
-1Be-7F(3)	108.4(2)	
1F(3)-1Be-7F(3)	110.5(3)	

Mean Be-F distance in other compounds containing BeF_4 ion

$Na_3Li(BeF_4)_2$	1.552(3)A^{o}
NH_4LiBeF_4	1.60 A^{o}
$CsLiBeF_4$	1.65 A^{o}

Table 3.3(b)

Numerals 1 and 7 in front of atom symbols indicate symmetry positions x,y,z and x,1/2-y,z respectively

Environment of N(1) within a radius of 3.01 A^{o}

1N(1)-1H(1)	0.83(5)
-1H(2)	0.83(5)
-1H(3)	0.95(3)
-7H(3)	0.95(3)
1H(1)-1N(1)-1H(2)	123(4)
-1H(3)	101(3)
-7H(3)	101(3)
1H(2)-1N(1)-1H(3)	109(2)
-7H(3)	109(2)
1H(3)-1N(1)-7H(3)	114(3)

1N(1)-F(2)(1/2-x,-y,z-1/2)	2.987(1)
-F(2)(1/2-x,1-y,z-1/2)	2.987(1)
-F(3)(x-1/2,1/2-y,1/2-z)	3.009(5)
-F(3)(x-1/2,y,1/2-z)	3.009(5)
-F(3)(1/2-x,-y,z-1/2)	3.005(4)
-F(3)(1/2-x,1/2+y,z-1/2)	3.005(4)
-F(1)(1/2+x,1/2-y,1/2-z)	2.826(6)

Table 3.3(c)

Numerals 1 and 7 in front of atom symbols indicate symmetry positions x,y,z and x,1/2-y,z respectively

Environment of N(2) within a radius of 3.01 A°

1N(2)-1H(4)	0.72(6)
-1H(5)	0.79(5)
-1H(6)	1.01(3)
-7H(6)	1.01(3)
1H(4)-1N(2)-1H(5)	117(5)
-1H(6)	108(3)
-7H(6)	108(3)
1H(5)-1N(2)-1H(6)	109(3)
-7H(6)	109(3)
1H(6)-1N(2)-7H(6)	105(2)
1N(2)-F(2)(1/2+x,1/2-y,3/2-z)	2.785(5)
-F(2)(x,y,z)	2.903(5)
-F(3)(1/2-x,-y,1/2+z)	2.880(4)
-F(3)(1/2-x,1/2+y,1/2+z)	2.880(4)
-F(3)(1-x,1/2+y,1-z)	2.869(4)
-F(3)(1-x,-y,1-z)	2.869(4)
1N(2)-F(1)(1/2-x,-y,1/2+z)	3.094(2)
-F(1)(1/2-x,1-y,1/2+z)	3.094(2)

N-H distances and H-N-H angles. In $(NH_4)_I$ and $(NH_4)_{II}$ tetrahedra the mean value of N-H distances are 0.89(4) Å and 0.88(4) Å respectively and the mean value of H-N-H angle is 109°(3) in each case. Based on the neutron diffraction analysis of $(NH_4)_2SO_4$, Schlemper and Hamilton [51] have for the room temperature phase reported the mean N-H distance as 0.97(1) and H-N-H angle 109°(1).

The two symmetrically independent nitrogen atoms of the unit cell have somewhat different surroundings. Within a sphere of radius 3.01 Å, N(1) has seven and N(2) has six fluorine atoms with an average N(1)-F distance of 2.975(4) Å and N(2)-F of 2.864(4) Å. The van der Waals contact length between N-F atoms is 2.85 Å. Around N(1) only one fluorine F(1) is at a distance less than 2.9 Å whereas all the six fluorines around N(2) lie within 2.9 Å. If a sphere of radius 3.1 Å is considered, two more fluorines can be added around N(2) but none around N(1). The average N(2)-F distance then becomes 2.922(4) Å. The environment of N(1) and N(2) within a radius of 3.01 Å has also been shown in tables 3.3(b) and 3.3(c) respectively.

In table 3.4, H...F distances less than 2.6 Å along with the corresponding N-H...F bond angles are given. The hydrogen bonding scheme is shown by dotted lines in fig. 3.1(b). Each NH_4^+ tetrahedron is bonded to its neighbouring

Table 3.4

Hydrogen Bonds

F(1)-H(1)	2.01(5) Å	F(1)...H(1)-N(1)	171(4)°
-H(2)	2.51(5)	H(2)-N(1)	149(4)
-H(6)	2.32(3)	H(6)-N(2)	133(2)
-H(6)	2.32(3)	H(6)-N(2)	133(2)
F(2)-H(4)	2.43(5)	F(2)...H(4)-N(2)	126(5)
-H(5)	2.01(5)	H(5)-N(2)	164(5)
-H(3)	2.19(3)	H(3)-N(1)	141(2)
-H(3)	2.19(3)	H(3)-N(1)	141(2)
F(3)-H(2)	2.49(4)	F(3)...H(2)-N(1)	122(3)
-H(3)	2.17(3)	H(3)-N(1)	146(2)
-H(4)	2.41(4)	H(4)-N(2)	123(3)
-H(6)	1.93(3)	H(6)-N(2)	155(3)
F(3)-H(2)	2.49(4)	F(3)...H(2)-N(1)	122(3)
-H(3)	2.17(3)	H(3)-N(1)	146(2)
-H(4)	2.41(4)	H(4)-N(2)	123(3)
-H(6)	1.93(3)	H(6)-N(2)	155(3)

BeF_4 tetrahedra by eight hydrogen bonds. If H...F distances less than 2.01 Å are considered, then $(NH_4^+)_I$ is strongly hydrogen bonded to its neighbouring BeF_4 tetrahedra by one (2.01(5) Å) and $(NH_4^+)_{II}$ by three (1.93(3), 1.93(3), 2.01(5)Å) hydrogen bonds. The corresponding distances in $(NH_4)_2SO_4$ are 1.97 Å and 2.05, 2.05, 1.85 Å respectively.

The difference in the surroundings of N(1) and N(2) and the hydrogen bonding of $(NH_4^+)_I$ and $(NH_4^+)_{II}$ to its neighbouring BeF_4^{--} tetrahedra indicates different inter-ionic interactions involving $(NH_4^+)_I$ and $(NH_4^+)_{II}$. One of the implications of this is that it should lead to the observation of their individual and separate bands in the Raman spectrum of AFB. This has been experimentally observed in the Raman spectrum investigations[52] of a single crystal of AFB. Similar results have also been observed in $(NH_4)_2SO_4$[53].

3.2.2 Interpretation of Thermal Motion

Table 3.1(b) gives the anisotropic temperature factors for each atom. Lengths and directions of principal axes of the thermal ellipsoids for different atoms are depicted in table 3.5. A careful study of these tables indicates a large anisotropy in the thermal motion of fluorine atoms as compared to other atoms. Therefore an interpretation of anisotropic temperature factors in terms of librational motion of BeF_4^{--} has been attempted.

Table 3.5

The thermal ellipsoids

q_i :r.m.s. thermal-vibration parameters for for the three principal axes of the ellipsoid.

	q_i	Angle w.r.t crystal axes		
N(1)	0.208	86.7°	90.0°	3.3°
	0.175	90.0	0.0	90.0
	0.155	3.3	90.0	86.7
N(2)	0.184	2.6	90.0	87.5
	0.187	90.0	0.0	90.0
	0.156	87.5	90.0	2.6
Be	0.166	86.0	90.0	4.0
	0.165	90.0	0.0	90.0
	0.133	4.0	90.0	86.0
F(1)	0.290	85.4	90.0	4.6
	0.260	90.0	0.0	90.0
	0.155	4.6	90.0	85.4
F(2)	0.249	4.3	90.0	85.7
	0.259	90.0	0.0	90.0
	0.164	85.7	90.0	4.3
F(3)	0.265	101.2	74.7	160.9
	0.224	162.8	105.6	83.1
	0.183	102.9	22.1	72.3

Considering BeF_4^{--} as rigid body, the atomic vibration tensor (U) for each atom has been expressed in terms of two symmetric (T,L) and one non-symmetric (S) tensors (sec. 1.A.4). There are five atoms in the rigid group BeF_4^{--} giving 30 such equations. With respect to the orthogonal crystal axes, the value of T and L tensors as determined by the method of least squares and symmetrizing S is given by

$$T(\text{Å}^2) = \begin{bmatrix} 0.0205 & 0 & 0.0018 \\ & 0.0275 & 0 \\ & & 0.0307 \end{bmatrix}$$

$$L(\text{deg.}^2) = \begin{bmatrix} 58.5 & 0 & 4.7 \\ & 66.1 & 0 \\ & & 38.7 \end{bmatrix}$$

Since the value of T_{13} and L_{13} are small as compared to their respective diagonal elements, the principal axes of T and L can be taken to coincide with the crystal axes. The r.m.s. amplitudes of translational oscillations obtained from the square roots of the diagonal elements of T are 0.143, 0.166 and 0.175 Å respectively. The corresponding r.m.s. amplitudes of angular oscillation obtained from L are 7.65°, 8.13° and 6.22° respectively. The increase in individual Be-F bond lengths in BeF_4^{--} ion thus obtained from L tensor is given in table 3.3(a). The mean Be-F bond length thus increases

from 1.531 Å to 1.556 Å. The new bond length agrees well with those in other crystals containing BeF_4^{--} ions. All the above calculations have been done on IBM 7044 using the computer programme TLS [54].

From the amolitudes of angular oscillations the frequencies of oscillation of BeF_4^{--} have also been obtained from eqn. 1.15

$$(L)_I = \frac{h}{8\pi^2 I} \left(\frac{1}{\nu} \coth \frac{h\nu}{kT}\right)$$

This transcendental equation has been solved for ν by Newton Raphson iterative method for each value of the estimated moment of inertia 199, 197, 200 x 10^{-40} g cm^2 of BeF_4^{--} about a, b, c axis respectively. Thus the three rotational frequencies of BeF_4^{--} about a, b and c are 57, 54, 70 cm^{-1} respectively. These frequencies should show up in Raman spectrum of AFB.

For a perfect tetrahedral (T_d) symmetry, the librational modes are forbidden in both Raman and IR spectra. Since the BeF_4^{--} ions do not differ significantly from regular tetrahedral symmetry, it is highly probable that the Raman intensity of the librational modes of BeF_4^{--} ions is too weak to be detected. This is found to be so in the Raman spectrum of single crystal of AFB analyzed by Jain [52].

However, he has estimated the mean librational frequency of BeF_4^{--} from the difference of internal mode frequency (ν_4) plus librational frequency (l) of BeF_4 ($(\nu_4 + l)_{BeF_4} \simeq 472$ cm^{-1}) and the internal mode frequency (ν_4) of BeF_4 ($\nu_4 \simeq 372$ cm^{-1}) to be around 100 cm^{-1}.

4. THERMAL DIFFUSE SCATTERING OF X-RAYS FROM $(NH_4)_2BeF_4$: RESULTS AND DISCUSSION

The plots of ratio of thermal diffuse intensity to direct beam intensity (I_d/I_o; after applying all the corrections described in sec. 2.B.3) and the square of the thermal wave length ($\lambda^2 = \frac{1}{q^2}$) have been shown in figs. A1-A12. These plots are straight lines passing through the origin. The slopes of these lines give the average value of $K[uvw]_{hkl}$ from which the respective C_{ij} can be calculated. The details of calculations of the individual elastic constants are given in Appendix II.

4.1 Elastic Constants Based on Old (Voigt's) Theory of Elasticity

From the diffractometer study of diffuse reflections, the nine elastic constants, based on old (Voigt's) theory, of orthorhombic $(NH_4)_2BeF_4$ at room temperature are given in table 4.1.

Ramachandran and Wooster (1951)[15] developed this method and used it for cubic crystals. Later other workers notably Prince and Wooster (1953)[55], Prasad and Wooster (1955,1956)[36], Srivastava and Chakravorty (1962)[56],

Table 4.1: Elastic constant values and the corresponding $K[uvw]_{hkl}$ from which they have been evaluated

Elastic constant	$K[uvw]_{hkl}$	Elastic constant $\times 10^{-11}$ dynes.cm^{-2}	Mean C_{ij} $\times 10^{-11}$ dynes.cm^{-2}
C_{11}	$K[\bar{1}00]_{301}$	3.822	3.82(30)
C_{22}	$K[0\bar{1}0]_{013}$	3.555	3.56(28)
C_{33}	$K[00\bar{1}]_{301}$	2.451	2.45(19)
C_{44}	$K[00\bar{1}]_{040}$	0.959	0.96(05)
	$K[0\bar{1}0]_{004}$	0.963	
C_{55}	$K[\bar{1}00]_{004}$	1.016	1.01(05)
	$K[00\bar{1}]_{400}$	1.008	
C_{66}	$K[\bar{1}00]_{020}$	0.776	0.79(04)
	$K[\bar{1}00]_{040}$	0.808	
C_{12}	$K[\pm\frac{1}{\sqrt{2}}, \pm\frac{1}{\sqrt{2}}, 0]_{020}$	1.759	1.78(18)
	$K[\pm\frac{1}{\sqrt{2}}, \pm\frac{1}{\sqrt{2}}, 0]_{040}$	1.801	
C_{13}	$K[\pm\frac{1}{\sqrt{2}}, 0, \pm\frac{1}{\sqrt{2}}]_{004}$	1.520	1.52(15)
C_{23}	$K[0, \pm\frac{1}{\sqrt{2}}, \pm\frac{1}{\sqrt{2}}]_{004}$	1.406	1.41(14)
	$K[0, \pm\frac{1}{\sqrt{2}}, \pm\frac{1}{\sqrt{2}}]_{040}$	1.416	

Joshi and Kashyap (1954)[57], Chandra and Hemkar (1972)[58] and Phatak, Srivastava and Subbarao (1972)[59] applied it to non-cubic crystals. Ramachandran and Wooster employed counter diffractometer and large crystals of cross-section ~5 mm x 5 mm which were required to be cut along particular directions and polished. Some of the later workers mentioned above have used photographic method and small crystals. The method as developed for small crystals obviates the need for cutting the crystals and also results in small divergence correction. Phatak et al.[59] have employed small crystals of volume of the order of 10^{-4} c.c, not only in the photographic method but also in the counter diffractometer using balanced filter for monochromatization. They have shown that the agreement between the results obtained by the two methods with small crystals is quite good. In the present case also we have been able to resolve and analyse I_d/I_o vs λ^2 curves along different directions around a relp. on small crystals of volume 10^{-3}-10^{-4} c.c. As a result one of the limitations of using large crystals normally associated with the counter technique is no longer considered necessary. The additional advantage with such small crystals is that the divergence correction is further reduced.

4.1.1 Accuracy of the Results

Each elastic constant is evaluated from at least two different directions of the thermal wave vector. The relationship between the K's corresponding to a particular direction of propagation of the thermal wave and the elastic constants based on old (Voigt's) theory as well as new (Laval's) theory has been given in table 1.1. $K[uvw]_{hkl}$ that have been used to evaluate elastic constants of AFB are listed in table 4.1.

Accuracy of the results of the elastic constants as determined by the X-ray diffuse scattering method depends upon the following factors

1. Choice of the reflecting plane and the rekha [uvw].
2. Various corrections (i) Divergence, (ii) Skew, (iii) Polarization, (iv) Absorption, (v) Second and higher order diffuse reflection, and (vi) General scattering.
3. Measurement of absolute intensity.
4. Corrections arising out of contribution from Cochran's optical mode or soft mode.

The first two factors affect the accuracy of the individual constant in different ways. On the other hand, the factors 3 and 4 affect all the elastic constants to nearly the same extent, so these have been discussed first.

The accuracy of the elastic constants mainly depends on the accuracy with which I_d and I_o can be measured in addition to the structure factor F_T, i.e. the accuracy of the crystal structure indirectly. The structure has been refined (sec. 3.1) to quite a good degree of accuracy (R = 0.049). The calculated values of structure factors F_T's have been used. The direct beam intensity I_o which is of the order of 10^5-10^6 times the diffuse intensity has been measured by using an intermediate standard such that the measured intensity leading to I_o is comparable to diffuse intensity. The details of the measurements of I_o are given in Appendix I. Such a standardization of the incident intensity can be made with an accuracy of 3%[55].

By measuring the intensity of diffuse reflection close to the reciprocal lattice point i.e. for low values of the thermal wave vector $\vec{q}$, it has been possible to neglect the contribution of optical mode of vibration because of their high frequency at such small q values. However, as mentioned earlier, $(NH_4)_2BeF_4$ is a ferroelectric crystal and ferroelectricity in many crystals has been attributed to the existence of low frequency transverse optical mode or so-called soft mode. A detailed theory of soft mode by Anderson[60] and Cochran[61] predicts the existence of a temperature dependent low frequency (ω_T) transverse mode which goes to zero as the Curie temperature (T_o) is approached,

i.e. $$\omega_T \propto (T - T_o) \qquad (4.1)$$

Such a low frequency optical mode, if exists in AFB, would also contribute to the diffuse intensity apart from the usual acoustic mode. Hence the values of the elastic constants determined on the assumption of negligible optical contribution would deviate from their true value. It is, therefore, necessary to examine the results of experiments which are likely to throw light on the existence of soft mode.

Popkov et al.[62] have measured the Raman spectrum of AFB and found no soft mode. Recently, Wada et al.[63] who found soft mode in different phases of K_2SeO_4 re-examined the Raman spectrum of AFB but did not find any such low frequency phonon mode for any orientation of the crystal down to the liquid nitrogen temperature. Iizumi and Gezi[64] have done the neutron diffraction study of $(ND_4)_2BeF_4$ but have not been able to observe such a mode. The dielectric measurements of AFB have been done by Hoshino et al.[65] but they have also not noticed any dielectric anomaly along any of the crystallographic directions at the transition temperature. These results rule out the possibility of explaining the ferroelectric behavior of $(NH_4)_2BeF_4$ on the basis of soft mode concept.

Further the transition from ferroelectric to paraelectric state in AFB takes place at 175 K while elastic constants have been obtained at room temperature 305 K in the present study. Looking at the difference in two temperatures, eqn. (4.1) shows ω_T is not low at this temperature. Hence even if soft mode existed (for which there is no evidence as discussed above) its contribution to diffuse scattering will be negligibly small at 305 K.

The first two factors are discussed now. C_{11}, C_{22}, C_{33} could, in principle, be determined independent of other constants by measuring intensity of diffuse reflection in the same direction as the reciprocal lattice vector, i.e. along $[100]_{hoo}$, $[010]_{oko}$, $[001]_{ool}$, but for such wave vectors the geometry of reflection is such that even for slight mis-setting from the Bragg angle, the value of q is very large. Thus a small error in measurement of the angle of mis-setting would introduce large errors in q. Moreover, large q makes the corresponding value of I_d/I_o very low and consequently less accurate. It was found to be more so for AFB crystals as the values of C_{11}, C_{22}, C_{33} are quite large as compared to other constants. Also the second order correction becomes large as q increases. So other reciprocal lattice points having two non-zero indices had to be used for evaluation of C_{11}, C_{22}, C_{33} making each of these dependent on another elastic constant. The divergence correction has

been reduced by using small crystals of volume $\sim 10^{-3}$-10^{-4}c.c. and has been properly taken care of. The absorption correction has been accurately determined by taking well shaped crystals and applied in all the cases. The variation in the general scattering (Compton scattering, fluorescent radiation and scattering due to optical waves, etc.) has been accounted for by making intensity measurements on either side of the reciprocal lattice point and calculating average value of the elastic constant from these measurements. The procedure for applying all the above mentioned corrections has been discussed in sec. 2.B.3. Thus taking into account all the above factors, the accuracy of C_{11}, C_{22}, C_{33} is estimated to be about 3%.

C_{44}, C_{55}, C_{66} have been evaluated by measuring the intensities of diffuse reflections in a direction perpendicular to the concerned reciprocal lattice vector. They are independent of any other elastic constant. The corrections are the same as for C_{11}, C_{22}, C_{33} except that thermal wave vectors involved are smaller and hence second order diffuse reflection correction is reduced. The accuracy of C_{44}, C_{55}, C_{66} is estimated to be about 5%.

C_{12}, C_{13}, and C_{23} each depends on the value of three other elastic constants, e.g. C_{12} can be determined from the following

$$C_{12} = -C_{66} + \sqrt{C_{66}^2 + C_{11}C_{66} + (C_{11}+C_{66})(C_{22}-2/K[\frac{1}{\sqrt{2}}, \frac{1}{\sqrt{2}}, 0]_{oko})}$$

The corrections are the same as for C_{11} etc. as discussed above. The accuracy of C_{12}, C_{13}, C_{23} is estimated to be about 10%.

4.2 Elastic Constants on the Basis of New (Laval's) Theory of Elasticity

It is seen in sec. 1.B.4 that fifteen elastic constants are necessary for completely specifying the elastic behavior of an orthorhombic crystal. Six of them do not occur independently but appear only in combination $(C'_{12} + C'_{69})$, $(C'_{23} + C'_{47})$, $(C'_{13} + C'_{58})$ in the expression for propagation of elastic waves in the crystals. Therefore, all the dynamical methods would only give these combinations and not the individual constants[66]. One is thus left with only twelve dynamical constants namely C'_{11}, C'_{22}, C'_{33}, C'_{44}, C'_{55}, C'_{66}, C'_{77}, C'_{88}, C'_{99}, $(C'_{12}+C'_{69})$, $(C'_{23}+C'_{47})$ and $(C'_{13}+C'_{58})$. Out of these C'_{11} to C'_{66} can be identified with the constants C_{11} to C_{66} of the old (Voigt's) theory. So the values of these constants are unaffected due to the implications of the new theory as applied to the present compound $(NH_4)_2BeF_4$ also.

Further, in the new (Laval's) theory, it is possible to distinguish between the following pairs of elastic constants: C'_{55} and C'_{88}; C'_{66} and C'_{99}; C'_{44} and C'_{77}; C'_{69} and C'_{66};

C'_{58} and C'_{55}; C'_{47} and C'_{44}. For example, according to the new theory the rekha $K[100]_{oo1}$ and $K[001]_{hoo}$ would give rise to elastic constants C'_{55} and C'_{88} respectively, but according to the old theory they give rise to the same elastic constant C_{55}. Measurements have been done along rekha $K[100]_{004}$ and $K[001]_{400}$ to determine C'_{55} and C'_{88} respectively. Details of observations and calculations are given in tables A-3(a,b) and A-4(a,b) respectively of Appendix II. Hence we get

$$C'_{55} = 1.016 \times 10^{11} \text{ dynes/cm}^2$$

$$C'_{88} = 1.008 \times 10^{11} \text{ dynes/cm}^2.$$

The difference (0.8%) between the two constants is not significant and is well within the limits of accuracy of our experiments. Similarly measurements have been made along $K[010]_{004}$ and $K[001]_{040}$ (tables A-1(a,b) and A-2(a,b) of Appendix II respectively) to distinguish between C'_{77} and C'_{44}.

$$C'_{77} = 0.963 \times 10^{11} \text{ dynes/cm}^2$$

$$C'_{44} = 0.959 \times 10^{11} \text{ dynes/cm}^2$$

The difference (0.4%) between the two is again not significant. Similarly the difference between C'_{66} and C'_{99} and other pairs stated above were found to be insignificant. It may be pointed out that if the difference between the two

constants say C'_{55} and C'_{88}, C'_{44} and C'_{77} etc. is not large compared to the inaccuracy of their determination, it is sufficient to interpret the results in terms of old theory.

Evidently, the difference between C'_{55} and C'_{88} and such differences in other constants can be employed to differentiate between the two theories, limitation being that the difference should be larger than 5-10% (depending on the constant) if X-ray method is employed. Due to limitation of the accuracy of the method employed, it is not possible on the basis of our experimental results to make any assertion regarding the difference between the old and the new theory of elasticity for the compound AFB which has been investigated.

Further as argued by Joel and Wooster[67], a centre of symmetry in the crystal necessitates the presence of parallel and opposite bonds, thus destroying the volume couples which are chiefly responsible for increasing the number of elastic constants. Hence it would not be expected that any centrosymmetric crystal like AFB would require the new theory for description of its elastic properties.

Few other workers have performed experiments to verify the new theory. For example, in cubic $NaBrO_3$ the difference in the pairs of elastic constants required by the new theory is about 0.1%[68] which is well within the limit of experimental error of pulse technique employed. Unequivocal results

justifying the validity of the new theory have yet to appear.

4.3 Isodiffusion Contours

Contours around a relp. over which diffuse intensity has a constant value are called isodiffusion or equiscattering contours. The information about the thermal vibration amplitudes in AFB has been obtained from the study of isodiffusion contours around the reciprocal lattice node 400. These contours have been calculated following the method of Jahn[18] and are drawn in reciprocal planes a*b*, b*c* and c*a* respectively in fig. 4.1. The intensity formula is given by eqn.(2.3) as follows

$$\frac{I_d}{I_o} = \frac{\varepsilon^2 kT\Omega}{V^2} F_T^2 \frac{|\vec{x}|^2}{|\vec{q}|^2} K[uvw]_{hkl}$$

For isodiffusion contours

$$\frac{I_d}{I_o} = \text{constant value}$$

$$\therefore \quad q^2 = \text{const. } K\,[uvw]_{hkl}$$

The value of the constant depends upon the particular relp. used.

For hoo node in a*c* plane

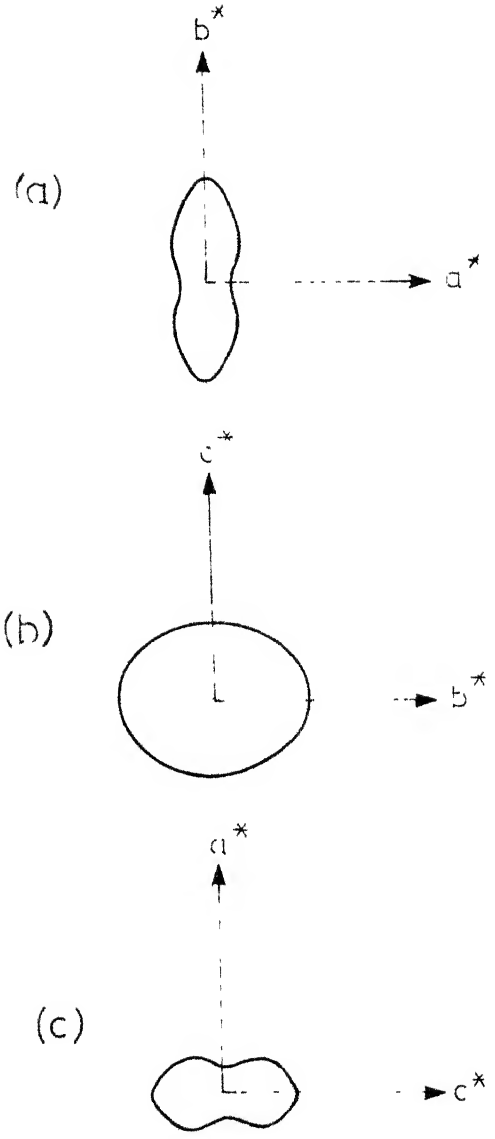

Fig. 4.1 Isodiffusion contours around 400 in (a) $a^* b^*$ (b) $b^* c^*$ (c) $c^* a^*$ reciprocal planes.

$L = 1,\ M = 0,\ N = 0$ and $v = 0$

$$q^2 = \text{const. } K[uow]_{hoo} = \text{const. } A_{11}^{-1}$$

where

$$A_{11}^{-1} = \frac{C_{55}u^2 + C_{33}w^2}{(C_{11}u^2 + C_{55}w^2)\ (C_{55}u^2 + C_{33}w^2) - (C_{13} + C_{55})^2 u^2 w^2}$$

$$= f\ (u^2, w^2)$$

$$q^2 = \text{const. } f\ (u^2, w^2) \qquad (4.2)$$

So the wave vector for a point on the contour is guided by the eqn. (4.2) which shows that the value of q^2 is dependent only on the squares of the direction cosines u and w of the thermal wave and hence the isodiffusion contours would be symmetrical about a* and c* axes in a*c* plane. Similar arguments follow for contours in a*b* and b*c* planes.

In AFB, the isodiffusion contours shown around 400 have almost circular shape (with a little elongation along b*) in b*c* plane while peanut shape in a*c* and a*b* planes. The elongation of the contours along b* in a*b* plane and c* in a*c* plane shows that the amplitude of vibration of the transverse wave is higher than that of the longitudinal wave. This is found to be true for 040 as well as 004 relps. The contours around 400 depict $|\vec{q}|_{100} < |\vec{q}|_{010}$, $|\vec{q}|_{100} < |\vec{q}|_{001}$ and $|\vec{q}|_{001}$ a little $< |\vec{q}|_{010}$. The above inequalities are

implicit in the values of the experimentally determined elastic constants requiring $C_{11} > C_{66}$, $C_{11} > C_{55}$ and C_{55} a little $> C_{66}$.

4.4 Debye Temperature and other Bulk Properties of $(NH_4)_2BeF_4$

Debye temperature is one of the important physical properties of a solid. It provides useful quantitative information regarding vibrational spectrum and is also used as a parameter in many thermodynamic relations. The Debye temperature of AFB has been calculated by finding the mean velocity of sound in the crystal from the elastic constants.

The mean sound velocity v_m is given by[69]

$$\frac{3}{v_m^3} = \int_0^{4\pi} \left(\frac{1}{v_l^3} + \frac{1}{v_{t_1}^3} + \frac{1}{v_{t_2}^3}\right) \frac{d\Omega}{4\pi} \qquad (4.3)$$

where $d\Omega = \sin\theta \, d\theta \, d\phi$

and v_l and v_{t_1}, v_{t_2} are the longitudinal and transverse velocities obtained from roots of the Cristoffel equations

$$|\Gamma_{ik} - \delta_{ik} \rho v_i^2| = 0 \qquad (4.4)$$

where $\delta_{ik} = 0 \quad i \neq k$

$= 1 \quad i = k$

and $\Gamma_{ik} = \Gamma_{ki} = l_j l_l C_{ijkl}$

where l_i are the direction cosines of the phase velocity vectors.

The integral in eqn. (4.3) has been solved numerically by replacing it by a summation of the following type[70]

$$\frac{3}{v_m^3} = \frac{S}{4\pi} \sum_{\theta=0}^{\theta_s-\Delta\theta} \sum_{\phi=0}^{\phi_s-\Delta\phi} \left(\frac{1}{v_l^3} + \frac{1}{v_{t_1}^3} + \frac{1}{v_{t_2}^3}\right) \Delta\Omega$$

where

$$\Delta\Omega = \left[\cos\theta - \cos(\theta + \Delta\theta)\right] \Delta\phi$$

and S is a symmetry constant dependent upon the limits of summation θ_s and ϕ_s.

$(NH_4)_2BeF_4$ belongs to orthorhombic system and hence it is only necessary to sum it over an octant (i.e. $\theta_s = \phi_s = 90^\circ$) and take S=8. The above calculations have been done on DEC 10 system. The interval chosen is $\Delta\theta = \Delta\phi = 5^\circ$ with a view of the fact that difference between v_m with $\Delta\theta = \Delta\phi = 5^\circ$ and v_m with $\Delta\theta = \Delta\phi = 2^\circ$ is less than 2% for calcite[71]. The mean sound velocity v_m thus calculated for AFB using the values of elastic constants given in table 4.1 is 2.54 km/sec. Using this value, the Debye temperature θ_D defined as

$$\theta_D = \frac{h}{k} \left(\frac{3n\ N\rho}{4\pi M}\right)^{1/3} v_m$$

where, n is the number of atoms in the molecule,

N is Avogadro's number,

ρ, M are the density and molecular weight respectively,

comes out to be 381 K.

An estimate of the accuracy of the elastic constants obtained experimentally can be seen by comparing θ_D as obtained above and that derived from specific heat measurement at low temperature where only low frequency lattice vibrations contribute to specific heat ($C_v \propto T^3$). Unfortunately, no such data in the T^3 region is available for AFB.

Some of the bulk properties of polycrystalline aggregate which consists of randomly oriented single crystals of AFB can also be estimated from the single crystal elastic constant values. Hill has shown by energy density considerations that for such an aggregate, the Voigt model of calculating bulk moduli from elastic constant values (C_{ij}) on the basis of uniform local strain and the Reuss model of calculating bulk moduli from compliance constant values (S_{ij}) on the basis of uniform local stress represent the extreme upper and lower bounds and hence an arithmetic average of the two is the best representation of the bulk elastic moduli. Using this simple averaging scheme (called VRHG approximation by Anderson[72]), the different elastic moduli calculated for AFB are as follows

Bulk Modulus (K_H) = 2.03 x 10^{11} dynes/cm^2

Shear Modulus (G_H) = 0.92 x 10^{11} dynes/cm^2

Young's Modulus (E_H) = 2.41 x 10^{11} dynes/cm^2

The average longitudinal ($\bar{v}_l$) and transverse ($\bar{v}_t$) velocities in the polycrystalline aggregate are then given by

$$\bar{v}_l = \sqrt{(K_H + \frac{4}{3} G_H)/\rho} = 4.40 \text{ km/sec}$$

$$\bar{v}_t = \sqrt{G_H/\rho} = 2.32 \text{ km/sec}$$

Hence the average mean velocity in the polycrystalline AFB is

$$\bar{v}_m = \left[\frac{1}{3}\left(\frac{2}{\bar{v}_t^3} + \frac{1}{\bar{v}_l^3}\right)\right]^{-1/3} = 2.60 \text{ km/sec.}$$

This value is in good agreement with the one (=2.54 km/sec) calculated by more rigorous integration technique above. This shows the correctness of the Bulk moduli calculated from VRHG approximation.

The complex nature of the velocity surfaces given by eqn. (4.3) is shown in different sections in fig. 4.2 for AFB. These curves have been drawn from the three real solutions of eqn. (4.3). The largest root corresponds to the longitudinal or quasi-longitudinal wave and the other two are transverse or quasi-transverse waves. A close inspection of these curves shows that velocity surfaces of each wave possess

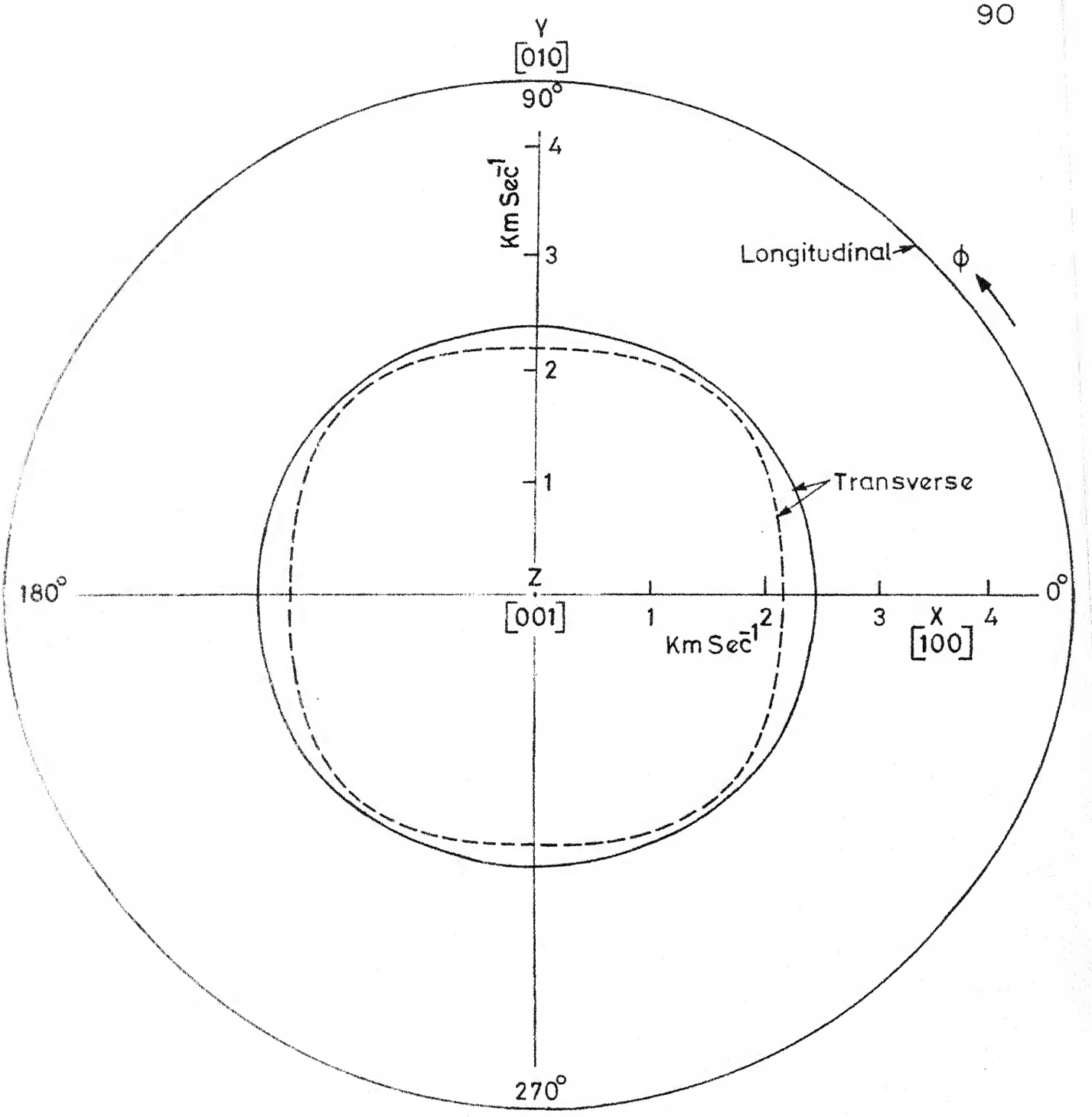

Fig. 4.2(c)

Cross-section of the wave velocity surfaces in (001) plane of $(NH_4)_2BeF_4$

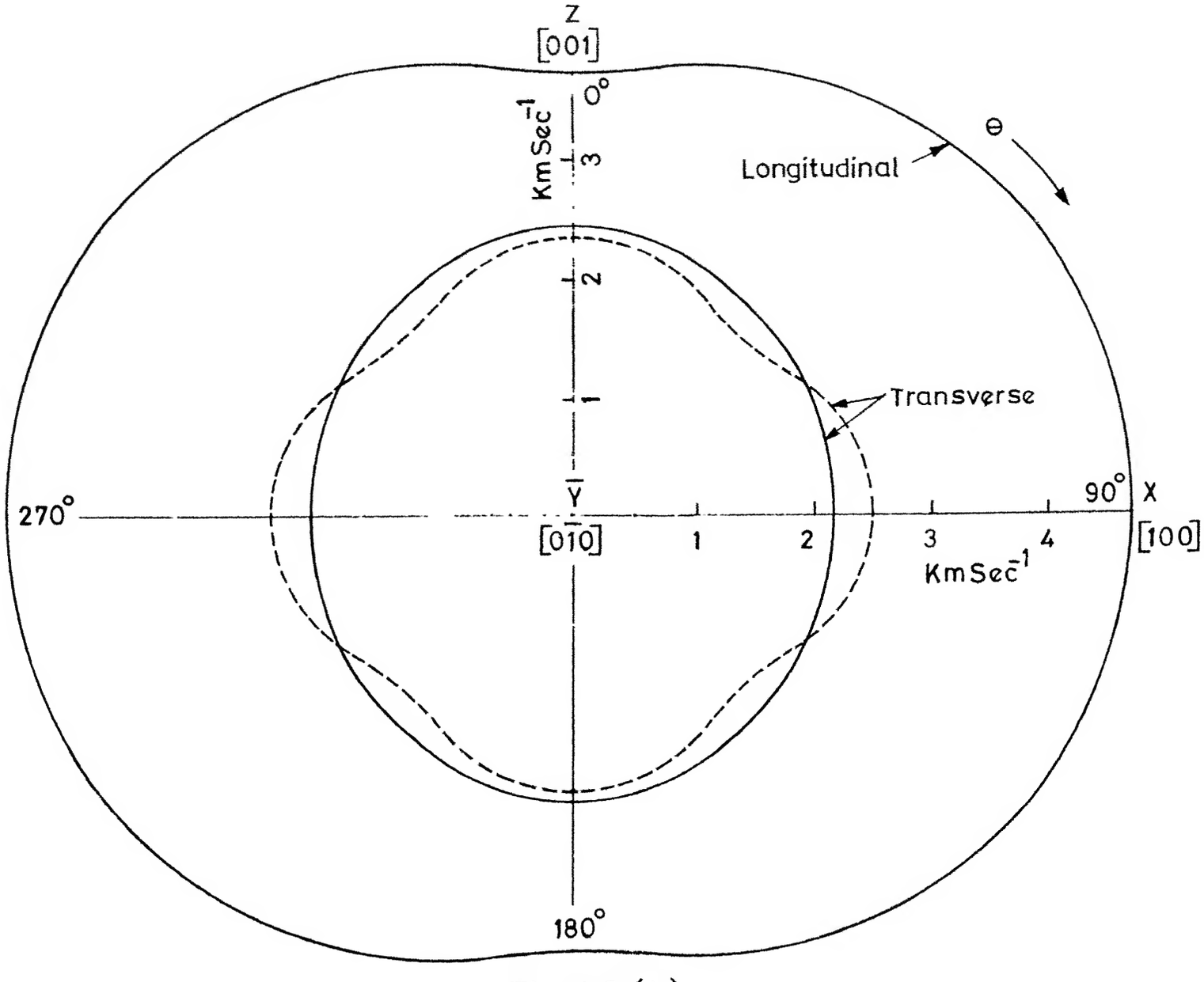

Fig.4.2 (b)

Cross-section of the wave velocity surfaces in (010) plane of $(NH_4)_2 BeF_4$

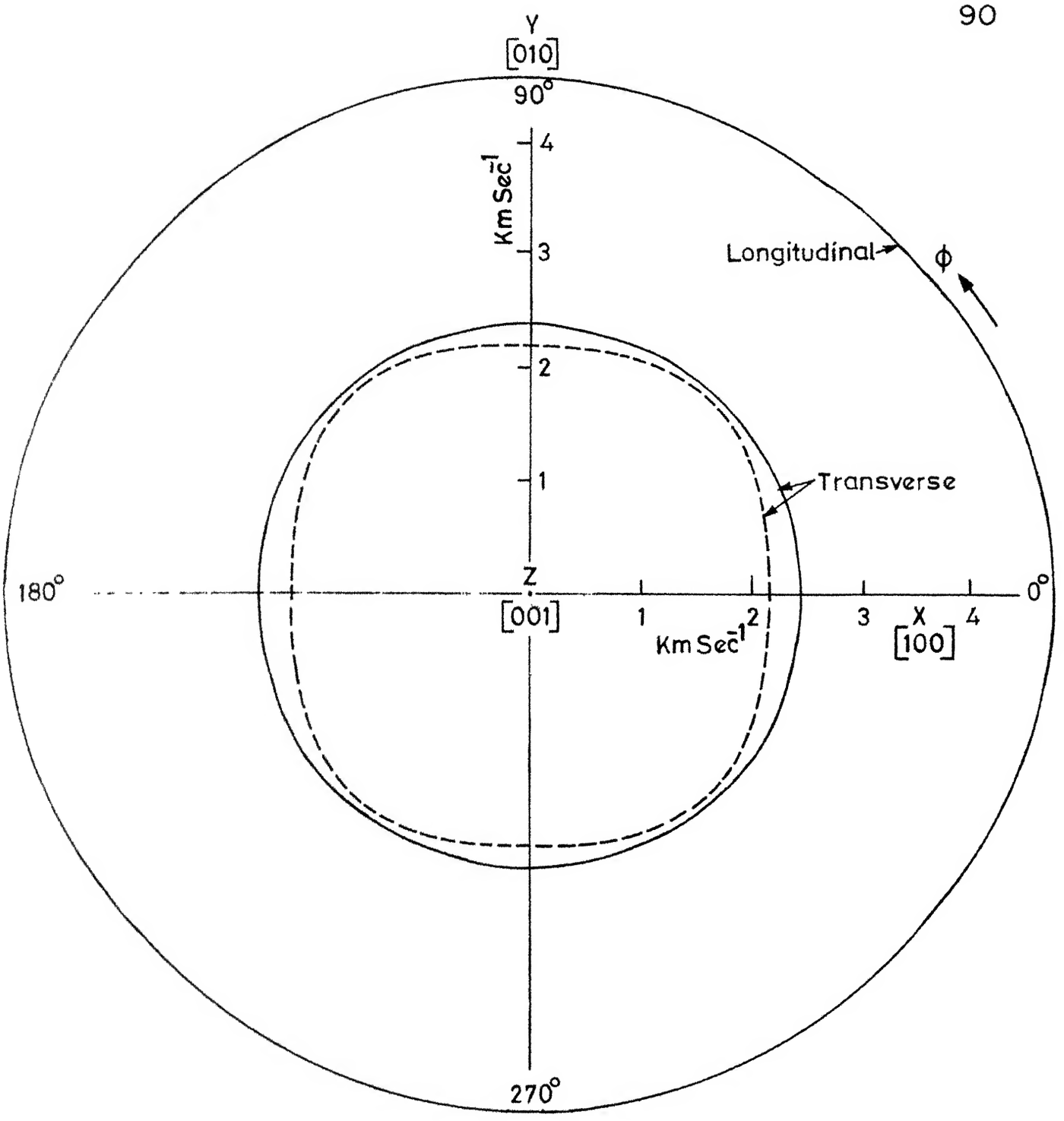

Fig. 4.2(c)

Cross-section of the wave velocity surfaces in (001) plane of $(NH_4)_2 BeF_4$

the symmetry of the particular projection drawn. So for the orthorhombic symmetry, it is only necessary to calculate the velocities (v_l, v_{t_1}, v_{t_2}) in one quadrant of a plane to reproduce the whole velocity surface in that plane. These velocity surfaces are helpful in finding out the directions (specific directions of Borgnis[73]) along which pure longitudinal waves may be propagated in the crystal.

4.5 Correlation of Elastic Constants and Crystal Structure

The elastic properties of crystals may be very useful in investigating the nature of binding forces. Although the elastic constants determine the thermal vibration spectrum only in the low frequency limit yet they may be employed to form semiempirical force models and used as a check for fundamental theories of binding in solids. The analysis is simple for cubic crystals but becomes complicated as the number of atoms in the asymmetric unit increases. Hence only a qualitative correlation could be made between the structure of AFB and its elastic constants.

A survey of elastic constants for different structures has been done by Wooster[74]. A more recent survey of diffuse scattering study leading to elastic constants has been done by Amoros and Amoros[37]. The broad generalization which emerges from these survey is that where the atomic binding

parallel to an axial direction is strong, the corresponding elastic constant is large. According to the classification of hydrogen bonded crystals to different structure types, done by Amoros and Amoros, AFB can be considered as the crystal whose molecules are joined in three dimensional framework. As has been shown in sec. 3.2.1, AFB consists of three types of tetrahedra $(NH_4)_I$, $(NH_4)_{II}$ and BeF_4. Their bond lengths and bond angles show that these tetrahedra are almost regular with very little anisotropy in the distribution of bond strengths. It does not possess any significant bonding feature along any direction as is present in layer or chain type structures. Hence one should not expect to observe much variation in the value of the constants C_{11}, C_{22}, C_{33}. Similar results should be expected for shear constants C_{44}, C_{55}, C_{66}. As seen in table 4.1, in fact, very little anisotropy is actually observed in experimentally obtained elastic constant values.

An estimate of hardness of AFB can be obtained from the mean value (C_{11}') of C_{11}, C_{22}, C_{33}. There is a rough correspondence[74] between C_{11}' and hardness H which is given by $C_{11}' = H^{7/4}$. The hardest known substance, diamond has $C_{11}' = 94 \times 10^{11}$ dynes/cm^2 and corresponding H is ~ 10. On the same scale corresponding to $C_{11}' = 3.3 \times 10^{11}$ dynes/cm^2 for AFB, H is ~ 2. From the crystal structure also one would expect AFB to have low hardness because its molecules are held together by hydrogen bonds which are quite weak as compared to strong covalent bonds in diamond.

REFERENCES

1. R. Pepinsky and F. Jona, (1957) Phys. Rev. 105, 344.

2. Y. Makita and Y. Yamauchi, (1974) J. Phys. Soc. Japan 42, 1425.

3. A. P. Levanyuk and D. G. Sannikov, (1969) JETP 28, 134.

4. M. M. Woolfson, (1961) Direct Methods in Crystallography, Oxford: O.U.P.

5. D. W. J. Cruickshank, (1956b) Acta Cryst. 17, 142.

6. V. Schomaker and K. N. Trueblood, (1968) Acta Cryst. B24, 63.

7. D. W. J. Cruickshank, (1956) Acta Cryst. 9, 1005.

8. M. Born, (1942-43) Rep. Prog. Phys. 9, 294.

9. R. W. James, (1967) "The Optical Principles of the Diffraction of X-ray", G. Bell and Sons, London.

10. J. C. Slater, (1958) Rev. Mod. Phys. 30, 197.

11. W. A. Wooster, (1962) "Diffuse X-ray Reflections from Crystals", Clarendon Press, Oxford.

12. W. Cochran, (1969) "Lattice Dynamics", Benjamin.

13. J. Laval, (1938) C.R. Acad. Sci. Paris 207, 169.
, (1943) J. Phys. Rad. 4, 1.
, (1951a) C.R. Acad. Sci. Paris, 232, 1947.
, (1957) J. Phys. Rad. 18, 247, 289, 369.

14. K. Lonsdale and H. Smith, (1941) Proc. Roy. Soc. A179, 8.
, (1941) Nature Lond. 148, 628.
, (1942) Ibid. 149, 21.

15. G. N. Ramachandran and W. A. Wooster (1951a,b) Acta Cryst. 4, 335 and 431.

16. I. Waller, (1923) Z. Phys. 17, 398.
, (1925) Dissertation, Uppsala.
, (1928) Z. Phys. 51, 213.

17. H. Faxen, (1923) Z. Phys. 17, 266.

18. H. A. Jahn, (1942) Proc. Roy. Soc. A179, 320.

19. W. Voigt, (1910-1928) "Lehrbuch der Kristall Physik", Leipzig, Tenbner.

20. M. Born, (1909-1915-1926), "Atom theorie des Festen Zustandes Ency. Math.", Wiss.

21. W. A. Wooster, (1938) "Crystal Physics", Camb. Univ. Press.

22. A.E.H. Love, (1944) "Mathematical Theory of Elasticity", Dover.

23. J.F. Nye, (1957) "Physical Properties of Crystals", Clarendon Press, Oxford.

24. R. S. Krishnan, (1958) Prog. in Crystal Phys. 1, 73.

25. H. B. Huntington, (1958) "Solid State Physics" 7, 213. Acad. Press.

26. S. Bhagavantam, (1966) "Crystal Symmetry and Physical Properties", Acad. Press.

27. K. Viswanathan, (1954) Proc. Ind. Acad. Sci. A39, 196.
, (1955) Ibid. A41, 98.

28. Le Corre, (1953) Bull. Soc. France. Miner. Cryst. 76, 464.
, (1954) Ibid. 77, 1363 and 1393.
, (1956) J. Phys. Rad. 17, 924.
, (1958) Ibid. 19, 541.

29. C. V. Raman and K. Viswanathan, (1955) Proc. Ind. Acad. Sci. 42(1), 51.

30. N. Joel and W. A. Wooster, (1958) Acta Cryst. 11, 573.
, (1960) Acta Cryst. 13, 516.

31. R. S. Krishnan, V. Chandrasekharan and E. S. Rajagopal, (1958) Nature, Lond. 182, 518.

32. P. L. Mukherjee, (1944) Indian J. Phys. 18, 148.

33. W.A. Wooster, G.N. Ramachandran and A. Lang, (1949), J. Sci. Instr. 26, 156.
D.A. Lind, W. J. West and J.W.M. DuMond, (1950), Phys. Rev. 77, 475.
J.M.J. Cowley, (1950) J. Appl. Phys. 21, 24.

34. L. V. Azaroff, (1955) Acta Cryst. 18, 88.

35. G. Albrecht, (1939) Rev. Sci. Instrum. 10, 221.

36. S. C. Prasad and W. A. Wooster, (1955) Acta Cryst. 8, 361, 507, 614, 682.
, (1956) Acta Cryst. 9, 35, 38, 169, 304.

37. J. L. Amoros and M. Amoros, (1968) "Molecular Crystals", John Wiley.

38. K. Lonsdale, (1968) Nature, Lond. 21, 149.

39. R. Hultgren, (1934) Zeitschr. f. Kristallographie. 88, 233.

40. B. Singh, (1962) "Ferroelectric and structural mechanism of the Ammonium sulphate transition", Doctoral Dissertation, The Pennsylvania State University.

41. Locally written normalized structure factor programme, McMaster University, Canada.

42. Locally written least squares programme, McMaster University, Canada.

43. "International Tables for X-ray Crystallography", (1974) Vol. IV, Birmingham: Kynoch Press.

44. D. Cromer and J. Mann, (1968) Acta Cryst. A24, 321.

45. W.J.A.M. Peterse and J.H. Palm, (1966) Acta Cryst. 20, 147.

46. W. R. Busing, K.O. Martin and H.A. Levy, (1962) Program reports ORNL-TM-305 Oak Ridge National Laboratory.

47. P. J. Vicat, D. Tranqui, S. Aleonard and P. Richard, (1974) Acta Cryst. B30, 2678.
J. LE. Roy and S. Aleonard, (1972) B28, 1383.

48. A. Garg and R. C. Srivastava, (1979) Acta Cryst. B35, 1429.

49. D.W.J. Cruickshank, (1956b) Acta Cryst. 9, 915.

50. E.G. Cox, D.W.J. Cruickshank and J.A.S. Smith, (1958) Proc. Roy. Soc. London 247, 1.

51. E. O. Schlemper and W. C. Hamilton, (1966), The Journal of Chemical Physics 44, no. 12, 4498.

52. Y. S. Jain, (1974) Ph.D. Thesis, I.I.T. Kanpur.
, (1978) Proc. Indian Acad. of Sci. 87, no. 1, 45.

53. P. Venkateswarlu, H.D. Bist and Y.S. Jain, (1975) J. Raman Spectroscopy 3, 143.

54. TLS Computer program of V. Schomaker and K.N. Trueblood, (1968) Acta. Cryst. B24, 63.

55. E. Prince and W. A. Wooster, (1951) Acta Cryst. 4, 191.
, (1953) Acta Cryst. 6, 450.

56. R. C. Srivastava and S. C. Chakraborty, (1962) J. Phys. Soc. Japan. 17, 1767.

57. S. K. Joshi and B. M. Kashyap, (1964) Acta Cryst. 17, 629.

58. S. Chandra and M. P. Hemkar, (1973) Acta Cryst. A29, 25.

59. S. D. Phatak, R. C. Srivastava and E. C. Subbarao, (1972) Acta Cryst. A28, 227.

60. P. Anderson, (1960) Fizika Dielectrikov, ed. G.I. Skanavi, Lebedeva, Moscow.

61. W. Cochran, (1960) Advan. Phys. 9, 387.
, (1961) Advan. Phys. 10, 401.
, (1967) Symp. Ferroelectricity, Ed. Weller, Elsevier, Pub. Co., 62.
, (1969) Lattice Dynamics, Benjamin, 93.

62. Yu. A. Popkov, V.F. Shabanov, V. V. Eremenko and K. S. Aleksandrov, (1976) Low Temperature Physics, 1, 936.

63. M. Wada, A. Sawada, Y. Ishibashi and Y. Takagi, (1977) J. Phys. Soc. Japan. 43, no. 3, 950.

64. M. Iizumi and K. Gesi, (1976) JAERI-memo 6796.

65. S. Hoshino, K. Vedam, Y. Okaya and R. Pepinsky, (1958) Phys. Rev. 112, no. 2, 405.

66. W. A. Wooster, (1961) Acta Cryst. 14, 571.

67. N. Joel and W. A. Wooster, (1957) Nature London 180, 430.

68. Radha and E. S. Rajgopal, (1968) Ind. Inst. Sci. 50, 26.

69. H.B. Huntington, (1958) "Solid State Physics", Vol. 7, Chap. III, Academic Press Inc., New York.

70. M. Blackman, (1955) "Handbuch der Physik" (Springer Verlag, Berlin), Vol. VII, part 1, 341.
J. de Launay, (1956) "Solid State Physics", Vol. 2, 286, Academic Press Inc. New York.
N.M. Wolcott, (1959) J. Chem. Phys. 31, 536.

71. R. A. Robie and J. L. Edwards, (1966) J. Appl. Phys. 37, no. 7, 2659.

72. O. L. Anderson, (1963) J. Phys. Chem. Solids 24, 909.

73. F.E. Borgnis, (1955) Phys. Rev. 98, 1000.

74. W. A. Wooster, (1953) Reports on Progress in Physics, 16, 76.

APPENDIX I

MEASUREMENT OF DIRECT BEAM INTENSITY (I_o)

To determine the elastic constants it is necessary to measure the absolute value of the incident intensity I_o. The direct beam is too strong to be measured directly by any counter hence if a direct measurement was desired, the beam must be attenuated first so that the mean time interval between the arrival of X-ray quanta is appreciably more than the dead time of the counter. Attenuation of monochromatic beam can be done by using multiple foils, but since the reduction factor is of the order of 10^6, small error in the measurement of thickness or μ can lead to large errors[1] in I_o. This method has therefore not been used.

Compton scattering from a substance consisting of light elements and known chemical composition such as diamond[2] can be used as an intermediate standard. The incident X-ray beam is allowed to fall on the diamond crystal set at any convenient angle (θ_{111} or θ_{220}) to the incident beam. The radiation of modified wave-length scattered in direction well away from Bragg reflections (about 8° to 10° on either side) has an intensity which may be calculated from the fundamental constants and may be

compared directly with the thermal diffuse scattering under investigation. The intensity of diffuse reflection is given by equation 2.3 as follows

$$\frac{I_d}{I_o} = \frac{\varepsilon^2 kT\,\Omega}{V^2} F_T^2 \frac{|\vec{X}|^2}{|\vec{q}|^2} K[uvw]_{hkl}$$

The symbols have been explained in sec. 1.B.1. Wooster[3] has defined thermal diffuse scattering power (D) as the ratio of the thermal diffuse intensity per unit cell of the crystal per unit solid angle to that scattered by a single Thomson electron under the same conditions. Its value is given by

$$D = \frac{kT}{V} F_T^2 \frac{|\vec{X}|^2}{|\vec{q}|^2} K[uvw]_{hkl}$$

Hence

$$\frac{I_d}{I_o} = \frac{\varepsilon^2 D\Omega}{V}$$

In an analogous manner, one can define Compton diffuse scattering power (D_c) as the ratio of the intensity scattered by the Compton effect per unit cell of the crystal per unit solid angle to that scattered by a single Thomson electron under the same conditions.

Hence

$$\frac{I_c}{I_o} = \frac{\varepsilon^2 D_c \Omega}{V} \qquad \text{(I-1)}$$

where I_c is the intensity (after applying absorption correction) of Compton scattering per unit volume of diamond, Ω is the solid angle subtended by counter collimator slit at the crystal and V is the volume of the unit cell of diamond.

For diamond, the Compton diffuse intensity can be calculated theoretically and is given by[4]

$$D_c = 8 (6 - \Sigma f_{ec}^2) / B^3$$

where Σf_{ec}^2 is a function which describes the effect of the individual carbon atom scattering incoherently and its values are listed[4] as a function of 2θ. B is the Breit-Dirac correction factor which arises due to the scattering by the recoiling electron in the Compton process. Its value is given by

$$B = 1 + \frac{2h\lambda}{mc} (\sin^2\theta/\lambda^2)$$

Hence from eqn. (I-1) the absolute intensity (I_o) of the incident beam can be determined.

The diamond crystal used in the present case was taken out from a glass cutter. It was ground in a spherizer to remove surface irregularities. The quality of the crystal was checked by taking Laue photographs. It was then aligned along [110] on Weissenberg camera and shifted over

to the diffractometer, fitted with a quartz crystal monochromator as discussed in sec. 2.B.1, for the measurement of Compton diffuse intensity. The volume of the crystal (δV) immersed in the X-ray beam was calculated graphically from the area of cross-section of the crystal and the width of the beam. Its value along with other quantities is given in the description of table I-1.

Description of Table I-1

Column	Description
1	Angle (θ) which the incident X-ray beam makes with $[\bar{1}10]$ of diamond crystal.
2	Polarization factor $P = \frac{1 + \cos^2 2\alpha \cos^2 2\theta}{1 + \cos^2 2\alpha}$, where 2α is the angle of diffraction of the monochromatic beam from the quartz crystal.
3	Value of B (Breit Dirac factor).
4	Calculated Compton diffuse scattering flux D_c.
5	Observed Compton diffuse intensity I_c, corrected for absorption, per unit volume of diamond crystal.
6	Direct beam intensity I_o.

For Diamond

Volume (V) of the unit cell	$= 4.50 \times 10^{-23}$ c.c.
Linear absorption coefficient (μ) for MoK_α	$= 1.9375$ cm^{-1}
Volume (δV) of the crystal immersed in the X-ray beam	$= 8.27 \times 10^{-4}$ c.c.
Solid angle (Ω)	$= 4.31 \times 10^{-4}$
ε^2	$= 7.935 \times 10^{-26} \times P$

Table I-1

Data for the Calculation of Direct Beam Intensity, I_o

Angle with [$\bar{1}$10]	P	B	D_c	I_c $\times 10^{-3}$	I_o $\times 10^{-7}$
24.365	0.724	1.0116	38.188	2.292	1.091
25.365	0.707	1.0125	38.580	2.245	1.083
26.365	0.691	1.0134	38.815	2.257	1.107
27.365	0.674	1.0144	39.038	2.225	1.113
28.365	0.658	1.0154	39.254	2.187	1.114

Average Value of the Direct Beam Intensity, $I_o = 1.102 \times 10^{7}$ c.p.s.

REFERENCES : APPENDIX I

1. W. A. Wooster, (1962) "Diffuse X-ray reflections from Crystals". Clarendon Press, Oxford.

2. E. Prince and W. A. Wooster, (1953) Acta Cryst. 6, 450.

3. Same as 1.
G. N. Ramachandran and W. A. Wooster (1951a) Acta Cryst. 4, 335.

4. R. W. James, (1948) "Optical Principles of the Diffraction of X-rays", G. Bell and Sons, London.

A. H. Compton and S. K. Allison, (1935) "X-rays in Theory and Experiments". 782, Von Nostrand.

International tables for X-ray Crystallography, (1963) Vol. III, 134, 135, 232, 247-253, Kynoch Press.

APPENDIX II

OBSERVATIONS AND CALCULATIONS : TABLES AND GRAPHS

for the determination of elastic constants from thermal diffuse scattering study.

Description of tables A-1 to A-14

Column	Description
1	The angle of incident beam with certain given direction
2	Observed diffuse intensity, I_{obs} (counts per second, c.p.s.) corrected for absorption, per unit volume of the crystal.
3	Correction factor = $\frac{\text{Skew (S)}}{\text{Polarization (P)}}$ x Divergence (D)
4	Corrected intensity I_d'' (I+II order) = I_{obs} x $\frac{S.D}{P}$
5	Ratio of I_d'' to direct beam intensity I_o
6	Square of the wavelength (λ^2) of the elastic wave relevant to the specific direction.

The intensity I_B due to general scattering is given at the end of each table. The graphs have been plotted between $\frac{I_d}{I_o}$ $(= \frac{I_d''}{I_o} - \frac{I_B}{I_o})$ vs λ^2 for a given rekha of a given plane for all the planes that have been used to calculate the elastic constants.

The formula (eqn. 2.3) used for the calculations of elastic constants is given as follows

$$\frac{I_d}{I_o} = \frac{\epsilon^2 kT\Omega}{V^2} F_T^2 \frac{|\vec{x}|^2}{|\vec{q}|^2} K[uvw]_{hkl} \qquad (2.3)$$

The symbols have been explained in sec. 1.B.1. Eqn. (2.3) can be written as

$$\frac{I_d}{I_o} \times |\vec{q}|^2 = \frac{I_d}{I_o}/\lambda^2 = \frac{\epsilon^2 kT\Omega}{V^2} F_T^2 \, |\vec{X}|^2 \, K[uvw]_{hkl}$$

or $$\frac{I_d}{I_o}/\lambda^2 = G \times K[uvw]_{hkl} \qquad (1)$$

where $$G = \frac{\epsilon^2 kT\Omega}{V^2} F_T^2 \, |\vec{X}|^2$$

and has a constant value at temperature T for a given reciprocal lattice point.

$K[uvw]_{hkl}$ and hence the corresponding C_{ij} (Table 1.1) can be evaluated from equation (1), knowing the slope of the graph between $\frac{I_d}{I_o}$ vs λ^2 for a given rekha [uvw] of a given plane (hkl) and G value of the same plane. Some relevant data required for the calculation of G for all the planes studied is given in Table A.

Table A

Data of Planes used and their G Values

Solid Angle (Ω) = 4.31×10^{-4}

Plane Studied	Axis of Rotation	Structure Factor F_T	Rec. Lattice Vector X $\times 10^{-8}$ cm^{-1}	Volume of the Crystal $\times 10^{4}$ cc	Constant G
040	100	55.43	0.6756	7.406	9114.47
004	100	72.94	0.3827	6.875	5063.63
013	100	42.13	0.3337	6.790	1284.76
004	010	72.94	0.3827	6.837	5063.63
400	010	14.53	0.5227	16.057	374.98
301	010	70.11	0.4043	15.670	5222.49
020	001	53.68	0.3378	7.175	2137.83
040	001	55.43	0.6756	7.338	9114.47

II.1

Observation data along different directions of propagation [uvw] of the thermal wave for various reciprocal lattice points hkl and calculations of the elastic constants.

Table A-1(a,b)

Angle of incident beam with [010]	Diffuse intensity corrected for absorption $\times 10^{-3}$	Correction factor SxD/P	Corrected intensity (due to I order) $I''_d \times 10^{-3}$	I''_d/I_o $\times 10^{4}$	$\lambda^2=1/q^2$ $\times 10^{-3}$
		Rekha [010] 004			
8.915	9.979	1.192	11.896	10.795	18.524
9.015	9.107	1.127	10.263	9.313	15.565
9.215	7.428	1.043	7.749	7.032	11.434
9.515	4.877	1.060	5.168	4.690	7.753
9.815	3.555	0.988	3.514	3.189	5.600
		Rekha [010] 004			
6.615	8.470	1.083	9.171	8.322	13.262
6.315	7.876	0.966	7.605	6.901	9.960
6.215	6.940	0.889	6.170	5.599	8.753
6.015	6.130	0.833	5.104	4.632	6.915
5.915	4.629	0.833	3.857	3.500	6.206

$K_{004}^{\pm}[010]=1/C_{44}$

	1(a)	1(b)
Value of (I_B/I_o)	$=0.9 \times 10^{-4}$	1.0×10^{-4}
Value of the slope $(I_d/I_o)/^2$ from Figs. A1 and A7	$=5.27 \times 10^{-8}$	5.50×10^{-8}
Value of C_{44}, uncorrected for 2nd order diffuse reflection, $\times 10^{-11}$	$=0.961$	0.921 dynes/cm^2
Corrected value of $C_{44} \times 10^{-11}$	$=0.977$	0.950 dynes/cm^2
Average value of C_{44}	$=0.963 \times 10^{11}$ dynes/cm^2	

Table A-2(a,b)

Angle of incident beam with [001]	Diffuse intensity corrected for absorption $\times 10^{-3}$	Correction factor SXD/P	Corrected intensity (due to I''_d order) $I''_d \times 10^{-3}$	I''_d/I_o $\times 10^{4}$	$\lambda^2 = 1/q^2$ $\times 10^{-3}$
		Rekha [001]$^{+}_{040}$			
12.89	6.307	1.226	7.731	7.015	7.192
12.69	5.800	1.140	6.611	5.999	4.994
12.49	4.552	1.020	4.643	4.214	3.669
12.29	3.879	0.993	3.852	3.496	2.808
12.09	2.900	0.971	2.815	2.555	2.219
		Rekha [001]$^{-}_{040}$			
14.99	6.348	1.183	7.507	6.813	5.943
15.19	4.986	1.112	5.545	5.032	4.255
15.39	4.873	1.017	4.957	4.498	3.195
15.59	3.240	1.022	3.312	3.005	2.488
15.89	2.361	1.026	2.423	2.199	1.797

$K[001]^{+}_{040} = 1/C_{44}$

	1(a)	1(b)
Value of (I_B/I_o)	$=0.8 \times 10^{-4}$	0.9×10^{-4}
Value of the slope $(I_d/I_o)/^{2}$ from Figs. A1 and A7	$=9.20 \times 10^{-8}$	9.61×10^{-8}
Value of C_{44}, uncorrected for 2nd order diffuse reflection, $\times 10^{-11}$	$=0.991$	0.949 dynes/cm^2
Corrected value of $C_{44} \times 10^{-11}$	$=0.962$	0.956 dynes/cm^2
Average value of C_{44}	$=0.959 \times 10^{11}$ dynes/cm^2	

Table A-3(a,b)

Angle of incident beam with [100]	Diffuse intensity corrected for absorption $\times 10^{-3}$	Correction factor SxD/P	Corrected intensity (due to I order) $I''_d \times 10^{-3}$	I''_d/I_o $\times 10^{4}$	$\lambda^2=1/q^2$ $\times 10^{-3}$
		Rekha [100]/004			
6.715	9.974	1.070	10.669	9.682	18.524
6.515	7.801	1.044	8.141	7.388	13.262
6.315	6.245	1.038	6.482	5.882	9.960
9.215	5.665	1.024	5.801	5.264	8.753
6.015	5.045	0.898	4.528	4.109	6.915
5.195	4.564	0.943	4.304	3.905	6.206
		Rekha $[\bar{1}00]/004$			
8.915	9.563	1.205	11.524	10.457	18.524
9.015	8.199	1.134	9.298	8.438	15.524
9.215	7.394	1.058	7.823	7.099	11.434
9.515	5.202	1.047	5.447	4.943	7.753
9.815	4.205	1.001	4.209	3.819	5.600

$K[\bar{1}00]^{+}_{004} = 1/C_{55}$

	1(a)	1(b)
Value of (I_B/I_o)	$=0.8 \times 10^{-4}$	0.9×10^{-4}
Value of the slope $(I_d/I_o)/^2$ from Figs. A3 and A9	$=5.10 \times 10^{-8}$	4.98×10^{-8}
Value of C_{55}, uncorrected for 2nd order diffuse reflection, $\times 10^{-11}$	$=0.993$	1.017 dynes/cm^2
Corrected value of $C_{55} \times 10^{-11}$	$=1.008$	1.024 dynes/cm^2

Average value of C_{55} $= 1.016 \times 10^{11}$ dynes/cm^2

Table A-4(a,b)

Angle of incident beam with [100]	Diffuse intensity corrected for absorption $\times 10^{-2}$	Correction factor SxD/P	Corrected intensity (due to I order) $I''_d \times 10^{-2}$	I''_d/I_o $\times 10^{5}$	$\lambda^2=1/q^2$ $\times 10^{-3}$
		Rekha [001]$^{+}_{400}$			
11.705	14.084	1.161	16.347	14.834	12.012
11.805	12.954	1.138	14.739	13.375	9.927
12.005	13.491	0.988	13.332	12.098	7.107
12.305	12.405	1.003	12.440	11.289	4.690
12.705	11.447	1.026	11.740	10.654	3.001
		Rekha [00$\bar{1}$]$^{+}_{400}$			
9.505	16.427	0.848	13.935	12.645	8.340
9.305	14.240	0.922	13.125	11.910	6.127
9.205	13.270	0.955	12.666	11.494	5.337
9.005	12.066	1.016	12.259	11.124	4.154
8.805	11.518	1.036	11.937	10.832	3.326

$K[00\bar{1}]^{+}_{400} = 1/C_{55}$

	1(a)	1(b)
Value of (I_B/I_o)	$=0.95\times10^{-4}$	0.93×10^{-4}
Value of the slope $(I_d/I_o)/^2$ from Figs. A4 and A10	$=.383\times10^{-8}$	$.381\times10^{-8}$
Value of C_{55}, uncorrected for 2nd order diffuse reflection, $\times10^{-11}$	$=0.978$	0.987 dynes/cm^2
Corrected value of $C_{55}\times10^{-11}$	$=0.998$	1.017 dynes/cm^2
Average value of C_{55}	$=1.008\times10^{11}$ dynes/cm^2	
Mean value of C_{55} from tables A-3(a,b) and A-4(a,b)	$=1.012\times10^{11}$ dynes/cm^2	

Table A-5(a,b)

Angle of incident beam with [100]	Diffuse intensity corrected for absorption $\times 10^{-3}$	Correction factor SxD/P	Corrected intensity (due to I order) $I''_d \times 10^{-3}$	I''_d/I_o $\times 10^{4}$	$\lambda^2=1/q^2$ $\times 10^{-3}$
		Rekha [100]$_{020}^{+}$			
7.895	7.372	1.331	9.810	8.902	28.757
7.995	6.446	1.281	8.260	7.496	23.765
8.095	5.652	1.250	7.067	6.413	19.968
8.295	4.286	1.189	5.009	4.627	14.667
8.495	3.752	1.166	4.376	3.671	11.230
8.895	2.621	1.135	2.975	2.700	7.185
		Rekha [$\bar{1}$00]$_{020}^{-}$			
5.795	8.542	1.075	9.183	8.333	23.765
5.595	7.026	1.021	7.174	6.510	17.014
5.395	6.010	0.940	5.651	5.128	12.778
5.195	5.036	0.888	4.471	4.057	9.947
4.995	4.662	0.832	3.879	3.520	7.762

$K[100]^{+}_{020}=1/C_{66}$

	1(a)	1(b)
Value of (I_B/I_o)	$=0.8 \times 10^{-4}$	0.8×10^{-4}
Value of the slope $(I_d/I_o)/^{2}$ from Figs. A5 and A11	$=2.80\times10^{-8}$	2.85×10^{-8}
Value of C_{66}, uncorrected for 2nd order diffuse reflection, $\times 10^{-11}$	$=0.764$	0.750 dynes/cm^2
Corrected value of $C_{66} \times 10^{-11}$	$=0.782$	0.769 dynes/cm^2
Average value of C_{66}	$=0.776\times10^{11}$ dynes/cm^2	

Table A-6(a,b)

Angle of incident beam with [100]	Diffuse intensity corrected for absorption I_d x10^{-3}	Correction factor SxD/P	Corrected intensity (due to I order) I''_d x10^{-3}	I''_d/I_o x10^{4}	$\lambda^2=1/q^2$ x10^{-3}
		Rekha [100]$_{040}^{+}$			
14.99	6.607	1.104	8.847	8.028	5.943
15.19	5.263	1.027	6.658	6.042	4.255
15.39	5.137	1.015	5.214	4.731	3.195
15.59	4.635	0.956	4.431	4.021	2.488
15.89	2.855	0.898	3.341	3.031	1.797
		Rekha [$\bar{1}$00]$_{040}^{-}$			
12.89	8.692	1.168	10.152	9.212	7.192
12.69	7.261	1.090	7.916	7.183	4.994
12.49	5.834	1.028	5.999	5.443	3.669
12.29	4.746	0.991	4.703	4.268	2.808
12.09	4.073	0.971	3.955	3.589	2.219

$K[100]_{040}^{+-}=1/C_{66}$

	1(a)	1(b)
Value of (I_B/I_o)	= 0.9 x10^{-4}	1.0 x10^{-4}
Value of the slope $(I_d/I_o)/^2$ from Figs. A5 and A11	=11.61x10^{-8}	11.82x10^{-8}
Value of C_{66}, uncorrected for 2nd order diffuse reflection, x10^{-11}	= 0.785	0.772 dynes/cm^2
Corrected value of C_{66} x10^{-11}	= 0.810	0.806 dynes/cm^2

Average value of C_{66} = 0.808x10^{11} dynes/cm^2

Mean value of C_{66} from tables A-5(a,b) and A-6(a,b) = 0.792x10^{11} dynes/cm^2

Table A-7(a,b)

Angle of incident beam with $\bar{[103]}$	Diffuse intensity corrected for absorption $\times 10^{-2}$	Correction factor SxD/P	Corrected intensity (due to I order) $I''_d \times 10^{-2}$	I_d/I_o $\times 10^{5}$	$\lambda^2 = 1/q^2$ $\times 10^{-3}$
		Rekha [100] 301			
7.36	20.905	0.935	19.546	17.728	4.879
7.26	17.994	0.967	17.404	15.793	3.891
7.06	14.078	1.025	15.235	13.825	2.619
6.86	12.627	1.082	13.665	12.400	1.864
6.66	11.317	1.134	12.838	11.651	1.382
		Rekha [100] 301			
9.16	23.195	0.941	21.831	19.810	6.314
9.36	16.967	1.073	18.199	16.515	4.304
9.56	14.502	1.122	16.269	14.763	3.190
9.76	12.899	1.129	14.573	13.224	2.459
9.96	10.961	1.282	14.056	12.755	1.964
10.16	10.006	1.323	13.235	12.010	1.612

$K^{\pm}_{[100]}{}_{301} = L^2/C_{11} + N^2/C_{55}$; L=0.9715 N=0.2371

	1(a)	1(b)
Value of (I_B/I_o)	$=0.95\times10^{-4}$	0.95×10^{-4}
Value of the slope $(I_d/I_o)/^2$ from Figs. A4 and A10	$=1.60\times10^{-8}$	1.67×10^{-8}
Value of C_{11}, uncorrected for 2nd order diffuse reflection, $\times10^{-11}$	=3.763	3.581 dynes/cm^2
Corrected value of $C_{11}\times10^{-11}$	=3.881	3.763 dynes/cm^2

Average value of C_{11} $=3.822\times10^{11}$ dynes/cm^2

Table A-8(a,b)

Angle of incident beam with $\bar{[031]}$	Diffuse intensity corrected for absorption $\times 10^{-2}$	Correction factor SxD/P	Corrected intensity (due to I order) $I''_d \times 10^{-2}$	I''_d/I_o $\times 10^{5}$	$\lambda^2=1/q^2$ $\times 10^{-3}$
		Rekha $[010]_{013}$			
8.01	27.320	1.217	33.249	30.172	19.607
8.11	24.790	1.183	29.327	26.613	16.697
8.31	22.075	1.168	25.784	23.398	12.521
8.51	18.063	1.197	21.622	19.621	9.739
8.81	15.641	1.141	17.847	16.195	7.017
		Rekha $\bar{[010]}_{013}$			
5.61	30.621	1.116	34.173	31.010	19.920
5.41	25.917	1.055	27.343	24.812	14.653
5.21	22.871	0.983	22.482	20.401	11.232
5.01	21.973	0.934	20.522	18.623	8.885
4.91	21.883	0.913	19.979	18.130	7.979

$K\bar{[010]}_{013} = M^2/C_{22} + N^2/C_{44}$; M=0.5073 N=0.8613

	1(a)	1(b)
Value of (I_B/I_o)	$=0.90 \times 10^{-4}$	0.90×10^{-4}
Value of the slope $(I_d/I_o)/^2$ from Figs. A2 and A8	$=1.083 \times 10^{-8}$	1.089×10^{-8}
Value of C_{22}, uncorrected for 2nd order diffuse reflection, $\times 10^{-11}$	=3.671	3.440 dynes/cm^2
Corrected value of $C_{22} \times 10^{-11}$	=3.671	3.440 dynes/cm^2

Average value of C_{22} $= 3.555 \times 10^{11}$ dynes/cm^2

Table A-9(a,b)

Angle of incident beam with $\bar{[103]}$	Diffuse intensity corrected for absorption $\times 10^{-3}$	Correction factor SxD/P	Corrected intensity (due to I order) $I''_d \times 10^{-3}$	I''_d/I_o $\times 10^{4}$	$\lambda^2=1/q^2$ $\times 10^{-3}$
		Rekha [001] $\bar{3}01$			
9.46	7.028	1.223	8.597	7.801	13.025
9.66	4.934	1.231	6.075	5.513	9.552
9.86	4.809	1.145	5.508	4.998	7.300
10.06	4.320	1.098	4.743	4.304	6.678
10.26	2.765	1.088	3.008	2.730	4.654
		Rekha [001] $\bar{3}01$			
6.96	8.274	0.906	7.496	6.802	11.337
6.76	5.621	0.978	5.496	4.988	8.529
6.56	4.462	0.994	4.437	4.026	8.650
6.36	3.839	1.002	3.846	3.490	5.332
6.16	3.329	1.034	3.442	3.124	4.372

$K[001]^{+}_{\bar{3}01} = L^2/C_{55} + N^2/C_{33}$; L=0.9715 N=0.2371

	1(a)	1(b)
Value of (I_B/I_o)	$=0.95\times10^{-4}$	0.9×10^{-4}
Value of the slope $(I_d/I_o)/^2$ from Figs. A3 and A9	$=4.98\times10^{-8}$	5.00×10^{-8}
Value of C_{33}, uncorrected for 2nd order diffuse reflection, $\times10^{-11}$	=2.636	2.267 dynes/cm^2
Corrected value of $C_{33}\times10^{-11}$	=2.636	2.267 dynes/cm^2
Average value of C_{33}	$=2.451\times10^{11}$ dynes/cm^2	

Table A-10(a,b)

Angle of incident beam with [100]	Diffuse intensity corrected for absorption	Correction factor	Corrected intensity (due to I order)	I_d''/I_o	$\lambda^2=1/q^2$
	$x10^{-2}$	SxD/P	$I_d'' \times 10^{-2}$	$x10^{4}$	$x10^{-3}$
		Rekha $[-1/\sqrt{2},1/\sqrt{2},0]_{020}$			
5.795	25.803	1.175	30.319	27.513	11.431
5.595	20.048	1.108	22.213	20.157	8.125
5.395	18.928	1.020	19.307	17.520	6.059
5.195	18.197	0.974	17.724	16.173	4.683
4.995	16.598	0.941	15.619	14.173	3.721
		Rekha $[1/\sqrt{2},-1/\sqrt{2},0]_{020}$			
7.895	31.981	1.119	35.787	32.475	14.885
8.095	26.361	1.086	28.628	25.978	10.407
8.295	20.373	1.031	21.005	19.061	7.697
8.495	18.625	1.062	19.780	17.949	5.933
8.695	16.965	0.982	16.660	15.118	4.719

$$K[1\bar{+}/\sqrt{2},1\bar{+}/\sqrt{2},0]_{020}=2(C_{11}+C_{66})/[C_{11}(C_{22}+C_{66})+C_{22}C_{66}-2C_{12}C_{66}-C_{12}^2]$$

	1(a)	1(b)
Value of (I_B/I_o)	$=0,8 \times 10^{-4}$	$0,8 \times 10^{-4}$
Value of the slope $(I_d/I_o)/^2$ from Figs. A6 and A12	$=1,47 \times 10^{-8}$	$1,50 \times 10^{-8}$
Value of C_{12}, uncorrected for 2nd order diffuse reflection, $x10^{-11}$	=1,722	1,776 dynes/cm^2
Corrected value of $C_{12} x10^{-11}$	=1,738	1,780 dynes/cm^2
Average value of C_{12}	$=1,759 \times 10^{11}$ dynes/cm^2	

Table A-11(a,b)

Angle of incident beam with [100]	Diffuse intensity corrected for absorption $\times 10^{-2}$	Correction factor SxD/P	Corrected intensity (due to I order) $I''_d \times 10^{-2}$	I''_d/I_o $\times 10^{5}$	$\lambda^2=1/q^2$ $\times 10^{-3}$
		Rekha $[-1/\sqrt{2},1/\sqrt{2},0]_{040}$			
12.89	29.928	1.161	34.746	31.530	3.471
12.69	27.707	1.095	30.339	27.531	2.393
12.49	24.487	0.990	24.242	21.998	1.746
12.29	19.479	0.963	18.758	17.022	1.327
12.09	15.732	0.947	14.898	13.519	1.041
		Rekha $[1/\sqrt{2},-1/\sqrt{2},0]_{040}$			
14.89	29.247	1.283	37.524	34.051	3.723
14.99	26.796	1.254	33.602	30.492	3.087
15.19	22.719	1.169	26.558	24.100	2.225
15.39	20.208	1.120	22.633	20.538	1.683
15.59	17.228	1.056	18.193	16.509	1.319

$$K[1/\sqrt{2},\bar{1}/\sqrt{2},0]_{040}=2(C_{11}+C_{66})/[C_{11}(C_{22}+C_{66})+C_{22}C_{66}-2C_{12}C_{66}-C_{12}^2]$$

	1(a)	1(b)
Value of (I_B/I_o)	$=0.9 \times 10^{-4}$	0.9×10^{-4}
Value of the slope $(I_d/I_o)/^2$ from Figs. A6 and A12	$=6.41\times10^{-8}$	6.50×10^{-8}
Value of C_{12}, uncorrected for 2nd order diffuse reflection, $\times 10^{-11}$	=1.842	1.876 dynes/cm^2
Corrected value of $C_{12} \times 10^{-11}$	=1.809	1.793 dynes/cm^2
Average value of C_{12}	$=1.801\times10^{11}$ dynes/cm^2	
Mean value of C_{12} from tables A-10(a,b) and A-11(a,b)	$=1.780\times10^{11}$ dynes/cm^2	

Table A-12(a,b)

Angle of incident beam with [100]	Diffuse intensity corrected for absorption $\times 10^{-3}$	Correction factor SxD/P	Corrected intensity (due to I order) $I_d'' \times 10^{-3}$	I_d''/I_o $\times 10^{4}$	$\lambda^2=1/q^2$ $\times 10^{-3}$
		Rekha $[-1/\sqrt{2},0,1/\sqrt{2}]_{004}$			
8.815	5.315	1.288	6.846	6.212	10.820
9.015	4.195	1.243	5.218	4.735	7.460
9.315	3.128	1.132	3.541	3.213	4.723
9.515	2.478	1.062	2.632	2.388	3.650
9.815	2.023	1.099	2.223	2.018	2.608
		Rekha $[1/\sqrt{2},0,-1/\sqrt{2}]_{004}$			
6.815	5.153	1.176	6.060	5.499	11.603
6.615	4.559	1.091	4.974	4.513	8.112
6.315	3.713	0.959	3.561	3.231	5.244
6.115	3.735	0.826	3.085	2.799	4.110
5.815	2.981	0.809	2.412	2.188	2.999

$$K[1/\sqrt{2},0,1/\sqrt{2}]_{004}=2(C_{11}+C_{55})/[C_{11}(C_{33}+C_{55})+C_{33}C_{55}-2C_{13}C_{55}-C_{13}^2]$$

	1(a)	1(b)
Value of (I_B/I_o)	$=0.8 \times 10^{-4}$	0.9×10^{-4}
Value of the slope $(I_d/I_o)/^2$ from Figs. A3 and A9	$=4.80\times10^{-8}$	4.67×10^{-8}
Value of C_{13}, uncorrected for 2nd order diffuse reflection, $\times 10^{-11}$	$=1.410$	1.491 dynes/cm^2
Corrected value of $C_{13} \times 10^{-11}$	$=1.496$	1.544 dynes/cm^2

Average value of C_{13} $=1.520\times10^{11}$ dynes/cm^2

Table A-13(a,b)

Angle of incident beam with [001]	Diffuse intensity corrected for absorption $\times 10^{-2}$	Correction factor SxD/P	Corrected intensity (due to I order) $I''_d \times 10^{-2}$	I_d/I_o $\times 10^{5}$	$\lambda^2=1/q^2$ $\times 10^{-3}$
		Rekha $[0,1/\sqrt{2},-1/\sqrt{2}]_{040}$			
14.99	24.671	1.341	33.084	30.022	2.859
15.19	22.068	1.225	27.033	24.531	2.032
15.39	17.482	1.197	20.926	18.989	1.515
15.59	15.877	1.148	18.227	16.540	1.171
15.89	13.119	1.112	14.588	13.238	0.931
		Rekha $[0,-1/\sqrt{2},1/\sqrt{2}]_{040}$			
12.89	30.924	1.249	38.624	35.049	3.723
12.69	23.042	1.199	27.628	25.071	2.603
12.49	22.040	1.084	23.891	21.680	1.925
12.29	21.219	0.981	20.816	18.889	1.484
12.09	18.487	0.958	17.711	16.072	1.180

$$K[0,1/\sqrt{2},1/\sqrt{2}]_{040}=2(C_{44}+C_{33})/[C_{22}(C_{44}+C_{33})+C_{44}C_{33}-2C_{23}C_{44}-C_{23}^2]$$

	1(a)	1(b)
Value of (I_B/I_o)	$=0.9 \times 10^{-4}$	0.9×10^{-4}
Value of the slope $(I_d/I_o)/^2$ from Figs. A2 and A8	$=6.62\times10^{-8}$	6.43×10^{-8}
Value of C_{23}, uncorrected for 2nd order diffuse reflection, $\times 10^{-11}$	$=1.491$	1.434 dynes/cm^2
Corrected value of $C_{23} \times 10^{-11}$	$=1.446$	1.386 dynes/cm^2
Average value of C_{23}	$=1.416\times10^{11}$ dynes/cm^2	

Table A-14(a,b)

Angle of incident beam with [010]	Diffuse intensity corrected for absorption $\times 10^{-3}$	Correction factor SxD/P	Corrected intensity (due to I order) $I''_d \times 10^{-3}$	I''_d/I_o $\times 10^{4}$	$\lambda^2=1/q^2$ $\times 10^{-3}$
		Rekha $[0,1/\sqrt{2},-1/\sqrt{2}]_{004}$			
8,915	4,551	1,335	6,076	5,513	9,621
9,115	3,658	1,206	4,410	4,002	6,935
9,315	3,556	1,092	3,884	3,524	5,244
9,515	2,854	1,059	3,021	2,722	4,110
9,715	2,070	1,063	2,199	1,996	3,312
		Rekha $[0,-1/\sqrt{2},1/\sqrt{2}]_{004}$			
6,815	5,887	1,182	6,956	6,312	10,820
6,615	4,153	1,063	4,415	4,006	7,460
6,415	3,883	1,017	3,947	3,582	5,441
6,215	3,292	0,943	3,103	2,816	4,136
6,015	2,623	0,849	2,227	2,021	3,244

$$K[0,1/\sqrt{2},1/\sqrt{2}]_{004}=2(C_{44}+C_{22})/[C_{22}(C_{44}+C_{33})+C_{44}C_{33}-2C_{23}C_{44}-C_{23}^2]$$

	1(a)	1(b)
Value of (I_B/I_o)	$=0,9 \times 10^{-4}$	$0,9 \times 10^{-4}$
Value of the slope $(I_d/I_o)/^2$ from Figs. A1 and A7	$=4,75\times10^{-8}$	$4,67\times10^{-8}$
Value of C_{23}, uncorrected for 2nd order diffuse reflection, $\times 10^{-11}$	$=1.443$	$1,409$ dynes/cm^2
Corrected value of $C_{23} \times 10^{-11}$	$=1.418$	$1,394$ dynes/cm^2
Average value of C_{23}	$=1,406\times10^{11}$ dynes/cm^2	
Mean value of C_{23} from tables A-13(a,b) and A-14(a,b)	$=1,411\times10^{11}$ dynes/cm^2	

II.2

Graphs showing the variation of diffuse intensity with the square of the wavelength of the thermal wave for various directions of propagation and various reciprocal lattice points: Plots of $\frac{I_d}{I_o}$ vs λ^2.

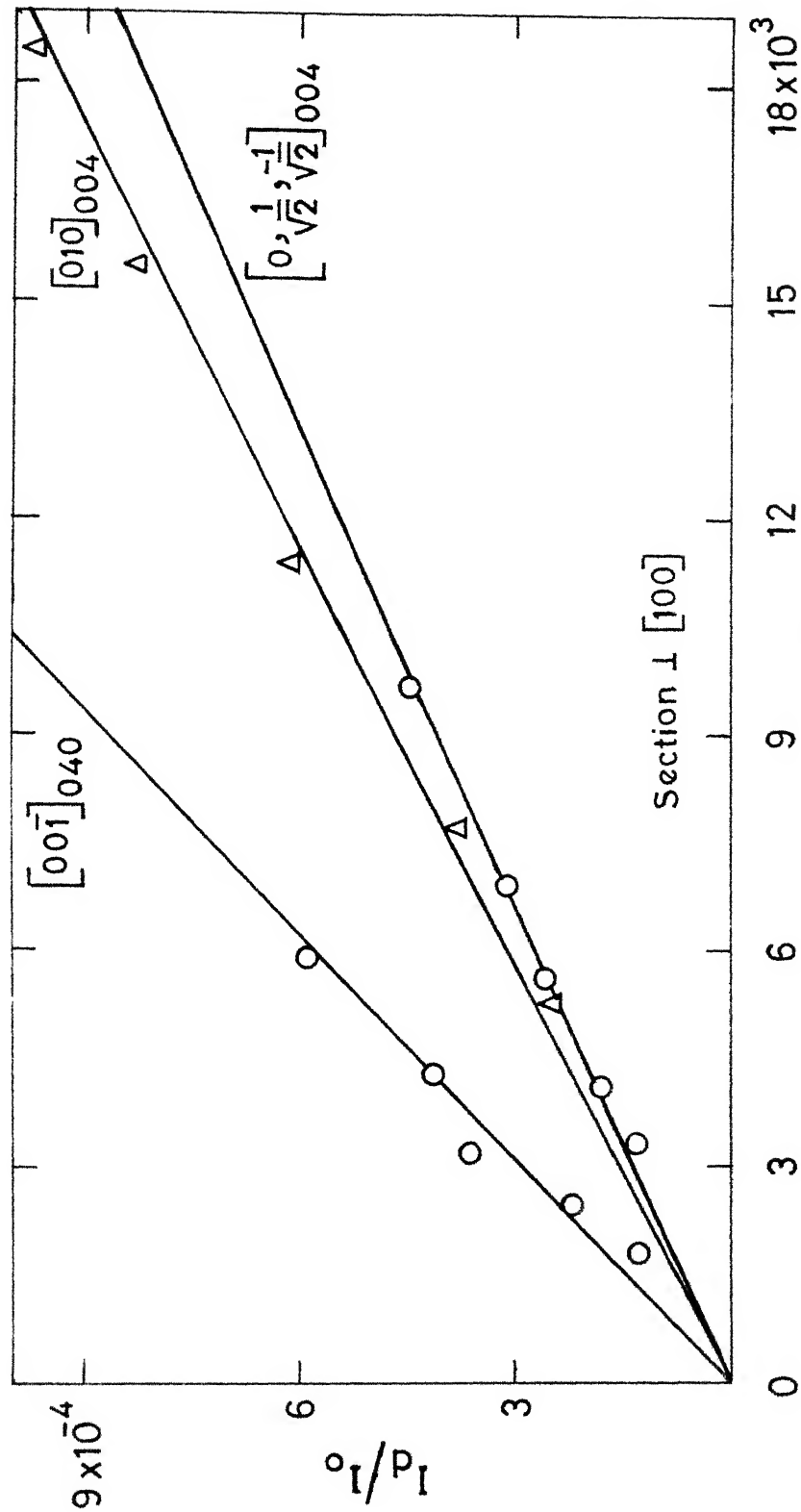
9×10^{-4}
6
3
I_d/I_o
0
3
6
9
12
15
18×10^{-3}
λ^2 in A^{o2}
Section ⊥ [100]
$[00\bar{1}]_{040}$
$[0\bar{1}0]_{004}$
$[0, \frac{1}{\sqrt{2}}, \frac{-1}{\sqrt{2}}]_{004}$

Fig. A1

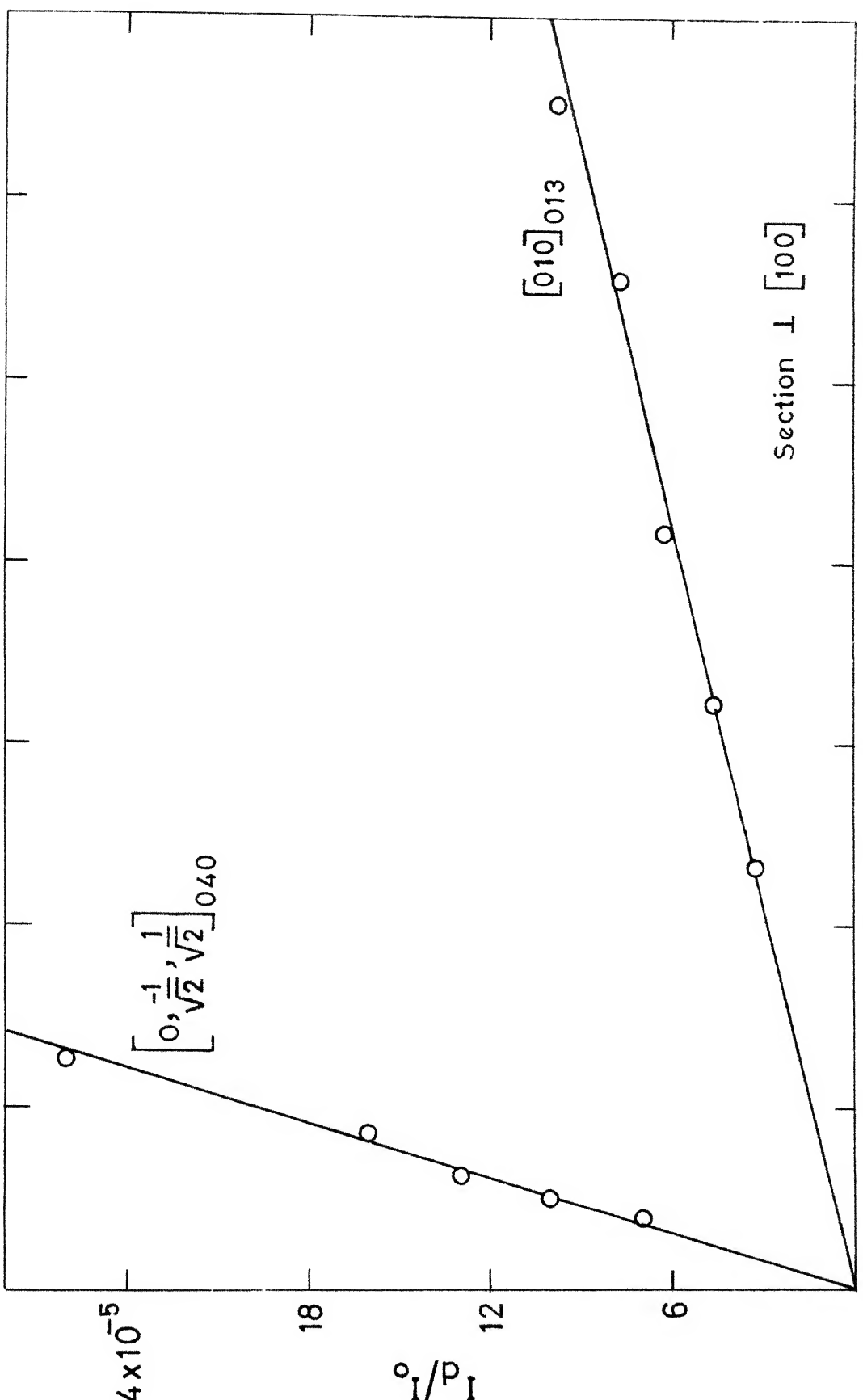
I_d/I_o
24×10^{-5}
18
12
6
0
3
6
9
12
15
18
21×10^3
λ^2 in A^{o2}
Section ⊥ [100]
$[010]_{013}$
$\left[0, \frac{-1}{\sqrt{2}}, \frac{1}{\sqrt{2}}\right]_{040}$

Fig. A2

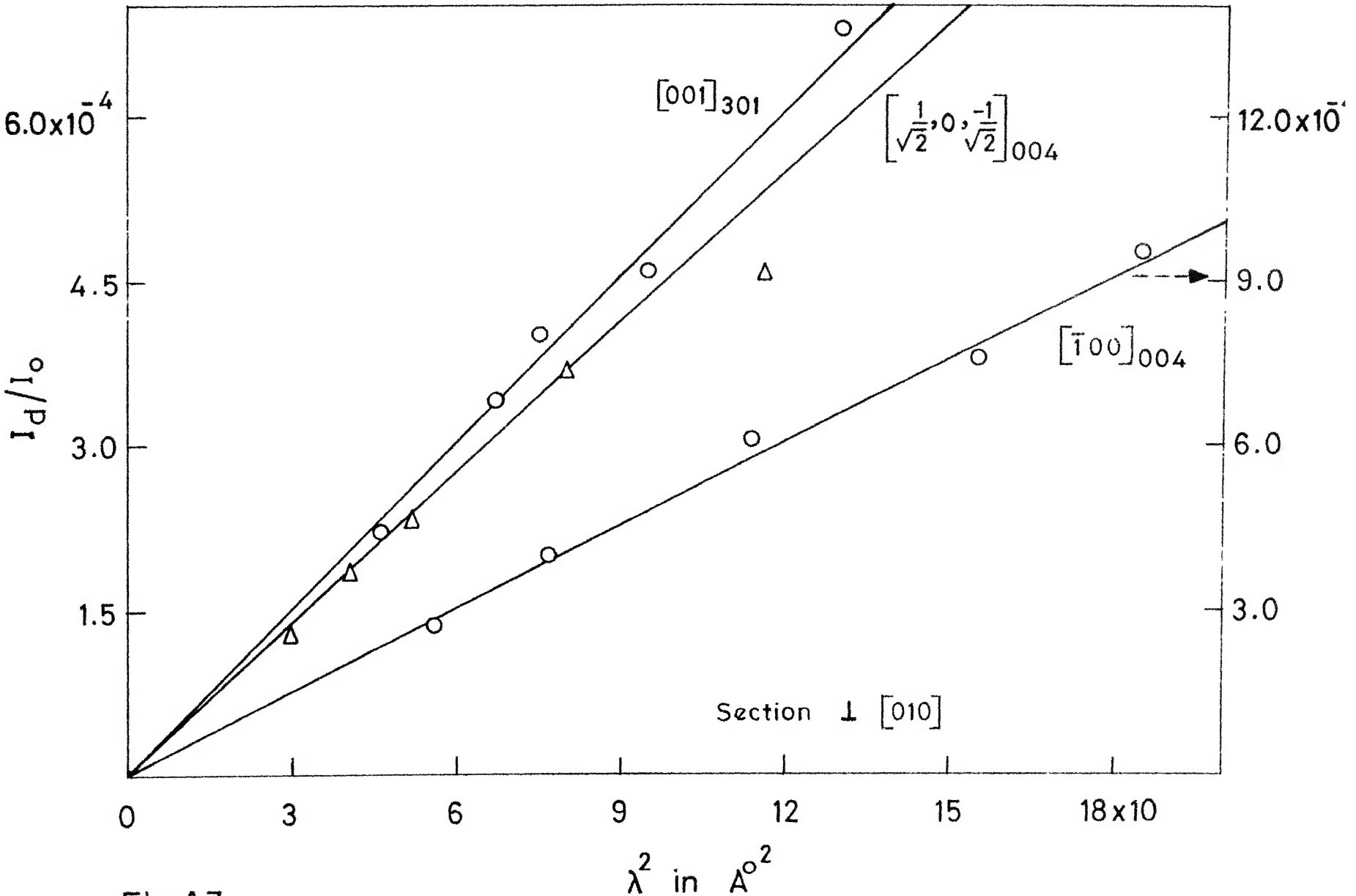
6.0x10⁻⁴
4.5
3.0
1.5
I_d/I_o
[001]301
$\left[\frac{1}{\sqrt{2}},0,\frac{-1}{\sqrt{2}}\right]_{004}$
[$\bar{1}$00]004
12.0x10⁻⁴
9.0
6.0
3.0
Section ⊥ [010]
0
3
6
9
12
15
18x10
λ^2 in A^{o2}

Fig.A3

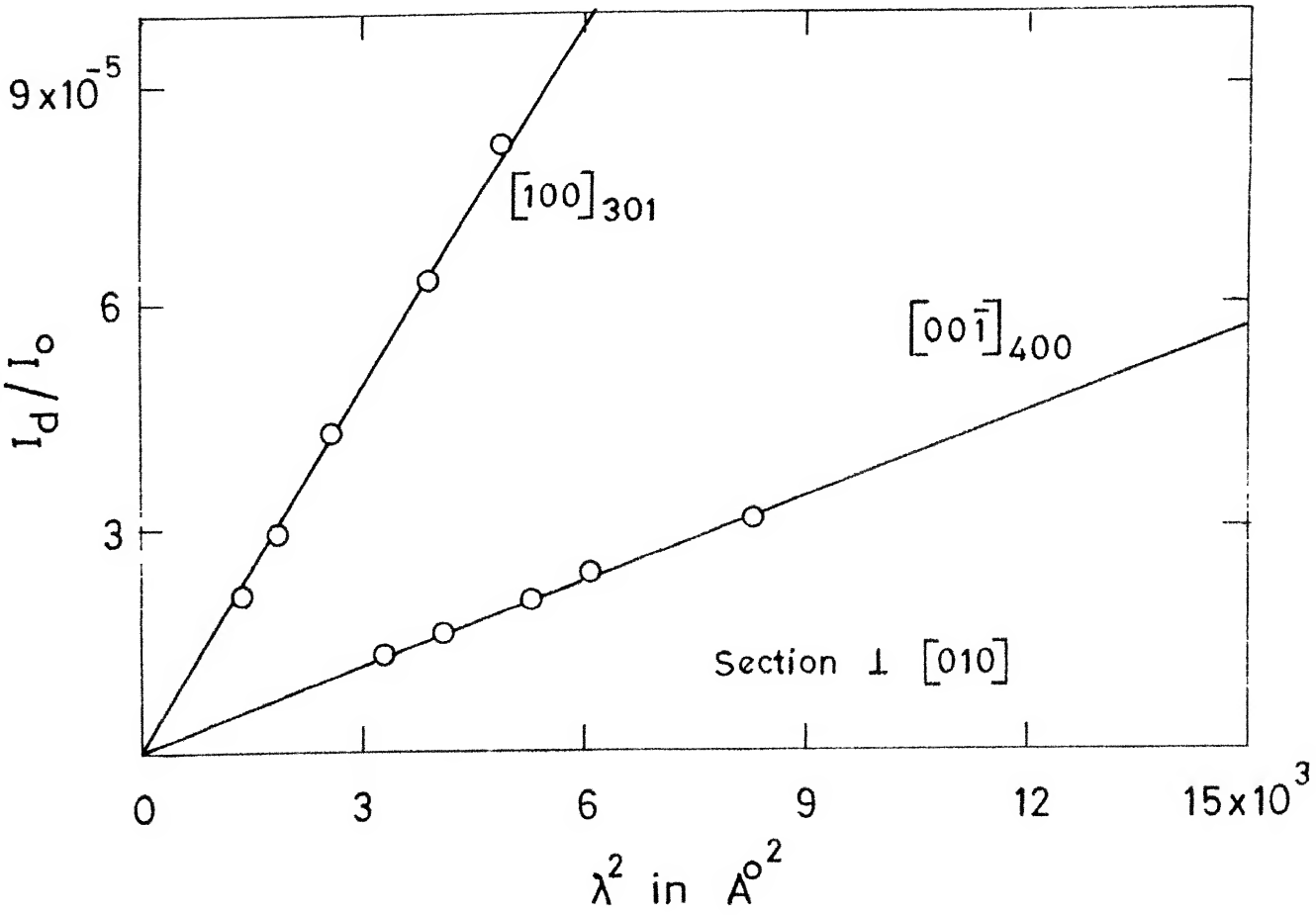
9x10⁻⁵
6
3
I_d / I_o
[100]301
[00ī]400
Section ⊥ [010]
0
3
6
9
12
15x10³
λ² in A°²

Fig. A4

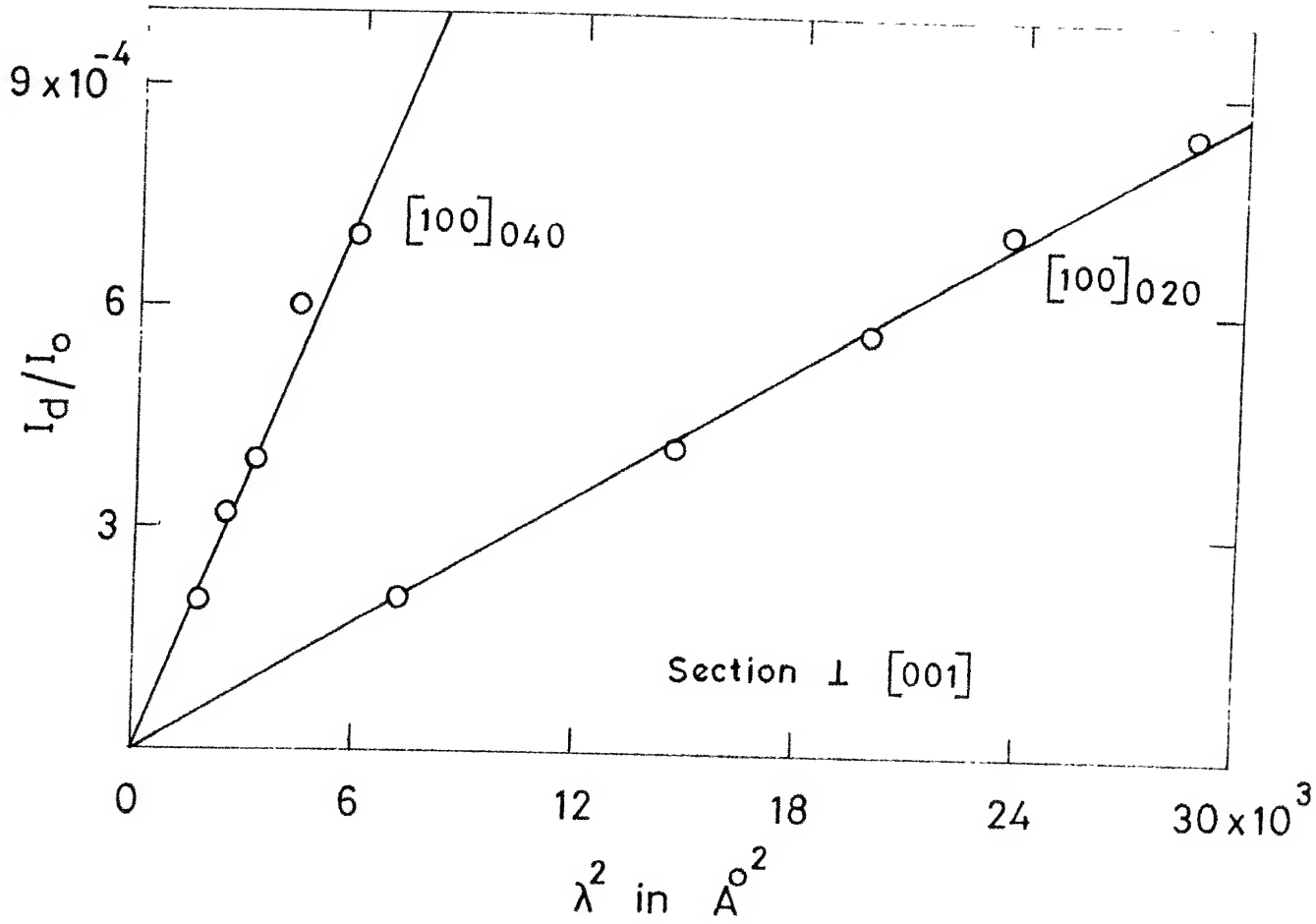
9 x 10^-4
6
3
I_d/I_o
[100]_040
[100]_020
Section ⊥ [001]
0
6
12
18
24
30 x 10^3
λ^2 in A°^2

Fig. A5

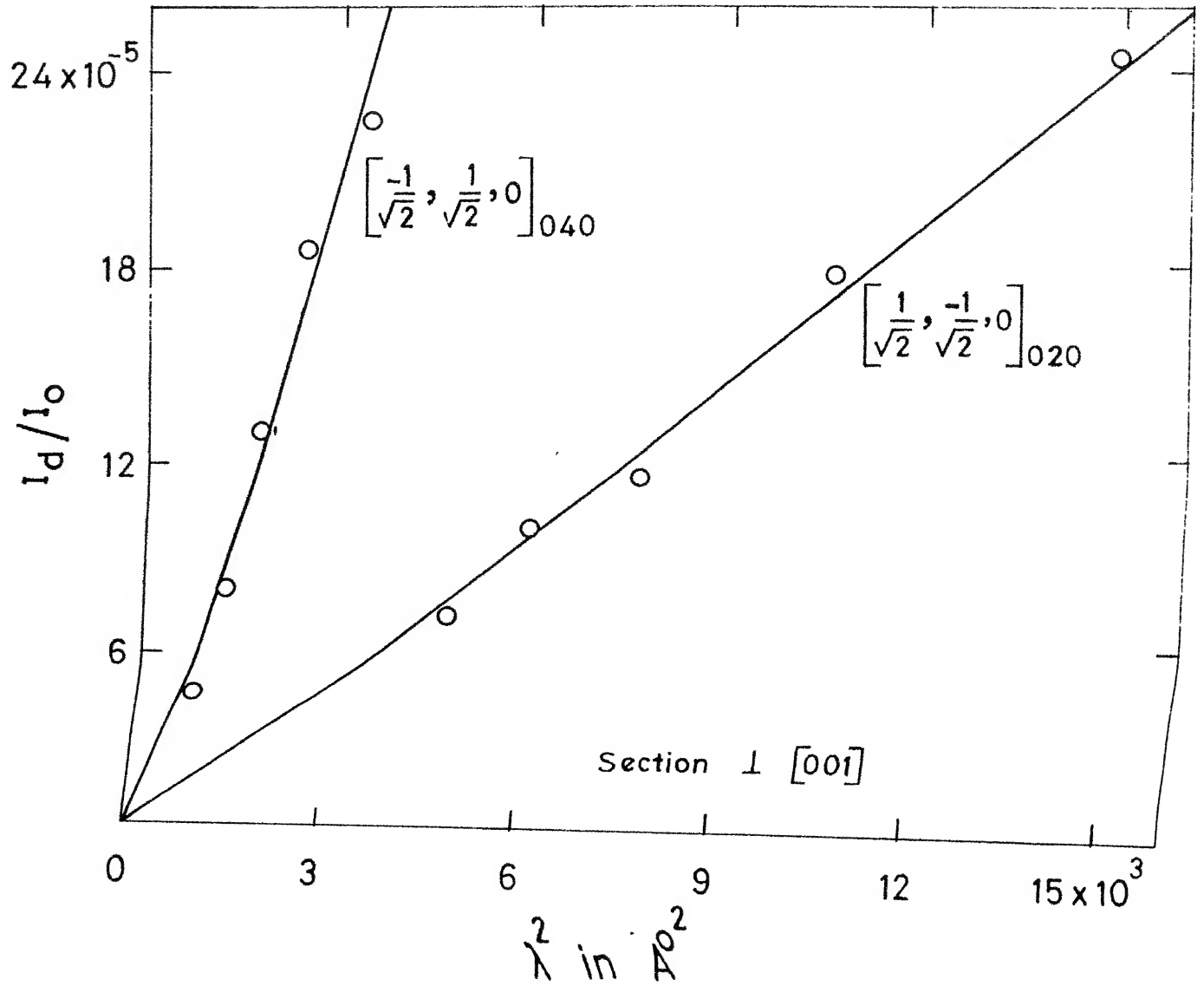
24 x 10^-5
18
12
6
0
3
6
9
12
15 x 10^3
I_d / I_o
λ² in A°²
[-1/√2, 1/√2, 0]040
[1/√2, -1/√2, 0]020
Section ⊥ [001]

Fig. A6

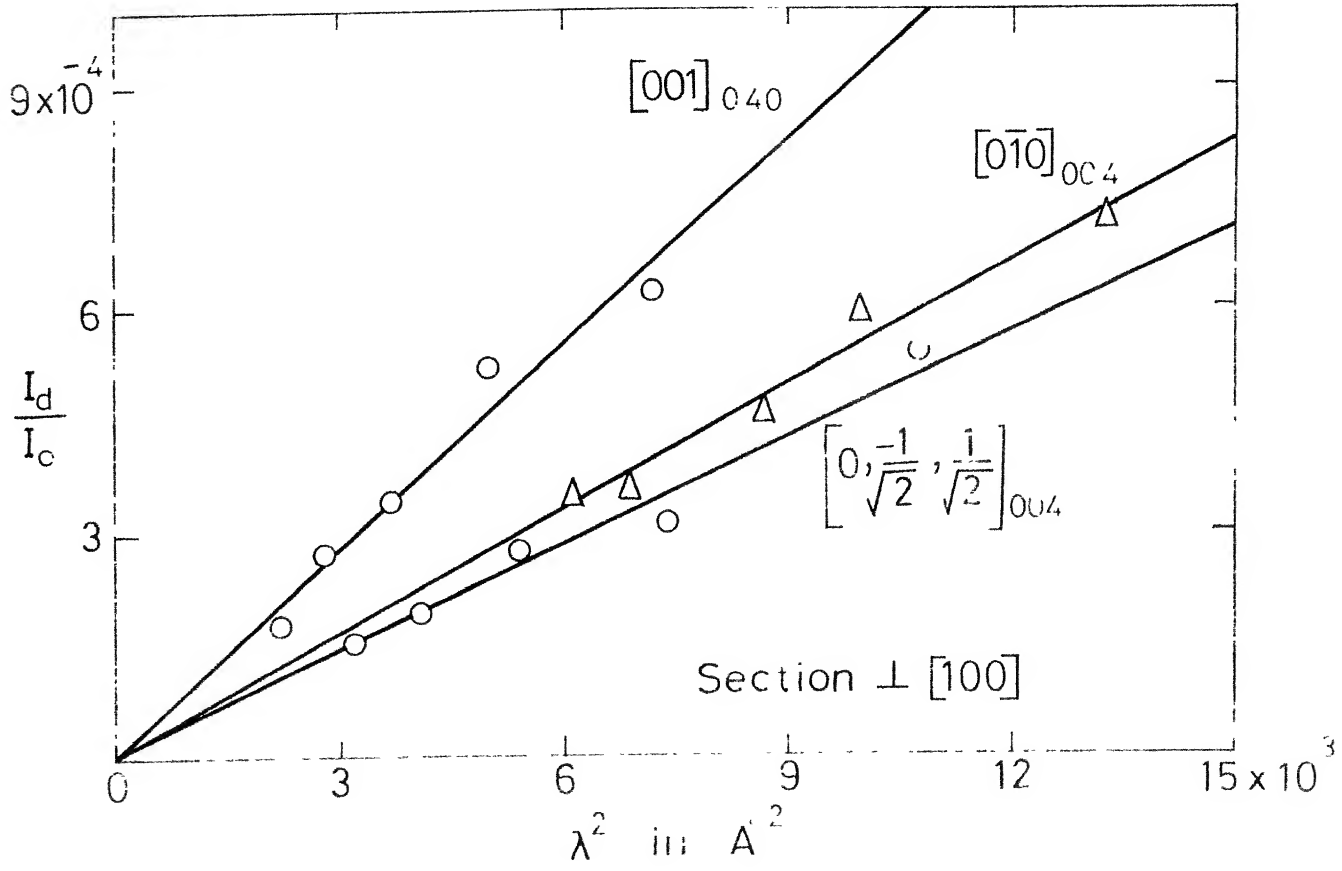
9x10^-4
6
3
0
3
6
9
12
15 x 10^3
$\frac{I_d}{I_c}$
λ^2 in A^2
[001] 040
[0$\bar{1}$0] 004
$\left[0, \frac{-1}{\sqrt{2}}, \frac{1}{\sqrt{2}}\right]$ 004
Section ⊥ [100]

Fig. A7

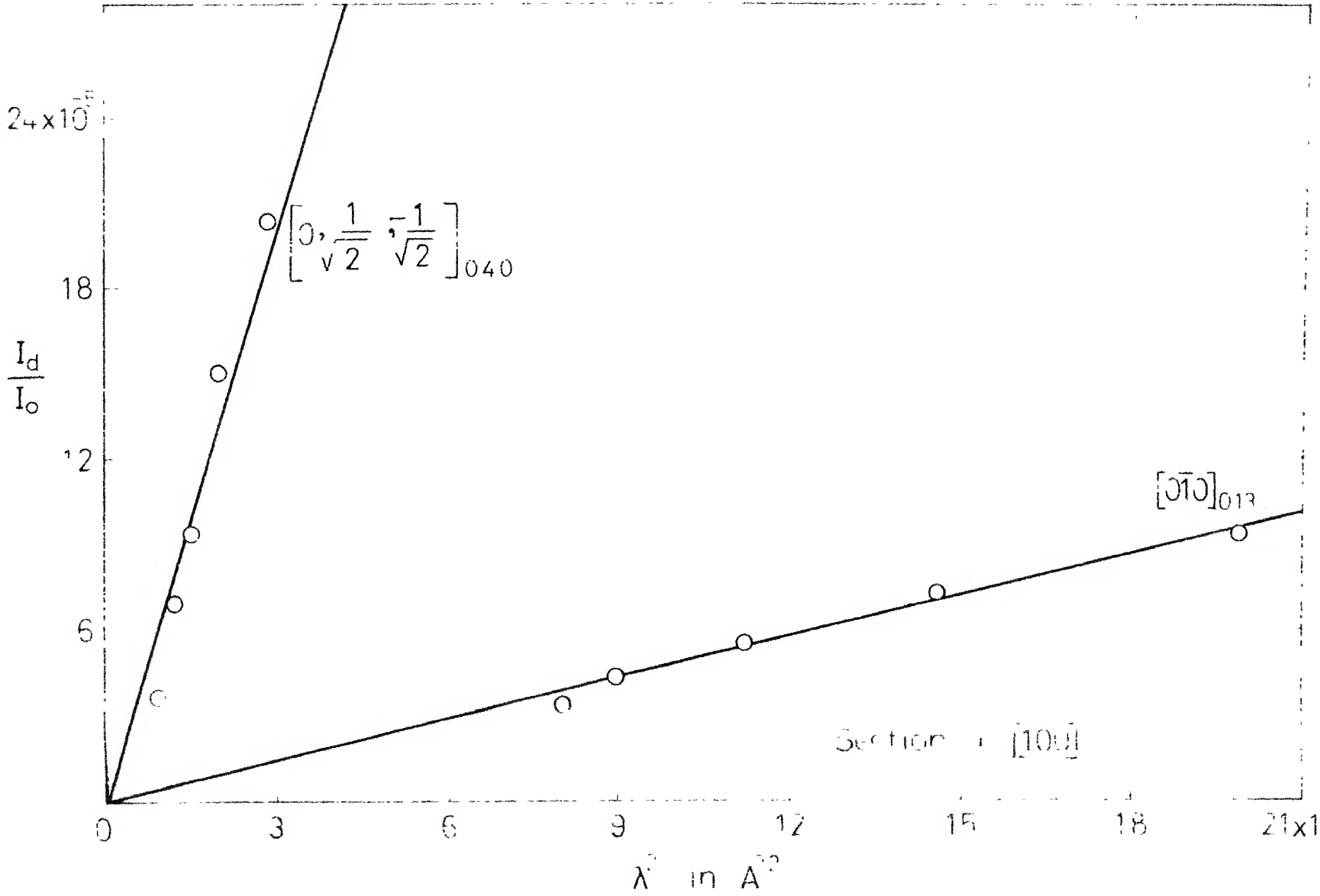
24x10⁻³
18
12
6
$\frac{I_d}{I_o}$
$\left[0, \frac{1}{\sqrt{2}}, \frac{-1}{\sqrt{2}}\right]_{040}$
$[0\bar{1}0]_{013}$
Section ⊥ [100]
0
3
6
9
12
15
18
21x10³
λ² in A²

Fig. A8

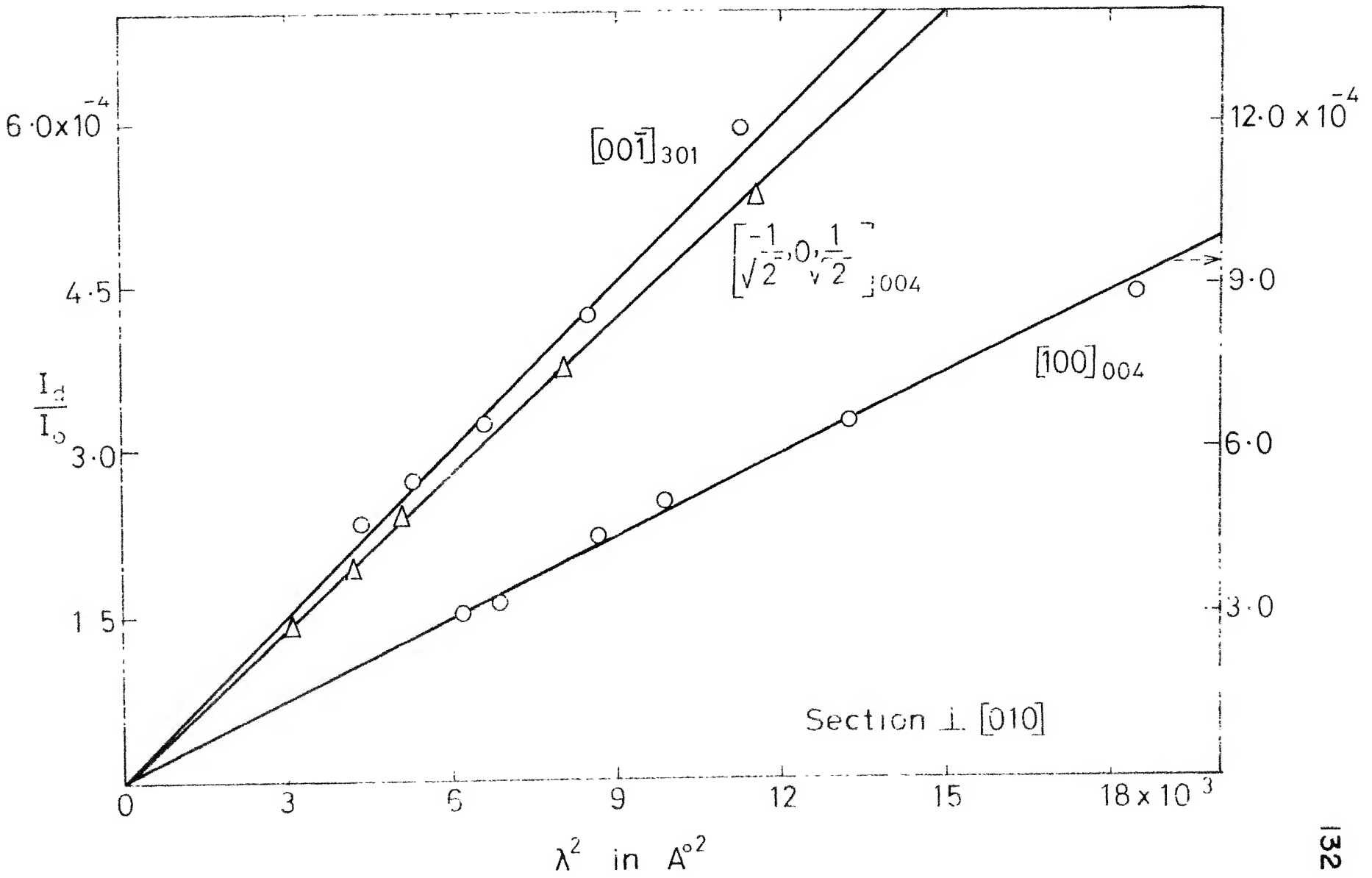
6·0x10⁻⁴
4·5
3·0
1 5
I_H / I_0
12·0 x 10⁻⁴
9·0
6·0
3·0
[001]301
[-1/√2, 0, 1/√2]004
[100]004
Section ⊥ [010]
0
3
6
9
12
15
18 x 10⁻³
λ² in A°²

Fig. A9

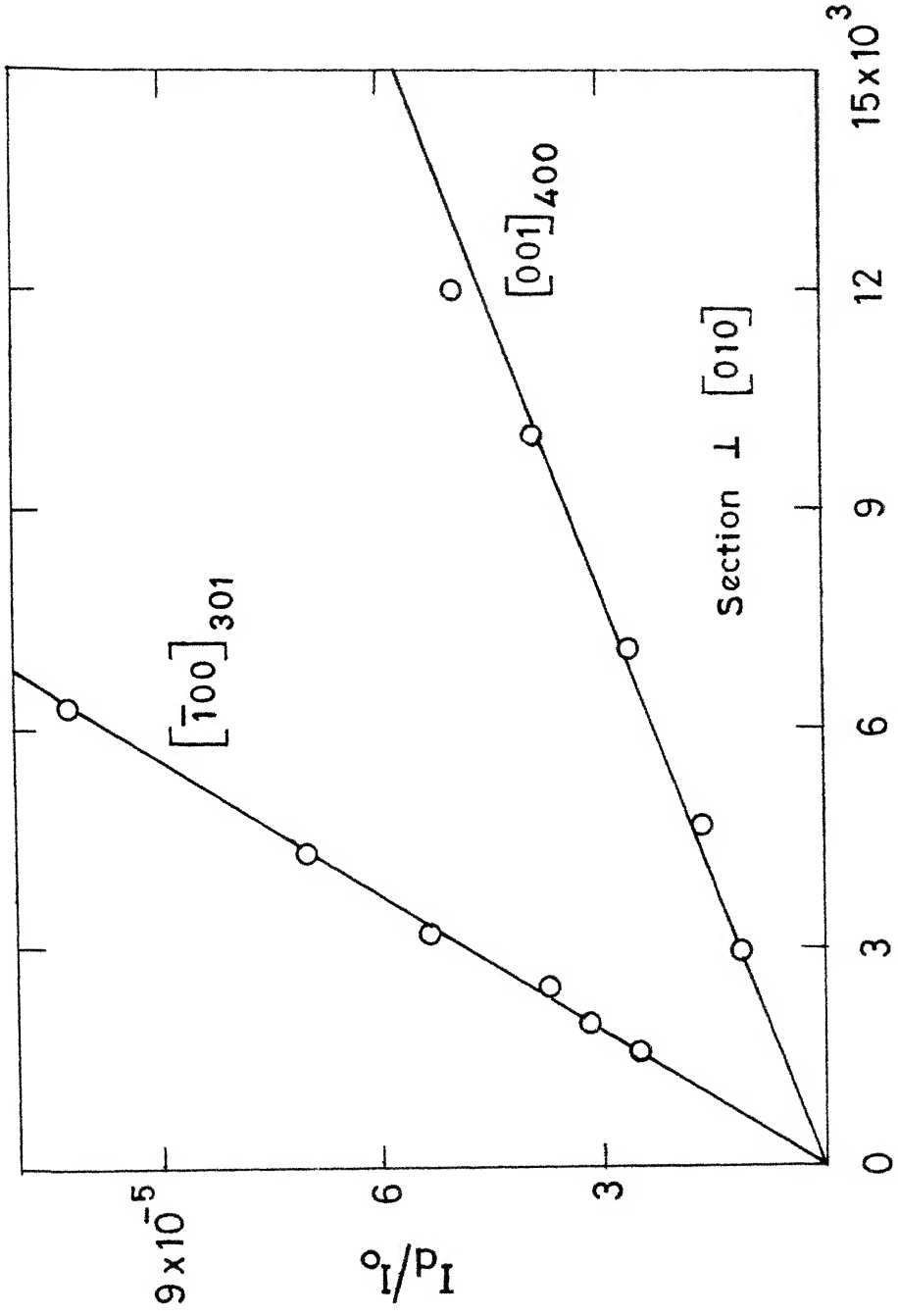
9×10^{-5}
6
3
I_d/I_o
0
3
6
9
12
15×10^3
λ^2 in A^{o2}
Section ⊥ [010]
$[\bar{1}00]_{301}$
$[001]_{400}$

Fig. A10

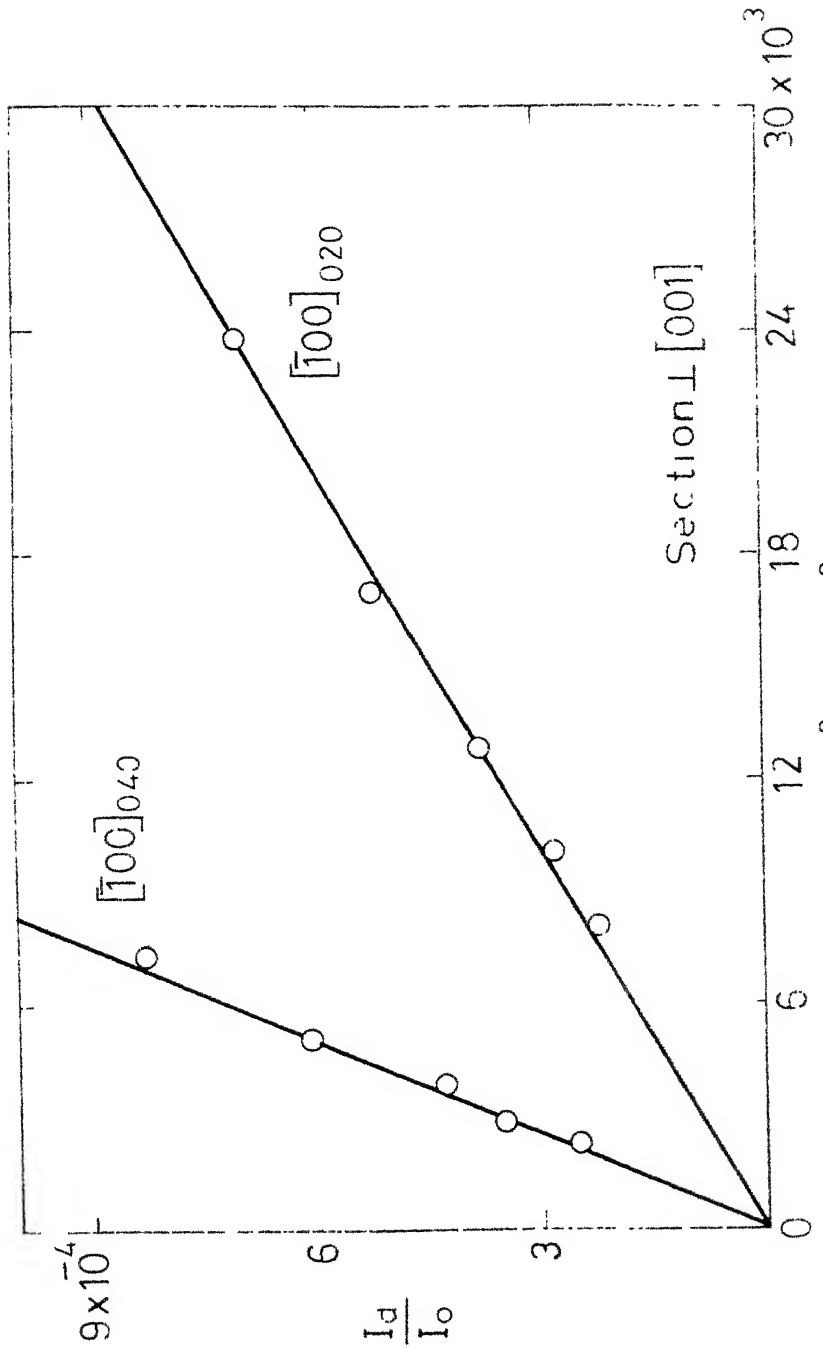
9×10^{-4}
6
3
0
$\frac{I_d}{I_o}$
$[\bar{1}00]_{040}$
$[\bar{1}00]_{020}$
Section ⊥ [001]
6
12
18
24
30×10^{3}
λ^2 in A^{o2}

Fig. A II

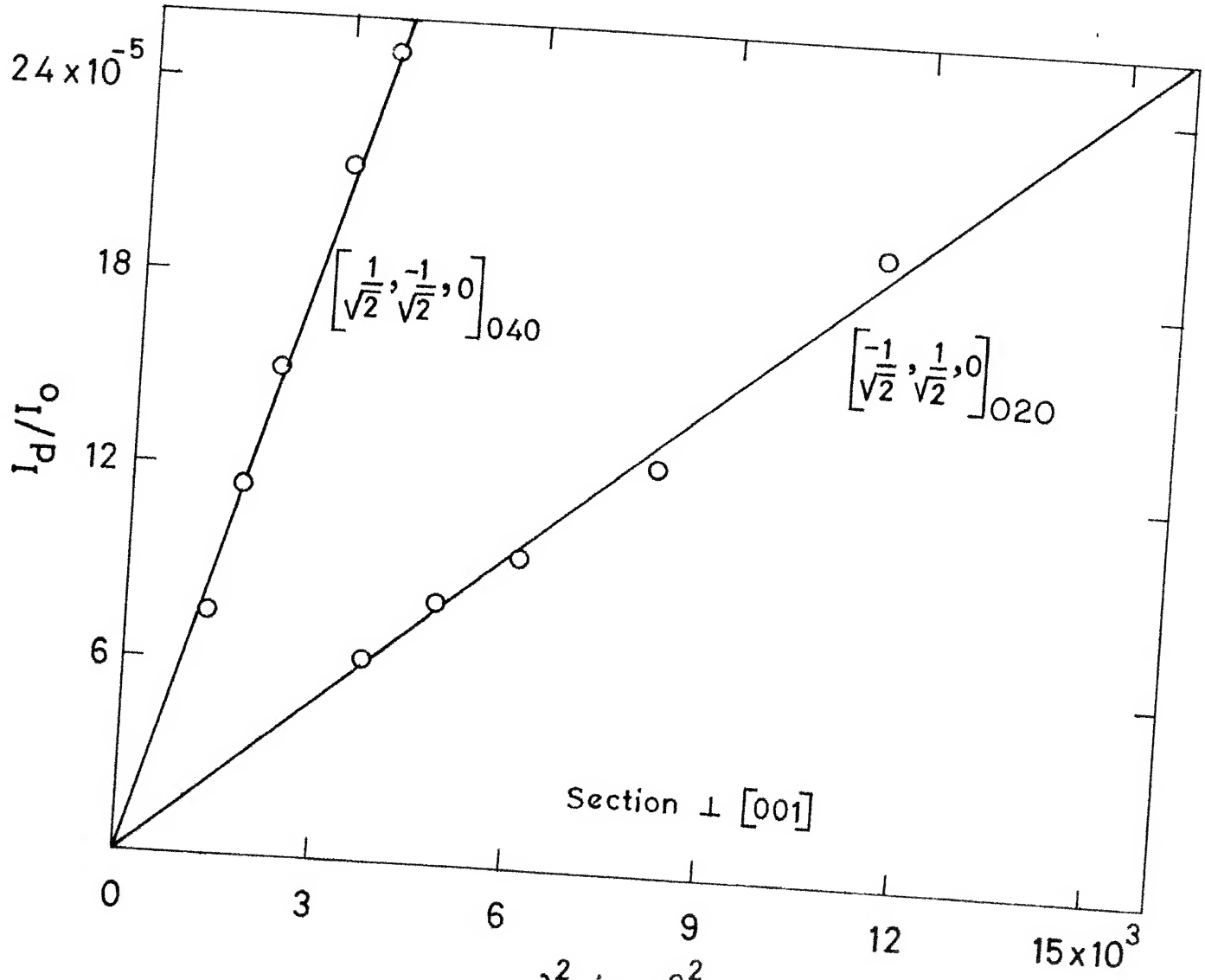
24 x 10^-5
18
12
6
0
3
6
9
12
15 x 10^3
I_d/I_o
λ² in A°²
[1/√2, -1/√2, 0]_040
[-1/√2, 1/√2, 0]_020
Section ⊥ [001]

Fig. A12

LIST OF PUBLICATIONS

Papers in Journals

1. A. Garg and R. C. Srivastava, (1979) Acta Cryst. "Ammonium Tetrafluoroberyllate" B35, 1429-1432.

2. A. Garg and R. C. Srivastava, (1980) Acta Cryst. "Elastic Constants of Ammonium Fluoberyllate by Thermal Diffusion Scattering of X-rays". Accepted for publication.

Papers Presented in Conferences

1. A. Garg and R. C. Srivastava, "Crystal Structure of Ammonium Fluoberyllate, $(NH_4)_2BeF_4$." 9th National Conference on Crystallography, Sardar Patel University, Gujarat, 1978, Paper D-1, p. 16.

2. A. Garg and R. C. Srivastava, "Anisotropy of Thermal Vibrations in $(NH_4)_2BeF_4$ and $(NH_4)_2SO_4$." 10th National Conference on Crystallography, B.H.U., Banaras, 1979, Paper 4.6, p. 63.

3. A. Garg, Y. Chandra and R. C. Srivastava, "Modifications in GE-XRD-5/6 Diffractometer to Accommodate Curved Crystal Monochromator." 10th National Conference on Crystallography, B.H.U., Banaras, 1979, Paper 12.4, p. 12

4. A. Garg and R. C. Srivastava, "Elastic Constants of Ammonium Fluoberyllate, $(NH_4)_2BeF_4$." 11th National Conference on Crystallography, I.A.C.S., Calcutta. 1980, Paper K-11.